

ABSTRACT

Title of Dissertation: PROBABILISTIC ASSESSMENT OF MULTI-MECHANISM FLOOD HAZARDS USING A BAYESIAN APPROACH

Somayeh Mohammadi, Doctor of Philosophy,
2022

Dissertation directed by: Assistant Professor Michelle Bensi, Department
of Civil and Environmental Engineering

Multi-mechanism floods (MMFs) are flood events caused by the simultaneous occurrence of multiple flood mechanisms such as storm surge, precipitation, waves, and tides. The term compound floods, which is a broader term frequently used in the current literature, includes MMFs as a subset. MMF events can have more severe impacts on communities and the built environment than single-mechanism floods. Therefore, a realistic probabilistic assessment of the frequency and severity of flood hazards requires the inclusion of the hazard contribution of MMFs. This dissertation addresses four objectives related to the probabilistic evaluation of MMFs. First, this dissertation develops a lexicon and framework for discussing a broad range of MMFs and then defines the gaps and shortcomings of the current literature. Second, this dissertation develops a Bayesian approach (BA) for performing a probabilistic assessment of a specific type of MMF hazard, namely tropical cyclone-induced increase in river discharge arising from multiple flood mechanisms. The Bayesian model is built using a Bayesian Network (BN). Five computationally

justifiable predictive "placeholder" models are developed in this approach to estimate conditional probability tables in the BN. Third, the performance of the BN is assessed for "reasonableness" using three historical storms that affected the study area. Fourth, the capability of the BN for information updating is demonstrated by setting information related to historical observations as evidence in the developed BN and conducting forward and backward inferences. Finally, this study concludes with a summary and synthesis of the gaps and weaknesses of current literature and practices in addressing compound flood hazards. This study further highlights the capabilities and challenges of the developed Bayesian approach and outlines proposed next steps to address these challenges.

PROBABILISTIC ASSESSMENT OF MULTI-MECHANISM FLOOD HAZARDS
USING A BAYESIAN APPROACH

by

Somayeh Mohammadi

Dissertation submitted to the Faculty of the Graduate School of the
University of Maryland, College Park, in partial fulfillment
of the requirements for the degree of
Doctor of Philosophy
2022

Advisory Committee:

Professor Michelle Bensi, Chair
Professor Katrina Groth, Dean's Representative
Professor Allison Reilly
Professor Kaye Brubaker
Dr. Meredith Carr

© Copyright by
Somayeh Mohammadi
2022

Dedication

To my family and friends, to whom I owe everything.

Acknowledgements

I would like to express my deepest gratitude to my advisor Professor Michelle (Shelby) Bensi, who constantly supported me throughout my Ph.D. Her continuous inspiration and encouragement always kept me motivated, even during the difficult times. Under her supervision, I have developed the necessary skills to be an independent researcher. I am thankful to my committee members, Professor Brubaker, Professor Reilly, Professor Groth and Dr. Carr, who provided valuable comments which improved this dissertation.

I also would like to thank the sponsors of this research. This work was supported by the U.S. Nuclear Regulatory Commission (NRC) Office of Nuclear Regulatory Research through Oak Ridge National Laboratory as part of the NRC Probabilistic Flood Hazard Assessment Research Program. I would also like to say thanks to Dr. Shih-Chieh Kao, Scott DeNeale, Dr. Joseph Kanney, and Dr. Elena Yegorova for their feedback and comments on certain sections of this dissertation.

I deeply appreciate the company of my family, even from long distances, during the difficult times. My special thanks also go to my dear friends, Sanaz Aliari, Maria Coelho, Maryam Froozan, Elnaz Peyghaleh, and Saeedeh Gilani, who supported me through the ups and downs of my journey. Without their heart-warming presence, my Ph.D. path would not have been as beautiful.

Finally, thanks to that very important piece of my heart, my cat Luna, (and her kitten Lola) who brought more beauty to this effort and stayed awake at nights with me to finish my work.

Table of Contents

Dedication.....	ii
Acknowledgements.....	iii
Table of Contents.....	iv
List of Tables.....	vi
List of Figures.....	vii
List of Abbreviations.....	ix
Chapter 1: Introduction.....	1
1.1 Motivation.....	1
1.2 Research Objectives.....	3
1.3 Methods.....	4
1.4 Dissertation Outline.....	5
Chapter 2: Probabilistic Multi-Mechanism Flood Hazard Assessment.....	7
2.1 Introduction.....	7
2.2 MMF Lexicon and Conceptual Framework.....	10
2.2.1 MMF Lexicon.....	10
2.2.2 Multi-Mechanism Flood Hazard Framework.....	12
2.3 Summary of Approaches to Develop Joint Distribution.....	14
2.3.1 Statistical Approaches.....	15
2.3.2 Bayesian Approaches.....	20
2.4 Summary of Available Literature.....	23
2.4.1 Study Scopes.....	24
2.4.2 Data Sources.....	26
2.4.3 Study Scale and Regions.....	27
2.4.4 Methods Applied.....	28
2.5 Discussion: Assessment of Current Literature.....	28
2.5.1 Length of Record and Characteristics of Available Data Series.....	28
2.5.2 Site-specific Assessments.....	29
2.5.3 Statistical Modeling Choices.....	30
2.5.4 Assumptions Regarding Occurrence and Concurrence of Extrema.....	31
2.5.5 Inconsistent Terminology.....	35
2.5.6 Lack of a Comprehensive Framework for Analyzing Dependence.....	36
2.6 Conclusion.....	38
Chapter 3: Bayesian Approach for Assessment of Hurricane-Induced Multi-Mechanism (Compound) Floods.....	43
3.1 Introduction.....	43
3.2 Bayesian Model.....	47
3.2.1 Background on BNs.....	47
3.2.2 Proposed BN for Coastal MMF.....	49
3.3 Case Study Location and Data Sources.....	51
3.4 Model Assumptions: Distributions and Predictive Models.....	54
3.4.1 Storm Parameter Distributions.....	54
3.4.2 Predictive Models Developed for Estimating Conditional Distributions.....	54
3.5 Generation of the Hazard Curve.....	71

3.6	Assessment of the Model Performance.....	72
3.7	Conclusion	77
Chapter 4:	Further applications of the developed Bayesian framework.....	79
4.1	Introduction.....	79
4.2	Information Updating in BNs	80
4.2.1	Forward Inference.....	81
4.2.2	Backward Inference	83
4.2.3	Mixed Inference.....	88
4.3	Conclusion	91
Chapter 5:	Conclusion, a Summary of the Contributions and Next Steps.....	94
5.1	Conclusion	94
5.2	Summary of contributions.....	97
5.3	Future research.....	99
Appendices.....		102
Appendix 1: Summary of Reviewed Research Studies		102
Bibliography		113

List of Tables

Table 3-1. Distributions and corresponding parameters for hurricane parameters (based on Nadal-Caraballo et al. (2015)).....	56
Table 3-2. Discretized values for the parameters required in the Bayesian formulation.....	70
Table 3-3. Storm parameters and surge and discharge values related to USGS gage and modeling results.	74
Table 4-1. Parameters and corresponding storm surges and discharges related to historical storms.....	83

List of Figures

Figure 2-1. Compound flood lexicon.....	11
Figure 2-2. Categories of flood mechanism combinations	14
Figure 2-3: Illustration of key steps in the implementation of Bayesian-motivated approaches	21
Figure 2-4: Example Bayesian graphical model used for generation of numerical expressions.....	22
Figure 3-1. The foundational BN used in this study.....	49
Figure 3-2. Left: The case study location with simulated landfall locations (red dots) and upstream watershed (blue dots); Right: The location of the USGS gage, NOAA tide gage, save point 5373, and the location of the rock riffles upstream of the save point 5373.	53
Figure 3-3. Hurricane-induced precipitation in the upstream area (mm/hr) for an example storm track at discrete time steps (represented as hours after storm landfall, LF) and total daily upstream rainfall (mm/day) (lower right map); the red star represents storm center at specific points after landfall; the color bar represents rainfall (mm/hr for hourly precipitation and mm/day for daily precipitation).....	62
Figure 3-4. Left: Time series of precipitation-induced discharge (top) and basin-wide average daily precipitation (bottom); Right: Scatterplot of discharge and basin-wide average daily precipitation.	63
Figure 3-5. Scatterplot of discharge and basin-wide average daily precipitation (blue dots) superimposed with second-order polynomial regression line (red line).....	64
Figure 3-6. Left: Scatterplot of stage and discharge (blue dots) with poor fitted data highlighted in black circles and fitted third-order polynomial model (red line) ;Right: time series of stage (blue) and discharge (orange) with poor fitted data highlighted using black circles.....	66
Figure 3-7. Empirical CDF (left) and PMF related to high and low tides.	68
Figure 3-8. Illustration of Monte Carlo simulation approach for generating CPTs.	71
Figure 3-9. Illustrative/representative hazard curve showing annual exceedance frequency for river discharge caused by hurricane occurrence, developed considering simplified/illustrative modeling assumptions.....	72
Figure 3-10. Synthetic and observed storm track related to historical storms.....	73
Figure 3-11. Location of the representative point for extracting information at landfall location for historical storms.	74
Figure 3-12. Posterior distribution of the modeled discharge values for historical storms.....	75
Figure 4-1. A simple BN with two parent nodes and a child node	79
Figure 4-2. Developed BN for information updating	80

Figure 4-3. Updated distributions of effect (target) node using forward inference. ...83

Figure 4-4. Updated distributions of nodes representing model input parameters using observations related to the total river discharge node.....86

Figure 4-5. Landfall locations of three historical storms (blue stars) along with fifteen simulated landfall locations in this study (red circles).....88

Figure 4-6. Updated distributions of nodes using observed values of storm surge related to historical storms.....90

List of Abbreviations

AIC	Akaike information criterion
BA	Bayesian approach
BIC	Bayesian information criterion
BN	Bayesian Network
CDF	Cumulative distribution function
CHS	Coastal Hazard System
CPT	Referred to as conditional probability tables
EVA	Extreme value analysis
GLM	Generalized linear models
JPA	Joint probability analysis
JPM	Joint Probability Method
MMF	Multi-mechanism floods
NACCS	North Atlantic Coast Comprehensive Study
NOAA	National Oceanic and Atmospheric Administration
NRC	Nuclear Regulatory Commission
PFHA	Probabilistic flood hazard assessment
PMF	Probability mass function
POT	Peak over threshold
RIDM	Risk-informed decision-making
RMSE	Root mean square error
SLOSH	Sea, Lake and Overland Surges from Hurricane
SLR	Sea level rise

TRR	Tropical Rainfall Rate
USACE	United States Army Corps of Engineers
VIC	Variable Infiltration Capacity
WL	Water level
WRF	Weather and Research Forecasting

Chapter 1: Introduction

1.1 Motivation

Flood disasters are a major cause of economic losses and fatalities in the US (Brody et al. 2008; Cigler 2017; Kick et al. 2011). Flood mechanisms are physical processes that can cause the flow or accumulation of water on or near a site (e.g., storm surge, precipitation, tides, and waves). Among the 35,000 disaster events that occurred in the US between 1900 and 2015, 40 percent were caused by floods (Cigler 2017). Flood events can be caused by a single flood mechanism or a combination of flood mechanisms. The latter group of flood events is referred to herein as multi-mechanism floods (MMFs). Multi-mechanism floods are a subset of compound floods. Compound floods may involve a broader range of compounding processes over a range of time durations.

MMFs can have more severe impacts on societies and built environments than single-mechanism floods. Hurricane Harvey (in 2017) was one of the costliest flood disasters in the US and an example of MMFs (Huang et al. 2021; Valle-Levinson et al. 2020). The estimated costs of this hurricane was \$143 Billion USD (Smith 2020).

Probabilistic flood hazard assessment (PFHA) uses probabilistic models and/or statistical assessments to assess the annual frequency (or probability) of exceedance associated with one or more measures of flood severity. Traditional methods for PFHA typically consider one flood mechanism and assess the frequency of exceedance of a single measure of flood severity (e.g., river discharge or surge elevation). Focusing on

a single mechanism can underestimate or mischaracterize flood hazards. Therefore, for a realistic PFHA, it is necessary to consider multiple flood mechanisms. However, consideration of more than one flood mechanism in the PFHA introduces new challenges. These challenges arise from the need to model the physical interactions between multiple flood mechanisms and capture the dependence structure between involved variables.

Common methods in the current literature and practice used to capture the dependence between multiple variables and develop joint distributions are the copula and direct estimation of the parametric bivariate distributions (Bender et al. 2016; Bevacqua et al. 2020; Ghanbari et al. 2021; Gilja et al. 2018; Hawkes et al. 2002; Hawkes 2008; Kao and Chang 2012). These methods typically focus on the statistical analysis of representative metrics of flood mechanisms (e.g., precipitation depth, river flow, and surge height) without explicitly leveraging physical process knowledge. These methods are often adversely impacted by the limited availability of data related to these representative metrics.

To capture the dependence structure between involved variables, many commonly employed methods directly construct joint distributions using defined functional forms and limiting assumptions. For example, some studies have constructed joint distributions using parametric bivariate distributions (e.g., bivariate normal distribution) (Hawkes et al. 2002; Hawkes 2008; Wadey et al. 2015). In this case, there is the requisite assumption of similarity of functional forms between marginal and joint distributions. The copula method relaxes this limiting assumption and can be applied to any functional form of marginal distributions (Bender et al. 2016; Bevacqua et al.

2020; Gilja et al. 2018; Kao and Chang 2012). However, a new challenge arises due to the absence of a well-defined scientific process to select the “best” functional form of copula from among the many available functional forms.

Bayesian approaches (BA) provide an alternative means of developing the joint distribution over multiple random variables. BAs are commonly employed in the probabilistic assessment of seismic and selected coastal hazards. In this method, using the chain rule of probability, each joint distribution of the random variables can be written as a product of the conditional distributions, which are estimated using models that reflect both the physical and statistical relationships between variables. As such, BA can incorporate the knowledge of physical processes into the analysis. Incorporating the knowledge of the physical processes in the PFHA is particularly valuable in cases where the long historical record of data related to representative metrics are not available.

1.2 Research Objectives

Compound flooding, including MMFs, has received attention recently. This has led to a broad and diverse set of applications. Still, no studies have systematically analyzed and reviewed the current literature/resources to define the gaps and weaknesses of available practices and approaches. Therefore, this dissertation first aims to critically review current literature and practices related to MMFs and define the associated gaps and challenges. The comprehensive review of the current state of the art identified several challenges related to current practices and a need for a framework that addresses these challenges. In response, this study develops a Bayesian framework for

probabilistic assessment of compound floods using a case study located in Trenton, NJ, on the Delaware River.

Specifically, this study focuses on the following four main objectives:

Objective 1: Develop a lexicon and a framework to describe different elements related to the probabilistic assessment of MMFs and use the lexicon/framework to (1) systematically review the current literature related to MMFs and (2) define the gaps and weaknesses.

Objective 2: Develop a BA for probabilistic assessment of MMF hazards related to storm surge, precipitation, river flow, and tides to build a representative model using a Bayesian Network (BN).

Objective 3: Use historical storm data to evaluate the performance of the developed Bayesian model.

Objective 4: Apply the information updating capability of the developed BN to illustrate the capability to update the probability distributions of involved parameters using observed data.

This study addresses Objective 1 in Chapter 2 and Objectives 2 and 3 in Chapter 3. Objective 4 is addressed in Chapter 4.

1.3 *Methods*

This dissertation uses a BA to develop a framework for the probabilistic assessment of compound floods. The framework is demonstrated using a coastal case study located in Trenton, NJ, on the Delaware River. The severity metric of interest in this study is river discharge.

A probabilistic assessment of compound floods using a BA requires the development of joint distributions of involved random variables. In this work, the Bayesian model is built using a BN as the computational mechanism. The BN is developed using the relationships between variables related to multiple flood mechanisms based on statistical and physical process models. This study uses five predictive “placeholder” models to illustrate the application of the proposed framework and demonstrate the development of conditional distributions in the associated BN. Then, using the BN, a probability distribution (conditioned on the occurrence of a hurricane) for total river discharge is generated, which accounts for storm surge, precipitation, tides, and river antecedent flow. The (conditional) probability of exceedance for different values of total hurricane-affected river discharge is estimated. The estimated (conditional) probability of exceedance is multiplied by the annual occurrence rate of a hurricane in the study area to generate a hazard curve.

While the framework is demonstrated using “placeholder models” that have been individually validated, the overall reasonableness of the model is assessed using historical observations. Finally, the capability of BNs for information updating is leveraged to update the probabilities of different nodes using observed data.

1.4 Dissertation Outline

The remainder of this dissertation includes the following chapters: Chapter 2 provides a comprehensive critical review of current literature and approaches. It focuses on developing a framework and lexicon, defining the challenges and gaps related to the current approaches, and summarizing the literature. Chapter 3 focuses on developing

the proposed BN for probabilistic assessment of MMFs in a coastal area and application to a case study. The chapter also includes a performance assessment of the developed framework based on a reasonableness metric. Chapter 4 focuses on applications of developed BN for information updating. Chapter 5 provides the conclusions, research contributions, and potential future research related to this dissertation.

Chapter 2: Probabilistic Multi-Mechanism Flood Hazard

Assessment

2.1 Introduction

Among all natural hazards, floods rank first in terms of economic consequences and loss of lives, and this impact is expected to grow in the coming decades (Brody et al. 2008; Brussee et al. 2021; Cigler 2017; Crawford et al. 2022; Hallegatte et al. 2013; Hu et al. 2021; Kick et al. 2011; Koç et al. 2021; Lazin et al. 2021; Lüdtke et al. 2019; Lv et al. 2021; Mazzoleni et al. 2021; Mileti 1999; Schoppa et al. 2021; Schröter et al. 2018; Shrestha et al. 2021; Wang et al. 2021a; Yildirim and Demir 2019; Zhang et al. 2021). A global-scale study (Hallegatte et al. 2013) estimated that the average yearly flood loss for coastal port cities could be eight times larger in 2050 (US\$52 billion) compared to 2005 (US\$6 billion).

Floods can result from the occurrence of individual flood mechanisms as well as combinations of multiple flooding mechanisms (i.e., compound or multi-mechanism floods). Given the joint behavior among mechanisms, compound floods may be more severe or have different characteristics than single-mechanism floods in terms of the negative consequences and the extent of the impacts on critical infrastructure and communities. To facilitate comprehensive risk-informed decision-making (RIDM) associated with efforts to protect against and mitigate the effects of flood events, it is important to understand hazards posed by both single and multiple (compounding)

flood mechanisms. Several studies have shown that ignoring compound, multi-hazard effects can underestimate the annual exceedance probability or expected likelihood of a given water level (Bevacqua et al. 2017; Eilander et al. 2020; Gori et al. 2020; Hsiao et al. 2021; Kumbier et al. 2018; Moftakhari et al. 2017; Saharia et al. 2021; Santos et al. 2021).

With the steadily increasing literature related to compound floods, there is a need for a systematic review and integrated evaluation. Within the content of RIDM for critical infrastructure facilities (e.g., nuclear power plants, high-hazard dams, power distribution systems), probabilistic assessment of compound floods is particularly relevant. Probabilistic flood hazard assessment (PFHA) provides information about the frequency and severity of flood hazards. PFHAs are typically characterized by a hazard curve providing the annual exceedance probabilities of a flood severity metric such as flood volume or water elevation. To develop realistic probabilistic estimates of flood hazards (particularly for low annual exceedance probabilities), and to better support RIDM, analysis of a single flood mechanism is generally not sufficient and will likely underestimate the hazard. This fact directs us to explore joint probability analysis (JPA) for flooding. The use of JPA for assessing flood hazards is not new, particularly when considering the joint occurrence of multiple parameters related to one flooding mechanism (Hsu et al. 2018; Razmkhah et al. 2022; Toro et al. 2010a; b; Yue 2001; Yue et al. 1999; Zhang and Singh 2006) and when assessing hazards for short to moderate return periods which are inversely related to high and moderate annual exceedance probabilities. However, when assessing hazards from more than one

flooding mechanism and for longer return periods, literature is more limited. In general, existing studies are reported in disparate disciplines using varying terminology.

To help synthesize the existing knowledge related to probabilistic compound flood assessment, a literature review is conducted that: (1) surveys reported compound flood assessment methods, and (2) identifies and categorizes challenges involved in the reported approaches. To help meet these objectives, we present a conceptual structure and lexicon for describing and integrating insights from existing MMF assessment sources. This structured approach to aggregating insights and identifying current research challenges/gaps across a disparate literature landscape represents this research's primary contribution. In this review, we include studies that strive to perform a complete PFHA-related to MMFs and studies that could serve as building blocks for MMF assessment. Some of these building block studies focus on deterministic MMF assessment and associated numerical model development. Other building block studies develop statistical or mechanistic models to understand the interaction between flood mechanisms.

In the sections that follow, a conceptual framework for the assessment of MMF (Section 2.2) is introduced and a summary of approaches used to probabilistically assess MMFs (Section 2.3) is provided. Then a summary of available literature (Section 2.4) is provided and critical insights are offered (Section 5).¹

¹ This chapter summarizes, complements, and extends the work in Bensi et al. (2020)

2.2 MMF Lexicon and Conceptual Framework

The current literature on MMF assessment is spread over several disciplines with no unified terminology or conceptual framework. To provide a concise and logical review, we first propose a lexicon and conceptual framework to organize the disparate semantics, approaches, methods, and applications.

2.2.1 MMF Lexicon

This section provides a lexicon (vocabulary) that facilitates the systematic review and discussion of the current literature related to MMFs. This is needed, in part, because the existing literature lacks consistent and unified terms of reference. Different sources often use different terms to describe the same concepts (and sometimes vice versa, using similar terms for different concepts). For example, a range of words have been used in the literature to refer to "combinations of flood hazards" without implying unique differences; e.g., coincident, combined, concurrent, compound, joint, cascading, concomitant, simultaneous, and successive.

The proposed MMF lexicon includes three main terms: (1) flood-forcing phenomena (events), (2) flood mechanisms, and (3) flood severity metrics. *Flood-forcing phenomena* are natural or man-made events that can lead to flooding of a site. Flood-forcing phenomena include severe weather events (hurricanes, local intense precipitation, rapid temperature changes, etc.), land movement events (earthquakes, landslides, etc.), operational events (releases from dams, equipment aging, and failure, etc.), and natural cyclic or quasi-cyclic events (e.g., the arrival of tides or swells).

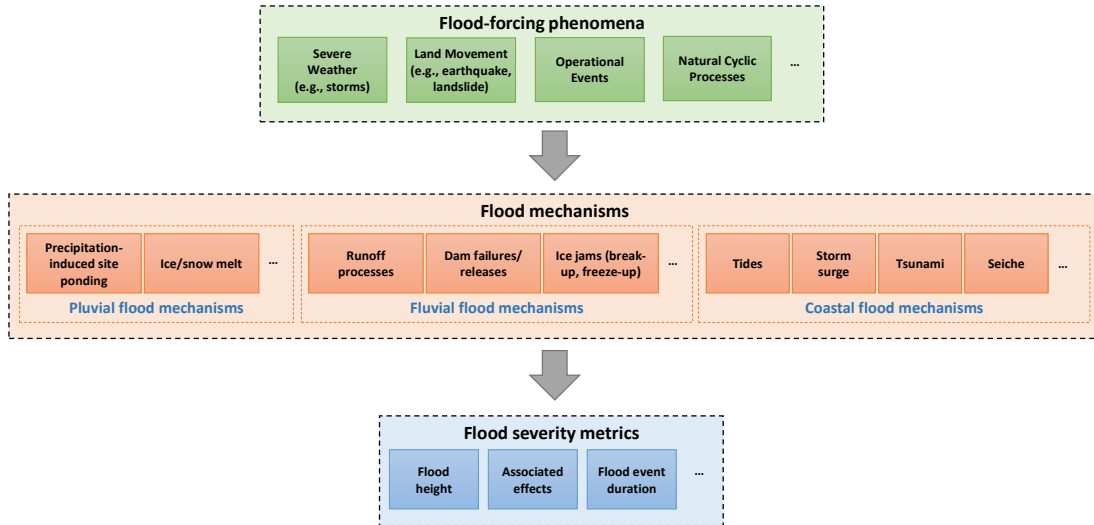


Figure 2-1. Compound flood lexicon

Flood mechanisms are the physical processes by which a flood-forcing phenomenon can cause flows or accumulation of water on or near a site. Generally, flood mechanisms are divided into three types/classes: fluvial, pluvial, and coastal flood mechanisms. Fluvial flood mechanisms are associated with non-local watershed processes (e.g., surface runoff, snowmelt, flood wave routing, and baseflow) that result in overflow of a river or water body (such as a reservoir), at the site location. Pluvial flood mechanisms are those involved when flooding occurs due to local precipitation or snowmelt directly at the site, independent of hydrologic processes in nearby watersheds or water bodies. Pluvial flooding is often associated with urban locations with inadequate conveyance. Coastal flood mechanisms are meteorological, hydrodynamic, and hydrologic processes that cause an open or semi-enclosed water body (e.g., an ocean, bay, or lake) to flood adjacent land.

Flood severity metrics are used to measure the severity of a flood event at a site location. Flood severity metrics include (1) flood height or still water elevation, (2)

flood volume, (3) peak discharge, (4) flood event duration, (5) associated effects (e.g., wind waves, velocity effects, debris/sedimentation), and (6) other metrics that are study-specific (USNRC 2012). Combinations of flood mechanisms can increase flood severity metrics such as flood height (e.g., superposition of the water level contributions from multiple flooding mechanisms), lead to differing associated effects, and can change the flood timing and flood event duration (e.g., increase the period of inundation, decrease warning time, generate multiple flood pulses). In the sections that follow, we will use this terminology to offer consistency in reviewing and assessing approaches and methods reported in the current literature.

2.2.2 Multi-Mechanism Flood Hazard Framework

In this study, we are mainly interested in literature that addresses flooding due to combinations of flood mechanisms (i.e., multi-mechanism flooding). However, we also expand our scope to include literature related to combinations of flood-forcing phenomena and flood severity metrics so that we can identify and address a broader range of techniques and tools that may be useful in assessing MMFs. Overall, we observed that relevant current literature focuses primarily on assessment combinations of flood mechanisms and flood severity metrics, which are the most tangible characteristics of a flood event.

Figure 2-2 illustrates three broad categories of MMFs, which we will discuss in this paper. In **Figure 2-2**, random processes are represented by nodes (ovals), and the dependency between random variables is shown by links (arrows). Flood mechanisms are categorized into two main types: (1) combinations related to the coincident

occurrence of flooding mechanisms and (2) combinations related to the correlated occurrence of flood mechanisms.

Coincident flood mechanisms are independent in nature and result from independent flood-forcing phenomena (**Figure 2-2a**). An example is a seismically induced dam failure occurring with high reservoir water levels induced by rainfall-runoff. The severity of this flood could be characterized by one flood severity metric (e.g., flood elevation or peak discharge) or several flood severity metrics.

Correlated mechanisms are those caused directly or indirectly by the same flood-forcing phenomenon. These flood mechanisms are further divided into concurrent correlated flood mechanisms and induced correlated flood mechanisms. Concurrent correlated flood mechanisms (**Figure 2-2b**) are a combination of flood mechanisms, which are all caused by the same flood-forcing phenomena. An example of this case is flooding due to simultaneous occurrences of storm surge and precipitation in coastal areas caused by the same hurricane. Induced correlated mechanism refers to the case in which the flood-forcing phenomenon leads to one flood mechanism that, in turn, leads to another flood mechanism (**Figure 2-2c**). An example of induced correlated mechanisms is when storm rainfall causes riverine flooding that induces a dam failure, and flooding at a site is due to the combined effects of the rainfall-runoff and the dam failure flood wave.

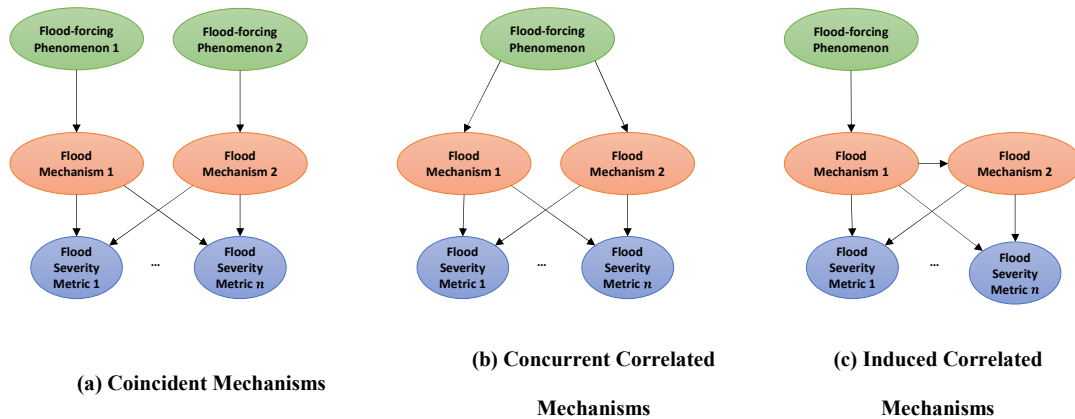


Figure 2-2. Categories of flood mechanism combinations

2.3 Summary of Approaches to Develop Joint Distribution

The three MMF combinations described above have implications for probabilistic flood assessment, based on assumptions that can be made regarding independence and dependence of the involved mechanisms. Estimating the joint probability of occurrence for coincident mechanisms is relatively straightforward, generally requiring only the multiplication of marginal probabilities of occurrence associated with the individual mechanisms. On the other hand, modeling of correlated mechanisms is complicated by the need to characterize the correlation between mechanisms. This correlation is caused by the common phenomenological origin or dependence, which is itself due to a function of spatiotemporal factors. Capturing the interactions between (coincident or correlated) flood mechanisms to estimate their contributions to one or more flood severity metrics is challenging, and analytical, empirical, or numerical models are often used to represent the physics of these interactions. Statistical and probabilistic (Bayesian) approaches to describe the dependence structure between processes shown

in **Figure 2-2** and develop requisite joint and conditional distributions, are discussed in the following sections.

2.3.1 Statistical Approaches

Statistical approaches for MMF JPA generally comprise four main steps: (1) preparation of paired or grouped data, (2) statistical analysis of marginal quantities, (3) multivariate analysis (using direct estimation of joint distributions or copula-based approaches), and (4) generation of a hazard curve related to one or more severity metrics.

Existing studies have used observed data as well as synthetic and reanalysis data generated using numerical or empirical process models. To support multivariate assessments, data are prepared as sets of grouped (e.g., paired simultaneous) values. The selection of grouped values is a notable decision point in the assessment. In conventional statistical extreme value analysis (EVA), block maxima (e.g., annual maxima) are often extracted from time-series data. When dealing with multiple data series, each related to one flood-forcing phenomenon, flood mechanism, or flood severity metric, it is possible (and often probable) that annual extreme values of each data series will not coincide, so modeling decisions are necessary to define data groups (pairs). Strategies used in EVA include (1) extraction and grouping of annual maxima values (regardless of the time of occurrence) (Bermúdez et al. 2021; Eilander et al. 2020; Gilja et al. 2018a; Jalili Pirani and Najafi 2020; Saharia et al. 2021; Wang et al. 2009; Wang 2016a), (2) extraction of annual maxima of one quantity, and the temporally concurrent extraction of other quantities (Lian et al. 2012; Masina et al.

2015; Tu et al. 2018; Xu et al. 2014), (3) extraction of annual maxima of one quantity and the extraction of the peak value of other quantities within some time window (Moftakhari et al. 2017; Nasr et al. 2021; Wahl et al. 2015a), and (4) clustering approaches (Bevacqua et al. 2020a; Eilander et al. 2020; Pappadà et al. 2018; Santos et al. 2020; Zscheischler et al. 2020).

Following the preparation of input data, it is generally necessary to first understand the marginal distributions of involved variables $\mathbf{X} = \{X_1, \dots, X_n\}$; i.e., $f_{X_1}(x_1), \dots, f_{X_n}(x_n)$, where $f_{X_1}(x_1), \dots, f_{X_n}(x_n)$ are the probability density functions for continuous random variables $\mathbf{X} = \{X_1, \dots, X_n\}$. This process involves the selection of candidate distributions, parameter estimation, goodness of fit assessment, and selection of (one or more) best fit distributions. In PFHA, this step often uses EVA for one or more of the involved random variables. After defining marginal distributions, joint distributions $f_{\mathbf{X}}(x_1, \dots, x_n)$ for the vector \mathbf{X} are constructed. Two of the most common statistical approaches to develop joint distributions used in current literature are the direct estimation of joint distributions and copula-based approaches.

2.3.1.1 Direct Estimation of Joint Distributions (Multivariate Parametric Distributions)

Direct estimation of joint distributions is conceptually similar to that used for univariate analysis. It starts by selecting candidate distributions and then uses a sample of paired data for parameter estimation. Bivariate normal or gamma distributions are examples of parametric joint distributions used in the PFHA-related literature (e.g., Hawkes et al. 2002; Wadey et al. 2015; Yue 2001). Different parameter estimation techniques can

be used to estimate the distribution parameters (e.g., method of moments, maximum likelihood estimation, L-moments, or Bayesian parameters estimation). To select the best model(s), goodness of fit between data and fitted distributions are evaluated using different methods, including graphical assessments, formal hypothesis tests, measures of divergence, and information criteria. However, the goodness of fit techniques may have limited value in assessing the distribution fit for extremal analysis, which is relevant here because PFHA is often interested in extreme values and distribution tails. There are also limiting assumptions inherent in the direct estimation approach. In particular, parametric joint distributions impose requirements on the functional form of the marginal distributions (e.g., a multivariate normal distribution necessitates that the marginal distributions of involved random variables are likewise normal).

2.3.1.2 Copula Method

Copula-based approaches for the development of joint distributions are widely used because they relax the limiting assumption of similarity between marginal and joint distributions. A copula has the flexibility of being applicable when variables are associated with different marginal distributions. To implement a copula-based approach, a functional form is assumed for the copula and marginal distributions. Estimation of marginal distributions follows the same process described above. The estimation of the copula begins with the selection of candidate copulas, based on physical considerations or other quantitative considerations (e.g., availability of explicit solutions). Parameters of the copula function are then estimated, typically using measures of correlation between variables. The fit of the copula-generated joint

distribution to the data is then assessed. Additional information regarding copulas can be found in multiple references (e.g., Balakrishnan and Lai 2009; Genest and Favre 2007; Haugh 2016; Nelsen 2002).

Given the flexibility offered by copulas and the variety of functional forms defined, this method is commonly used for constructing the joint distribution of variables in the PFHA-related literature (Bender et al. 2016a; Bevacqua et al. 2020b; De Michele et al. 2007; Ghanbari et al. 2021; Gilja et al. 2018a; Jane et al. 2020; Jang and Chang 2022; Kao and Chang 2012a; Lian et al. 2012; Lu et al. 2022; Lucey and Gallien 2021; Masina et al. 2015; Moftakhari et al. 2017; Saharia et al. 2021; Santos et al. 2020, 2021; Wahl et al. 2015a; Zhong et al. 2013, 2021). Studies using copulas have been conducted throughout the world, including Italy (Bevacqua et al. 2017; Masina et al. 2015), the Netherlands (Zhong et al. 2013), China (Lian et al. 2012), and the U.S. (Moftakhari et al. 2017; Wang et al. 2009). Studies conducted in the United Kingdom (Hawkes et al. 2002; Hawkes 2008; Wadey et al. 2015) have focused more frequently on the use of direct estimation methods.

While the copula approach offers flexibility in the variety of copula functions for capturing dependency structures between variables, the question that arises is: which copula is the best choice for the analysis? This is still an ongoing research question, and literature lacks a general process for understanding and selecting which copula is a better choice in each case study. There are some measures for the goodness of fit, but these measures are for comparison between different copulas, regardless of the basis for the initial selection of candidate copulas. Most research appears to select a functional form of copula on ease of construction, the prevalence in previous studies,

or having the capability of capturing a wide range of dependencies. Most of these studies did not focus on identification of the best fit copula, but rather on discussing a procedure under the assumption that the best (or an acceptable) copula has been selected (Bender et al. 2016; De Michele et al. 2007; Gilja et al. 2018; Kao and Chang 2012; Lian et al. 2012; Masina et al. 2015; Moftakhari et al. 2017; Wahl et al. 2015; Zhong et al. 2013).

In many PFHA-related studies, the estimation of the joint distribution represents the primary objective of the work while other studies seek to use the joint distributions to develop hazard curves. A conventional hazard curve includes one axis that represents the flood severity metric (e.g., flood height) while the other axis represents the annual probability (or frequency) of exceedance of the specified level of the flood severity metric. In univariate PFHA, this typically involves the statistical analysis of gauge data to estimate the distribution of a random variable representing the annual maxima of flood severity; i.e., $P(Z > z) = 1 - F_Z(z)$, where $F_Z(z)$ is the cumulative distribution function (CDF) of annual maximum Z . In multivariate analysis, the severity parameter Z is often estimated as a function of the random variables, \mathbf{X} , for which the joint distribution was developed; i.e., $Z = g(\mathbf{X})$. The exceedance probability of Z can then be defined as $P(Z > z) = \int P(g(\mathbf{X}) > z | \mathbf{x}) f_{\mathbf{X}}(\mathbf{x}) d\mathbf{x}$, with the integral computed using direct integration or simulation. Alternatively, in the case of multivariate analysis, the involved random variables \mathbf{X} may directly represent flood severity parameters, in which the joint exceedance probability is defined over all random variables; i.e., $P(\cap_i \{X_i > x_i\})$. Other exceedance quantities of relevance may focus on other logical

combinations such as the probability that *any* severity measure is in the exceedance state; i.e., $P(\cup_i\{X_i > x_i\})$.

2.3.2 Bayesian Approaches

In the methods described above, the goal was the estimation of joint distributions that can be used for estimating the marginal distribution of a flood severity metric or joint (or similar) exceedance probabilities. In Bayesian-motivated approaches, instead of directly estimating joint distributions using empirical data, conditional distributions for variables are used to build up the joint distributions, typically leveraging the knowledge of physical processes.

Figure 2-3 presents a high-level summary of the process involved in implementing a Bayesian-motivated approach, adapted to the case of MMFs and using the lexicon introduced earlier in the chapter.

To illustrate this concept, consider a simple case of one flood-forcing phenomenon characterized by the vector of parameters (random variables) \mathbf{X} , two flood mechanisms defined by the random variables Y_1 and Y_2 and a single flood severity metric Z driven by both mechanisms, as to reflect in the graphical model shown in **Figure 2-4**.

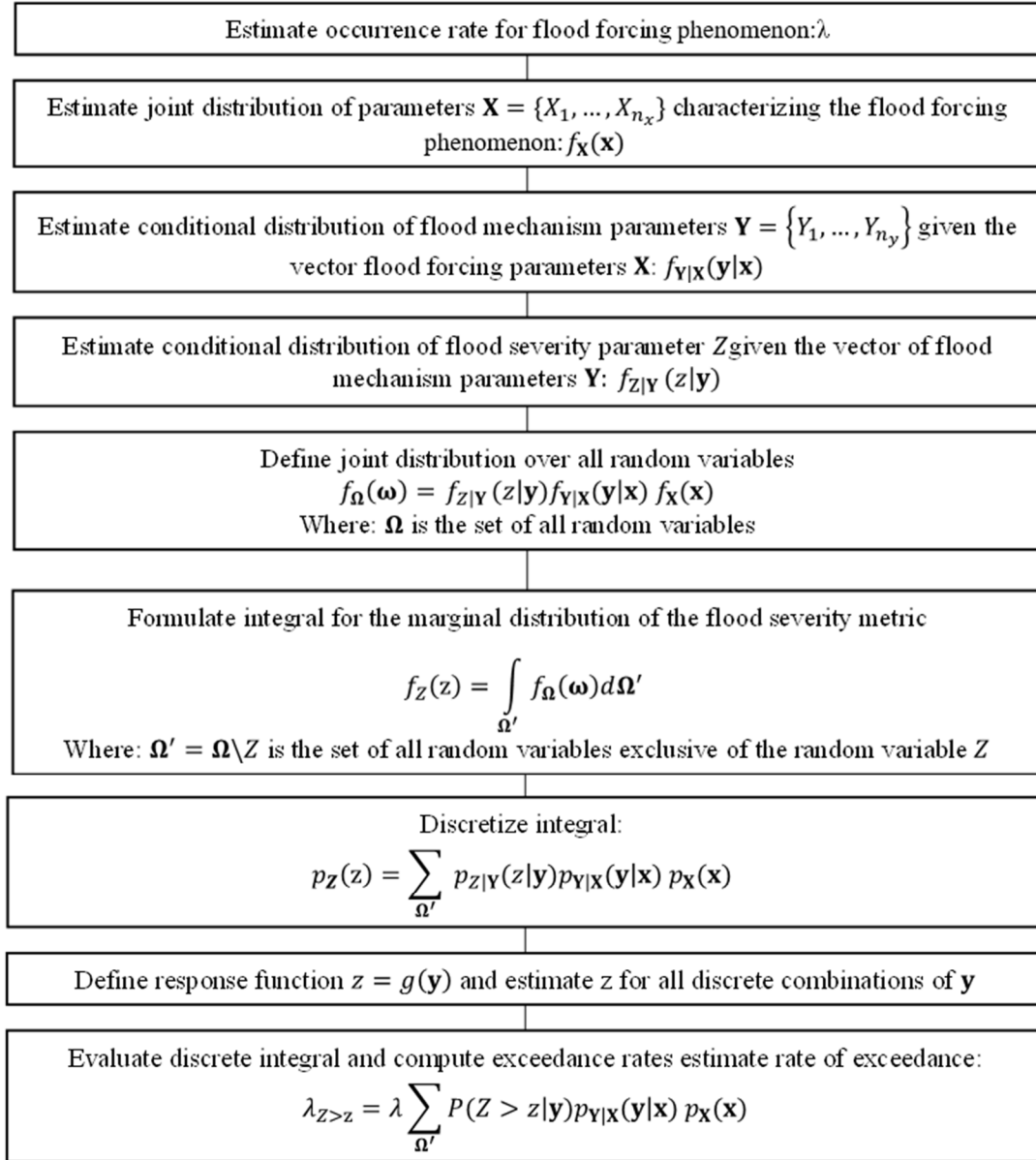


Figure 2-3: Illustration of key steps in the implementation of Bayesian-motivated approaches

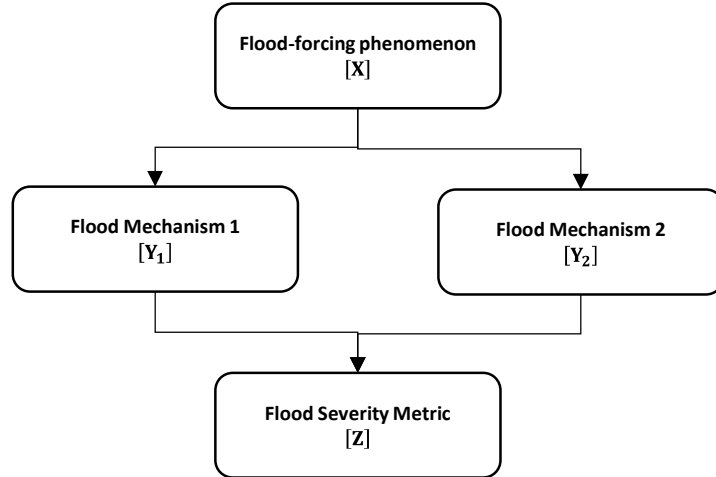


Figure 2-4: Example Bayesian graphical model used for generation of numerical expressions

The hazard can be estimated as:

$$\lambda_{Z>z} = \lambda \int_{\Omega'} \int_{Z^*>z} f_Z(z|y_1, y_2) f_{Y_1}(y_1|\mathbf{x}) f_{Y_2}(y_2|\mathbf{x}) f_{\mathbf{X}}(\mathbf{x}) d\Omega \quad (2-1)$$

where: λ is the annual occurrence rate of flood forcing phenomenon (X) and $\lambda_{Z>z}$ is the annual rate of exceedance of flood severity z (which can be converted to a probability through the use of a random process model; e.g., Poisson process); λ is the occurrence rate of the flood-forcing phenomenon; $f_Z(z|y_1, y_2)$ is the conditional probability density function of severity metric Z given the values of flood mechanism parameters y_1 and y_2 , $f_{Y_1}(y_1|\mathbf{x})$ and $f_{Y_2}(y_2|\mathbf{x})$ are the conditional probability density functions of random variables associated with flood mechanisms Y_1 and Y_2 ; and $f_{\mathbf{X}}(\mathbf{x})$ is the joint probability density function over the vector of random variables \mathbf{X} characterizing the flood-forcing phenomena; and $\Omega' = \Omega \setminus Z$ is the set of all random variables (Ω) exclusive of the vector of random variable Z .

The expression shown in (2-1) is typically computed in discrete form as:

$$\lambda_{Z>z} = \lambda \sum_{\Omega'} P(Z > z|y_1, y_2) p_{Y_1}(y_1|\mathbf{x}) p_{Y_2}(y_2|\mathbf{x}) p_{\mathbf{X}}(\mathbf{x}) \quad (2-2)$$

In the above expression, the probability density functions $f(\blacksquare)$ are replaced with the discretized probability mass functions $p(\blacksquare)$ and $P(Z > z|y_1, y_2)$ is the conditional probability of exceedance of severity metric level z given the values of flood mechanism parameters y_1 and y_2 . The expressions in (2-1) and (2-2) are for the problem formulation described above; expressions can be derived using alternate model forms (e.g., see the technical report by Bensi et al. 2020).

Bayesian-motivated approaches are commonly used for estimation of seismic hazards (Baker 2008) and hazards from storm surge (single-mechanism flood), in which joint distribution of hurricane parameters is generated using the Joint Probability Method (JPM) (Toro 2008). In some cases Bayesian approaches are used in conjunction with a copula to capture the dependency of variables (Couasnon et al. 2018; Fan et al. 2021b; a; Liu et al. 2021; Luo et al. 2019; Naseri and Hummel 2022; Sarhadi et al. 2016; Sebastian et al. 2017).

2.4 Summary of Available Literature

A summary of MMF-related studies, separated by flood type, is presented in **Tables 1 to 4** in the Appendix. Where applicable, these tables draw on the lexicon/framework introduced above to provide reference information related to:

- Flood-forcing phenomena, flood mechanisms (and the associated pluvial, fluvial, and coastal types), and flood severity metrics considered in each study
- Case studies or geographic regions addressed by each study

- JPA approach (e.g., direct estimation of joint distributions, copula, Bayesian approach) used, when applicable
- Data sources and numerical models/software used

Given that distilling divergent research activities into a tabular summary format is somewhat challenging, **Table 1 to 4** do not include all details and challenges associated with each study.

The summary of literature provided in this section concentrates on JPA studies involving random variables associated with each of the terms related to the MMF lexicon introduced previously. Moreover, some building block studies that do not directly focus on probabilistic assessments but provide insights and information that are useful for probabilistic assessment of MMFs are also described in this summary section because they can provide information that supports the JPA of MMFs.

2.4.1 Study Scopes

The technical literature related to MMF hazard assessment is wide-ranging in application and scope. However, a review of the current literature revealed that concurrent flood mechanisms, and particularly concurrent correlated mechanisms, are the main subject addressed in the literature. Coincident flood mechanisms are rarely discussed in technical literature since the assumption of independence between involved variables makes the joint probabilistic assessment of these floods (relatively) trivial. Coastal flooding hazards were studied most frequently in available literature while other types of mechanisms received relatively less attention.

In the context of coastal flooding hazards, a significant portion of the literature focused on hazards induced by storm-related flood-forcing phenomena (e.g., tropical cyclones, extratropical storms). This includes several studies seeking to understand the dependence of coastal water levels combined with precipitation and/or river flow (Archetti et al. 2011; Bass and Bedient 2018; Bevacqua et al. 2017; Chen and Liu 2014; van den Hurk et al. 2015; Kew et al. 2013; Moftakhari et al. 2017; Orton et al. 2016, 2018; Serafin et al. 2019; Svensson and Jones 2002, 2004; Wahl et al. 2015; Zheng et al. 2013, 2014; Zhong et al. 2013). A smaller portion of the literature related to storm-induced coastal flooding analyzed the joint probability of surge, waves, and water levels (Hawkes et al. 2002; Masina et al. 2015; Wadey et al. 2015).

In addition to studies that focused on elements of the probabilistic assessment of MMFs, several studies have focused on the development of models for aggregating and capturing the interactions of multiple mechanisms. For example, several studies have developed models for predicting hurricane-induced precipitation (Langousis and Veneziano 2009; Lin et al. 2010; Lonfat et al. 2007; Tuleya et al. 2007). Other studies focused specifically on process-based models and simulating the physical interactions between flood mechanisms using coupled or integrated modeling tools. Chen and Liu (2014) conducted deterministic modeling of storm surge and river flow. Bunya et al. (2010) developed and validated a coupled model of river flows, tide, wind, wind wave, and storm surge for Southern Louisiana and Mississippi.

Beyond work involving storm-induced coastal hazards, the interaction between tsunami and tide has been analyzed in some studies (Kowalik and Proshutinsky 2010;

Zhang et al. 2011). These studies were generally motivated by modeling efforts and did not conduct a probabilistic assessment of flood hazard due to tide and tsunami.

Multiple researchers conducted studies to analyze the effects of sea level rise (SLR) combined with other flood mechanisms in coastal areas. Tebaldi et al. (2012) investigated the effects of SLR on water levels caused by storm surge along U.S. coastal areas, using extreme value theory. Vitousek et al. (2017) conducted a global-scale study to analyze the effects of SLR combined with other flood mechanisms, including tides, waves, and storm surges.

Inland MMFs have received less attention in the literature than coastal-related MMFs. Several of these inland studies have focused on JPA related to combined river discharges at river confluences (e.g., Bender et al. (2016); Gilja et al. (2018); Kao and Chang (2012); Wang et al. (2009)). Several studies performed JPAs of multiple flood severity metrics associated with fluvial flooding, including flood peak, volume, and duration (Yue 2001; Yue et al. 1999; Zhang and Singh 2006). A limited set of studies assessed rain-on-snow events. Sui and Koehler (2001) considered rain-on-snow associated with a combination of flood mechanisms, and (Berghuijs et al. 2019) addressed the relative importance of extreme precipitation and snowmelt concurrent with soil moisture excess in causing severe floods in Europe. No studies were identified to address MMFs within the context of dam failures or ice effects.

2.4.2 Data Sources

The data used in each study is noted in column 6 of Tables 1 to 4. Both observed and synthetic data are reported; though observed data for the tide, rainfall, or streamflow

gauges were most common. Daily data were used most frequently (Bender et al. 2016; Gilja et al. 2018; Svensson and Jones 2002, 2004), while a limited number of the studies used hourly data (Nasr et al. 2021; Serafin et al. 2019a; Wang et al. 2009). Data record lengths used varied from 10 years or less (e.g., Masina et al. 2015, Hawkes et al. 2002) to over 30 years (e.g., Svensson and Jones (2002, 2004); Wahl et al. (2015)). Synthetic data generation techniques such as Monte Carlo were used to supplement observed data in some studies (Hawkes et al. 2002; Wang 2016; Zhong et al. 2013). Some studies leveraged output data from numerical models, such as the Weather and Research Forecasting [WRF] model (Lu et al. 2018).

2.4.3 Study Scale and Regions

Studies reviewed addressed MMFs at local, national (regional), and global scales. For example, Hawkes et al. (2002), Lian et al. (2012), Masina et al. (2015), Moftakhari et al. (2017), Svensson and Jones (2002), Wadey et al. (2015), and Zheng et al. (2014) conducted local-scale studies. Wahl et al. (2015) conducted a national-scale study for the contiguous U.S. and van den Hurk et al. (2015) analyzed surge and precipitation hazards at the national-scale for the Netherlands. Vitousek et al. (2017) conducted a global-scale study involving the effects of SLR in combination with other flooding mechanisms (i.e., tides, waves, and storm surge). Studies were located most frequently in the United Kingdom or U.S. (Bass and Bedient 2018; Hawkes 2008; Hawkes et al. 2002; Kao and Chang 2012; Moftakhari et al. 2017; Tebaldi et al. 2012; Wadey et al. 2015; Wahl et al. 2015b; Wang et al. 2009).

2.4.4 Methods Applied

In the context of the methods applied for developing joint distributions, as shown in Tables 1 to 4, the copula approach is the most frequently used. This is likely due to the relatively limited computational demands required to perform the assessments and flexibility of application. The next most commonly used method applied for the construction of joint distributions is the direct estimation of parametric joint distributions, and in particular, bivariate normal distribution (Hawkes et al. 2002; Wadey et al. 2015). Unique challenges associated with copula and direct estimation approaches are described in Section 2.5. As noted earlier, Bayesian-motivated approaches, however, were rarely used for the analysis of MMFs.

2.5 *Discussion: Assessment of Current Literature*

The analysis of literature discussed in this paper indicates that MMF analysis is an ongoing research topic with the potential to assist risk-informed decision-making. However, this research area is not mature, and challenges remain. We outline insights related to the review of literature below.

2.5.1 Length of Record and Characteristics of Available Data Series

Assessment of risks to critical infrastructure facilities from flooding requires estimation of hazards associated with long return periods. The utility of statistical models used for PFHA relies on the availability of time-series data with sufficient length. This challenge applies to diverse data types, ranging from gauge records to satellite and down-scaled data. While data availability is a challenge for single-mechanism PFHAs, the challenge is exacerbated for MMF PFHAs. This increased challenge arises due to the need for

multiple data series with coverage over the same time period. As a result, some studies are constructed based on short data records (Masina et al. 2015). The temporal resolution of available data relative to the flood mechanism's characteristic time scale can also be problematic. Daily data was used most frequently in reviewed studies, while few studies used data at sub-daily scales. For example, Wahl et al. (2015) used mean daily precipitation data, and Bender et al. (2016), Svensson and Jones (2002, 2004), and Zhong et al. (2013) used daily mean discharge time-series. However, the use of mean daily data can miss the peak values in relevant flood severity metrics and affect (e.g., bias) statistical results.

2.5.2 Site-specific Assessments

The majority of the studies reviewed used site-specific data. Therefore, unless there is sufficient homogeneity across involved processes, the geographic generalization of quantitative conclusions from available studies will not be possible. However, other insights from these studies, including the methods and approaches, could be informative to studies performed for other locations.

A key component of MMF JPA is analyzing dependence level and structure between involved parameters. This dependence is a function of different factors, including hydraulic, hydrologic, and meteorological factors (Hawkes 2008), as well as environmental factors such as topographic/bathymetric features, which change from one location to the next. As a result, MMF hazard analysis using observed data related to these factors will lead to site-specific results. However, among the studies reviewed, there were a few studies that focused on JPA or analyzing dependence between

variables at larger spatial scales. These studies focused on understanding how the level and pattern of dependence between variables changed in different locations. For example, Wahl et al. (2015) analyzed the temporal and spatial changes in dependence between storm surge and precipitation for the contiguous United States. Svensson and Jones (2002, 2004) investigated spatial changes in dependence between storm surge, precipitation, and river flow in southern, eastern, and western Britain.

2.5.3 Statistical Modeling Choices

Statistical modeling assumptions made when performing PFHA include identification, processing, and filtering of input data; selecting candidate distributions and parameter estimation methods. In general, there is a limited amount of guidance related to statistical modeling assumptions for assessments involving MMFs and longer return periods. However, for targeted univariate applications, guidance is available. For example, England Jr. et al. (2019) provide explicit federal guidelines for the treatment of data, distribution selection, and parameter estimation for flood frequency analysis (univariate) for riverine applications in the U.S. for return periods up to 500 years. The absence of guidance for these modeling decisions can contribute to an increased level of epistemic uncertainty, which arises due to a lack of knowledge or immature techniques used in the assessment of flood hazards. These uncertainties will continue to grow when assessments are extended from univariate to multivariate cases and extended to longer return periods.

As described earlier, two common statistical approaches to generate joint distributions are based on direct estimation of joint distributions and copulas. There are some

challenges with these two approaches. One of these challenges is the assumption of similar marginal distribution in the case of direct estimation of joint distributions (though some statistical transformation techniques may help address this limitation). In contrast, there is the flexibility offered by the copula approach, but a significant modeling decision is choice and justification of a functional form for the copula. There is a variety of copula functional forms for capturing different dependency structures between variables, but no general process or guidance exists for defining which copula is the most appropriate choice for each case study. One potential solution for addressing uncertainties described above could be sensitivity analysis along with approaches established to identify and address epistemic uncertainty. Bayesian approaches or logic trees are some examples of these approaches (Angelikopoulos et al. 2012; Annaka et al. 2007; Cheung et al. 2011; Flath et al. 2011; Huard and Mailhot 2008; Marzocchi et al. 2015; Oliver and Moser 2011; Yang et al. 2007).

2.5.4 Assumptions Regarding Occurrence and Concurrence of Extrema

Two common approaches for extremal analysis of marginal distributions in current literature are peak over threshold (POT) and block extrema (or annual maxima). In the POT method, values exceeding a selected threshold are extracted from the data time-series and used for extremal analysis to estimate the rate and magnitude of exceedance events. In annual maxima analysis, one maximum value for each year is selected for the extremal analysis. PFHAs employing univariate assessment often apply EVA using an annual maximum series. Some researchers have followed the same approach for multivariate assessment by simply extending this approach to more than one

dimension. This extension is conducted by fitting distributions to the annual maximum series of involved variables, under the assumption that the peak values related to these variables occur at the same time. However, this approach is potentially inaccurate because it is unlikely that the annual maximal value for one variable coincides with the occurrence of the annual maxima value for the other variable. Bender et al. (2016) noted that "it might even be that the simultaneous occurrence is physically impossible or at least very unlikely." Nevertheless, this approach is used for multivariate assessments. Gilja et al. (2018) used pairs of annual maximum discharge values in two different rivers. Wang (2016) and Wang et al. (2009) used annual peak discharge data related to upstream tributaries of the river confluence. In conceptually similar work, Svensson and Jones (2002, 2004) conducted extremal dependence analysis using an extremal dependence measure, which was defined as the probability of one variable's being extreme, conditioned on the other variable's being extreme.

Some researchers have used approaches that do not assume extreme values occur at the same time. In some of these studies, data pairs were generated with an extremal (e.g., annual maximal) value specified for one variable and a contemporaneous value of the other variable. Other studies considered the extreme value of one quantity at time t and the maximum value of the other within an interval $t \pm \Delta t$, in which Δt is usually as some relatively limited time window (e.g., one day). For instance, Masina et al. (2015) conducted a study in which peak sea level caused by surge/tides and contemporaneous value of significant wave heights were used to analyze the joint probability of waves and water levels. Moftakhari et al. (2017) used annual maximum fluvial flow and the corresponding maximum coastal water level measured within a time interval of one

day to analyze the compounding effects of SLR and fluvial flooding. In a different study by Wahl et al. (2015), the highest annual storm surge and the highest precipitation within ± 1 day, and also the highest annual precipitation and corresponding highest storm surge within a time interval of ± 1 day, were used to analyze the joint occurrence of storm surge and precipitation. Lian et al. (2012) considered maximum annual 24-hour precipitation and the highest tide contemporaneous with the annual maximum 24-hour precipitation for JPA of precipitation and tidal levels.

Kao and Chang (2012) conducted a fluvial flood study confirming that pairs of annual maximum data related to two river flows correspond to floods at different times during that year. In the study, pairs of data were generated using high flows (top 20% of flow pairs) rather than using peak annual values. Bender et al. (2016) proposed a multivariate design framework for river confluences where extreme values of involved variables (daily discharge values of upstream rivers) do not occur at the same time. The study was conducted for both simultaneous and non-simultaneous occurrence of extremal values related to the variables. For the non-simultaneous occurrence of extrema values, the maximum value of daily river discharge of the first river along with the contemporaneous daily river discharge of the second river was used to generate data pairs. The results were distinctively different when using data pairs related to the non-simultaneous occurrence of extremal values, compared to a more conservative method assuming simultaneous occurrence of extremal values.

In summary, the most common approaches to defining temporal combinations of random variables are:

- Combination of both extreme values related to involved variables

- Combination of extremal value related to one variable and simultaneous value for the other variable
- Combination of extremal value related to one variable and the highest value of the second variable within a time window

What all these three approaches have in common is that they all focus on analyzing at least one component at an extreme value, which is similar to conventional univariate PFHA. The first approach will generally lead to the most conservative hazard estimates but may include physically implausible mechanism combinations. The last two approaches refine the first approach by decreasing the dimensionality of extremal values to just one variable. However, while reducing conservatism, they then raise the (still unanswered) question of whether it is guaranteed that a different combination of flood mechanisms, none of which are in extreme levels, cannot cause a more severe flood compared to the cases that consider one extreme value.

A related challenge arises from the lack of a scientific process or robust criteria for choosing threshold value in extreme value analyses using POT (partial duration series) approaches. The choice of the threshold value is a significant modeling decision related to extremal analysis using partial duration data series. Usually, threshold values are determined based on expert judgment or expert-defined methods. For example, Tebaldi et al. (2012) conducted a POT analysis by selecting a threshold value related to the 99th percentile of data. This threshold was selected based on trial and error. Zhong et al. (2013) defined a fixed threshold value for the peak surge residual. Kjeldsen et al. (2010) defined a threshold value corresponding to 5% of the 2-year return period rainfall data.

The challenge regarding the choice of threshold value aggregates when dealing with multivariate assessments. For example, Hawkes (2008) explained that "sometimes, when dependence exists, it is more marked among the higher observed values (stormy conditions) than among the lower values." Based on this explanation, the choice of the threshold value can affect the degree of dependence between involved variables as well as the availability of data series (i.e., higher thresholds are associated with less data availability), adding the significance of this modeling decision.

2.5.5 Inconsistent Terminology

Current literature is fragmented and uses inconsistent terminology. These inconsistencies can cause challenges in identifying relevant literature and applying it to specific research (or practical) problems. Inconsistencies can also affect the development of mathematical details of approaches and the presentation of the results. One of the phrases frequently used in MMFs hazard assessment is the phrase "joint probability analysis" (or a closely related terminology variant). Specifically, diversity exists in the definition of the word "joint." Different interpretations of the "joint hazard" found in the literature are: (1) two variables of interest related to flood mechanisms or flood severity metrics are both exceeded (Boolean "and" scenario); (2) one of the hazard relevant variables is exceeded (Boolean "or" scenario); and (3) one variable is exceeded conditioned on the other variable equal to a specified value or exceeding a defined threshold (conditional scenario). The different interpretations described above can be extended for cases involving more than two random variables. Furthermore,

"joint occurrence" can also be defined as the temporally simultaneous occurrence of involved variables or occurrence within a time interval.

For example, some researchers used the phrase "joint probability analysis" to refer to extremal analysis in which both involved variables were at extremal values (Gilja et al. 2018; Svensson and Jones 2002, 2004; Wang 2016; Wang et al. 2009). Other researchers used this phrase to refer to the simultaneous occurrence of one variable conditioned on the other variable being at extremal value (Bender et al. 2016a; Lu et al. 2012; Masina et al. 2015). A third group of researchers conducted analysis on the extremal value of one variable and the highest value of the other variable within a defined time span (usually ± 1 day) (Wahl et al. 2015). To conduct a JPA, Moftakhari et al. (2017) used "or" scenario logic for the definition of hazard to assess socioeconomic consequences of compound events. Serafin et al. (2019) defined "joint hazard" as a result of a coincident event and emphasized simultaneous occurrence of the events instead of having both variables at extremal values; i.e., the defined "a combination of physical processes in which the individual variables may or may not be extreme; however, the result is an extreme event with a significant impact." Hawkes (2008) defined "joint exceedance" as "the probability that a specified value of one variable will be exceeded at the same time as a specified value of a second variable."

2.5.6 Lack of a Comprehensive Framework for Analyzing Dependence

A key challenge in MMF JPA is capturing and quantifying the dependence structure between variables. There is currently not a generalizable framework available for tackling this issue. Dependence between variables is a function of both the severity of

the parameters and spatiotemporal factors. For example, a higher threshold value (e.g., when performing statistical analysis of partial duration series) can contribute to a higher degree of dependency between variables, since higher observed values can be caused by similar event conditions (Hawkes 2008).

Geographic-dependent factors can affect the occurrence and dependence structure between flood mechanisms. This includes factors that change from one location to another location; e.g., flood-forcing phenomena such as hydraulic, hydrologic forces and atmospheric forces. Cyclic processes such as tides also change at different geographic locations. Geospatial/geophysical features, including topography or bathymetry also change at different locations. The study conducted by Wahl et al. (2015) analyzed spatial changes in dependence level between surge and precipitation for major U.S. cities. Svensson and Jones (2002, 2004) investigated spatiotemporal changes between river flow, precipitation and sea surge for the south, west, and east of Britain. These studies demonstrated how dependence between variables changed by location. Svensson and Jones (2004) demonstrated that catchment with higher slopes (topographic features) responded quickly to precipitation in form of increased river flow at the same day of high sea surge caused by a cyclone.

Temporal changes in dependency between variables can be divided into short-term and long-term factors. Short-term factors can occur at multiple time scales. Bender et al. (2016); Gilja et al. (2018); Moftakhari et al. (2017); Wang (2016) and Wang et al. (2009) used annual data to analyze dependency between variables. However, using an annual metric for analyzing the dependence between variables can potentially mask the seasonal dependency that exists between variables. Seasonal dependence is especially

important when conditions leading to the generation of flood events change by season. Hawkes (2008) considered short-term, midterm (seasonal), and long-term dependence between variables. Svensson and Jones (2002, 2004) conducted a seasonal analysis for dependence level between sea surge, river flow, and precipitation in the south and west Britain. In a study by Masina et al. (2015), which estimated the joint probability of waves and water levels, the dependence between variables was analyzed at a seasonal time scale. Serafin et al. (2019) considered the effects of seasonality on dependence and joint probability of river discharge and still water level at the shore line of open coast. Long-term changes in the dependence structure between variables are often due to climate change. Long-term changes in dependence between variables were investigated in the studies by Hawkes (2008) and Wahl et al. (2015) to assess MMFs' hazard.

2.6 Conclusion

MMFs are flood events caused by more than one flooding mechanism. Compared to single-mechanism floods, MMFs may be associated with more severe or differing consequences for communities and the built environment. As a result, a realistic probabilistic assessment of flood hazards to a site requires techniques and methods for estimating the hazard contributions from MMFs. Probabilistic assessments of hazards from MMFs are generally more complicated than assessments focusing on single-mechanism floods and introduce new challenges. These challenges arise predominately from the need to capture the dependence between involved variables and the physical interactions between involved flood mechanisms. There is relatively limited guidance

and experience to inform modeling assumptions associated with the probabilistic assessment of MMFs (e.g., for performing extremal analysis and development of the joint distributions). Further, the existing literature is disparate in the terminology used and quantitative techniques employed to assess MMFs.

This chapter introduced a framework that provides a conceptual structure and a lexicon for describing and discussing probabilistic assessments of MMFs. The study draws upon that framework to (1) describe approaches that have been used to probabilistically assess MMFs, (2) summarize the available literature, and (3) offer critical insights, which are summarized below.

The majority of existing MMF-related literature focuses on assessments of coastal flooding mechanisms. Among those studies, hazards from storm surge combined with river flow and precipitation are addressed most frequently. A smaller portion of the literature focuses on JPA of waves and water levels and SLR combined with other flood mechanisms, including tides and storm surge. Inland flooding has received relatively less attention, with available studies most frequently focusing on combinations of river flows at river confluences. Limited studies address hazard contributions from the rain-on-snow. A noticeable gap was observed in the availability of literature addressing dam failure caused by excessive precipitation-induced river flow combined with precipitation and river flooding.

The scope and objective of modeling efforts for MMFs documented in current literature can be partitioned into three broad categories. The first category includes studies that conducted a probabilistic assessment for MMFs and, in most cases, generated a hazard curve showing exceedance frequencies versus flood severity. The second category

includes studies that used numerical (and often computationally expensive) models to capture the interaction between involved flooding mechanisms, but not necessarily in a probabilistic manner. Instead, most of these studies defined and modeled limited deterministic scenarios. The third group of studies comprise building blocks that provide the modeling input and insights that support JPA of MMFs. These include studies modeling (hurricane) storm-induced precipitation as well as studies capturing the interaction between flood mechanisms (e.g., tides and tsunami) and modeling how this interaction affects inundation areas.

Extremal analysis is a key tool used in developing hazard curves or associated probabilistic modeling inputs. There was notable variability between studies in the modeling assumptions used for the extremal analysis of hazards from MMFs, particularly with regard to the strategies used to extract concurrent/simultaneous values related to two or more variables. Once paired (or grouped) data series are developed, joint distributions can be assessed. Modeling assumptions related to the construction of the joint distributions also vary across studies. A subset of studies directly estimate joint distributions by assuming quantities follow, for example, bivariate normal or gamma distributions. Copulas were the most popular modeling technique used in literature focusing on probabilistic assessment of MMFs. However, a notable lack of guidance was observed in the literature regarding the choice of the copula. A variety of copula functions are used in existing studies and, in most cases, there is often limited reasoning for why a particular functional form of the copula is selected. The choice is often made based on ease of use, range of dependencies for which the copula is applicable, and the frequency of use in other studies.

Several observations were noted related to the resolution and duration of data used in existing studies. Most frequently, average daily data were used. While the use of average daily data can lead to missed peak values and mask mechanistic interactions that happen at sub-daily time intervals, data at sub-daily temporal resolution was often not available to support these existing studies. In many cases, time-series used in existing studies were also relatively limited in duration, often spanning less than 30 years. The availability of sufficiently long time-series is a challenge even in a single-mechanism flood hazard assessment (particularly when assessing hazards associated with long return periods). However, this problem is exacerbated when analyzing MMFs due to the need for concurrent data related to more than one flood mechanism.

As noted above, impediments to the probabilistic assessment of MMFs arise due to the limited availability of (simultaneous) data for multiple flood mechanisms as well as the need to capture the interaction between involved flood mechanisms (which often requires computationally expensive models). More broadly, the fundamental challenge in the JPA of MMFs is capturing the dependence between involved variables. This is challenging because the dependence between variables is a function of spatiotemporal factors as well as the severity of hazards considered in the analysis. For example, dependence is a function of the geographic characteristics of the area under study and the flood-forcing phenomena that generated flood mechanisms. The majority of existing studies are site (or region) specific, which may limit the general applicability of research insights. Furthermore, the dependence between variables may evolve over time as a result of climate change or other factors and, a comprehensive framework for

capturing this non-stationary nature of the dependence between variables was not identified in the existing literature.

Overall, the current literature has taken steps in developing approaches for the analysis of MMFs, typically focusing on site-specific applications and hazards associated with short to moderate return periods. Existing approaches are relatively divergent in terminology, quantitative PFHA details, and model assumptions. Progress continues to be made, but a generalized and consistent quantitative framework for probabilistic assessment of MMFs, particularly for long return periods, is needed. Several research challenges currently stand as barriers to the development of such a framework. These include the need for: (1) strategies to capture both geospatial and temporal changes in the dependence between involved variables, (2) guidance to support decisions related to statistical modeling assumptions used in the MMF analysis, (3) a consistent terminology and quantitative convention, (4) strategies for data preparation as well as dealing with limitations in data type, duration, quality, and resolution, and (5) criteria for when it is suitable to generalize study methods and results.

Chapter 3: Bayesian Approach for Assessment of Hurricane-Induced Multi-Mechanism (Compound) Floods

3.1 *Introduction*

Floods are the leading cause of hazard-induced economic consequences and fatalities (Brody et al. 2008; Cigler 2017; Kick et al. 2011; Mileti 1999). Traditional probabilistic flood hazard assessment (PFHA) methods consider one flooding mechanism. This can lead to the underestimation of flood hazards when coastal areas are exposed to the simultaneous occurrence of multiple flooding mechanisms, such as waves, surges, tides, or precipitation-induced discharge. To generate realistic probabilistic estimates of flood hazards, it is necessary to consider more than one flooding mechanism in the PFHA.

There are statistical and numerical modeling considerations that make PFHAs of multi-mechanism floods (MMFs) challenging. Statistical challenges arise from the need to capture the dependence structure between involved variables and the development of joint distributions. In the current literature, two common approaches for developing the joint distributions are the copula method and direct estimation of parametric multivariate distributions (Bensi et al. 2020; Hawkes et al. 2002; Kao and Chang 2012). These statistical approaches focus on joint probability analysis of response variables related to multiple flood mechanisms such as water level, river discharge, and wave height. However, these approaches are not without challenges. One of the challenges

associated with these statistical methods is the availability of sufficiently long data records of the response variables. While this challenge exists for all statistical analyses, the issue is exacerbated for MMFs due to the need for overlapping periods of record for multiple mechanisms.

Numerical/analytical modeling challenges associated with PFHA of MMFs arise from the complexity of capturing the physical interactions between multiple flood mechanisms, which may require computationally expensive and coupled models. Several modeling studies exist in the current literature for predicting storm-induced surge using storm parameters (e.g., central pressure deficit, the storm's forward velocity, heading direction, and radius to the maximum wind). These studies use numerical surge models such as the ADvanced CIRCulation (ADCIRC) model (Luettich et al. 1992; Park and Youn 2021; Shashank et al. 2021; Wang et al. 2021b; Westerink et al. 1994; Yang et al. 2021) and the Sea, Lake and Overland Surges from Hurricane model (SLOSH) developed by National Weather Service (Helderop and Grubestic 2019; Jelesnianski 1992; Mayo and Lin 2019; Turan et al. 2018). Increasingly, surrogate modeling techniques are also used to emulate sophisticated models such as ADCIRC model. Some examples of these predictive models include artificial neural network (Al Kajbaf and Bensi 2020; Bass and Bedient 2018b; Hsieh and Ratcliff 2013; Kim et al. 2015), support vector regression (Al Kajbaf and Bensi 2020; Rajasekaran et al. 2008; Sahana et al. 2020), and Gaussian process regression (also known as Kriging models) (Al Kajbaf and Bensi 2020; Jia and Taflanidis 2013; Kyprioti et al. 2021a; b).

Existing storm surge studies focus primarily on (1) validating models to accurately model surge elevations and (2) calculating probabilistic hazards associated with storm surge. In recognition of the potential for compound hazards, these studies may also include simplified treatment of factors such as river discharge (e.g., via deterministic, steady-state inflows at boundaries of surge models (Cialone et al. 2015)). However, the prediction of river discharge due to the simultaneous occurrence of the storm-induced surge and precipitation, tides, and river antecedent flow is more complicated and not addressed well in the current literature. There are no established (numerical/analytical/statistical) models for predicting storm-induced river discharge using the above mentioned storm parameters as predictors. However, some solutions could be identified by combining surrogate, analytical, and numerical models such as HEC-RAS (<https://www.hec.usace.army.mil/software/hec-ras/>) as a river hydrodynamic model, HEC-HMS (<https://www.hec.usace.army.mil/software/hec-hms/>) a watershed model, and ADCIRC (<https://adcirc.org/>) which is a coastal hydrodynamic model. While such approaches are computationally expensive due to the high complexity of processes being modeled, the growth in computational capabilities and the increasing use of machine-learning derived methods provide a foundation to model MMFs in support of robust PFHAs. For example, Bass and Bedient (2018) explored the use of surrogate modeling to emulate the loose coupling of multiple models to generate joint flood levels (i.e., water levels caused by joint effects of flood mechanisms) as a function of hurricane characteristics for a study region.

Recognizing the physical modeling capabilities that have or may become available in the near future, this paper introduces a novel Bayesian-motivated framework for

modeling river discharge from compound hazards. Specifically, this study leverages a Bayesian-motivated approach to probabilistically assess hazards from river discharge in the case of the simultaneous occurrence of the storm-induced surge, precipitation, tides, and river antecedent flow. In the Bayesian-motivated approach, instead of directly constructing joint distributions on response quantities, the joint distribution over all involved stochastic quantities is written as the product of conditional distributions using the chain rule of probability. These conditional distributions are developed using knowledge of physical processes involved in the analysis and are estimated using statistical, analytical, or numerical predictive models. While the data related to compound processes is sparse, Bayesian-motivated approaches provide a tool to incorporate physical process knowledge in the PFHA and provide more robust hazard estimates. Bayesian networks (BNs) are selected as calculation mechanism (i.e., the mechanism for calculating the joint distributions over involved random variables and quantifying hazard curves); however, the approach described herein remains valid more generally.

Section 3.2 presents the foundational BN proposed in this study and describes how it is used to generate a hazard curve for river discharge, accounting for compound flooding processes. To demonstrate the concept, we present the proposed model using a case study along the North Atlantic Coast, as described in Section 3.3. In Section 3.4, a series of predictive models are developed and combined to ultimately estimate river discharge hazards caused by storm occurrence in a coastal area. The predictive models are computationally efficient and enable the development of the conditional relationships necessary to quantify the hazard curve using the BN. While the models

have been individually assessed for reasonableness, the models primarily serve as placeholders to facilitate the presentation of the overall Bayesian-motivated framework, recognizing that modeling capabilities continue to evolve and improve. Section 3.5 presents the final representative hazard curve for the region (built using representative, placeholder models). Section 3.6 provides a high-level assessment of the results. Discussion of results and conclusions are presented in Section 3.7. The initial results of this study are also presented in a report by Mohammadi et al. (2021).²

3.2 *Bayesian Model*

3.2.1 Background on BNs

The joint distribution for a set of random variables $\mathbf{X} = \{X_1, \dots, X_n\}$ can be written as a product of conditional distributions using the chain rule of probability (Equation (3-1)):

$$f_{\mathbf{X}}(x_1, \dots, x_n) = f_{X_n|X_1, \dots, X_{n-1}}(x_n|x_1, \dots, x_{n-1})f_{X_{n-1}|X_1, \dots, X_{n-2}}(x_{n-1}|x_1, \dots, x_{n-2}) \dots f_{X_2|X_1}(x_2|x_1)f_{X_1}(x_1) \quad (3-1)$$

In the above equation, there is no predefined order for the variables; i.e., the variables can appear in any arbitrary order. However, strategic ordering lets us take advantage of local independence among variables to simplify the above expression and allows us to build up a complex joint distribution from a set of simpler, local conditional distributions. In this work, we use physical and causal relationships between variables

² This chapter is based on a case study documented in Oak Ridge National Laboratory technical report ORNL/TM-2021/2231, which was published as a deliverable to the US Nuclear Regulatory Commission. This manuscript has been submitted for peer review to the Journal of Waterway, Port, Coastal, and Ocean Engineering.

to develop a BN that we then use to define the joint distribution of involved variables using the chain rule, as illustrated below.

First, key terminology and concepts related to BNs are introduced. A range of references provides comprehensive information about BNs (Jensen 1996; Kjærulff and Madsen 2013) as well as their applications to natural hazard assessment (Bensi et al. 2013; Couasnon et al. 2018; Harris et al. 2021; de Kok 2021). BNs are directed acyclic graphs that represent the dependence and independence relationships among the involved random variables. BNs graphically consist of nodes (circles) representing random variables and directed links (arrows) representing the probabilistic dependence among random variables (typically reflecting causal relationships). BNs are conventionally described using family terminology. For example, suppose that “ $(X_1) \rightarrow (X_2)$ ” represents a BN with nodes X_1 and X_2 and a link from X_1 to X_2 . X_1 is referred to as the *parent* of node X_2 ; conversely X_2 is referred to as the *child* of X_1 . Because X_1 has no parents, it is called a root node and has a marginal probability distribution assigned to it. X_2 is assigned conditional probability distributions that changes based on the states of its parent X_1 .

Returning to the concept of the chain rule of probability and the strategic ordering of random variables, the discrete representation of the joint probability mass function, $p_{X_1, X_2, \dots, X_n}(x_1, x_2, \dots, x_n)$, of all nodes, X_1, X_2, \dots, X_n , in a BN is generally expressed as:

$$p_{X_1, X_2, \dots, X_n}(x_1, x_2, \dots, x_n) = \prod_{i=1}^n p_{X_i|pa(X_i)}(x_i|pa(x_i)) \quad (3-2)$$

Where: $p_{X_i|pa(X_i)}(x_i|pa(x_i))$ is the conditional probability mass function of the random variable X_i given its parents, which are denoted by $pa(X_i)$; and n is the number

of random variables in the BN. The conditional probability mass functions are often referred to as *conditional probability tables* (CPTs).

3.2.2 Proposed BN for Coastal MMF

In this study, the probabilistic analysis of flood hazards focuses on hurricane-induced riverine flooding (specifically discharge) caused by storm surge and local intense precipitation (rainfall-runoff). The foundational BN used in this study is presented in **Figure 3-1**. The grey boxes in the figure represent modeling components that will be discussed in later sections of this paper.

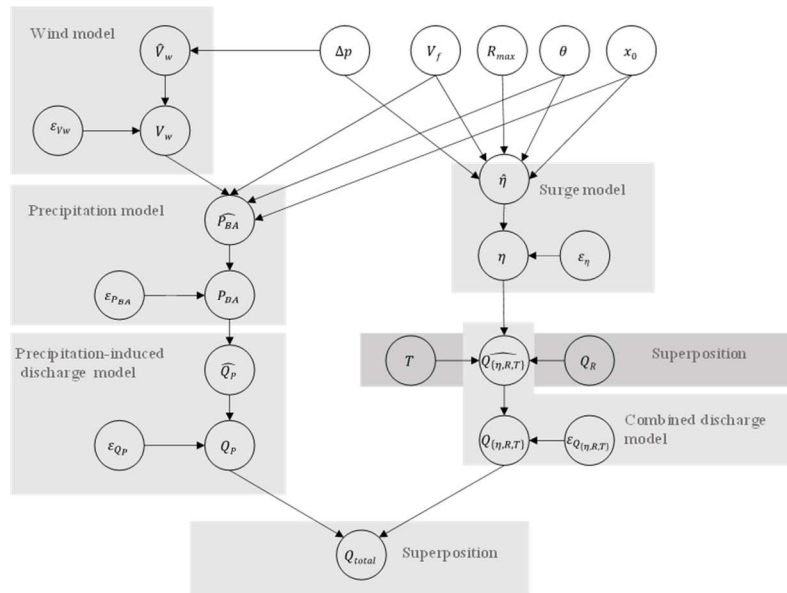


Figure 3-1. The foundational BN used in this study.

In **Figure 3-1**, the node labels in the BN correspond to the following quantities:

- Q_{total} : total discharge, accounting for hurricane-induced surge, precipitation-induced discharge, river antecedent flow, and tides (cms)
- Q_R : river antecedent flow (cms)
- Q_P : hurricane-induced precipitation discharge (cms)
- $Q_{\{\eta,R,T\}}$: discharge caused by surge, river antecedent flow, and tides (cms)
- T : elevation of the tides (m, mean sea level; MSL)

- P_{BA} : average basin precipitation (mm/day)
- η : surge elevation (m, MSL)
- Δp : storm's central pressure deficit (hPa), computed as the difference between a peripheral atmospheric pressure of 1,013 hPa and the storm's central pressure (hPa)
- V_f : storm's forward velocity (speed) (km/hr)
- R_{max} : storm's radius to the maximum wind (km)
- θ : storm's heading (direction) measured in degrees clockwise from North
- x_0 : storm's reference location (e.g., landfall location)
- V_w : wind velocity (km/hr)

The "hat" notation on certain nodes in the BN represents quantities that are predicted using a model. The “ ε quantities” refer to the errors associated with the predictive models with subscripts indicating the model to which they apply.

The root nodes in the BN in **Figure 3-1** represent the parameters used to characterize a hurricane: central pressure deficit (Δp), forward velocity (V_f), radius to the maximum wind (R_{max}), heading direction (θ), and landfall location (X_0). For the purposes of this study, these parameters are assumed to be independent (consistent with (Nadal-Carballo et al. 2015)), as indicated by their inclusion as root nodes in the BN. Estimated storm surge ($\hat{\eta}$) is defined as a function of these parameters, as represented in the BN by node $\hat{\eta}$ shown as a child of the nodes representing the storm parameters. Surge (η) is then equal to the superposition of the predicted value plus a model error (i.e., $\eta = \hat{\eta} + \varepsilon_\eta$), which is reflected by η having parent nodes $\hat{\eta}$ and ε_η . Similar superposition strategies to account for other model errors are used throughout the BN. Estimated hurricane-induced basin-average precipitation ($\widehat{P_{BA}}$) is defined as a function of maximum wind speed (V_w), forward velocity (V_f), heading direction (θ), and landfall location (X_0). $\widehat{V_w}$ is defined as a function of Δp . Precipitation-induced discharge ($\widehat{Q_p}$) is defined conditional on P_{BA} . Surge-, tide-, and river flow-induced

discharge, $(\widehat{Q_{\{\eta,R,T\}}})$ is defined as a function of storm surge (η), tidal elevation (T) and river antecedent flow (Q_R). Total river discharge (Q_{total}) is a function of surge-, tide-, and river antecedent flow-induced discharge ($Q_{\{\eta,R,T\}}$) and precipitation-induced discharge (Q_P).

Section 3.4 provides additional quantitative details related to the development of the marginal distributions of root nodes and the models that define the relationships between variables. Monte Carlo simulation is used to develop CPTs, as described in Section 3.4.2.7.

Using the BN in **Figure 3-1** as a guide and applying Equation (3-2), the summation for estimating the probability that total river discharge (Q_{total}) exceeds the value q is represented as:

$$\begin{aligned}
P(Q_{total} > q) = & \\
& \sum \dots \sum P(Q_{total} > q | Q_{\{\eta,R,T\}}, Q_P) p(Q_P | \hat{Q}_P, \varepsilon_{Q_P}) p(\varepsilon_{Q_P}) p(\hat{Q}_P | P_{BA}) \\
& p(P_{BA} | \hat{P}_{BA}, \varepsilon_{P_{BA}}) p(\varepsilon_{P_{BA}}) p(\hat{P}_{BA} | V_w, \theta, x_0, V_f) p(V_w | \widehat{V}_w, \varepsilon_{V_w}) p(\varepsilon_{V_w}) p(\widehat{V}_w | \Delta p) \\
& p(\Delta p) p(x_0) p(V_f) p(\theta) p(R_{max}) \left(Q_{\{\eta,R,T\}} | \widehat{Q}_{\{\eta,R,T\}}, \varepsilon_{Q_{\{\eta,R,T\}}} \right) p(\varepsilon_{Q_{\{\eta,R,T\}}}) \\
& p(\widehat{Q}_{\{\eta,R,T\}} | \eta, Q_R, T) p(Q_R) p(T) p(\eta | \hat{\eta}, \varepsilon_\eta) p(\varepsilon_\eta) p(\hat{\eta} | R_{max}, \theta, x_0, V_f, \Delta p)
\end{aligned} \tag{3-3}$$

3.3 Case Study Location and Data Sources

The case study considered in this paper is a site along the North Atlantic Coast located on the Delaware River near Trenton, New Jersey. The location of the case study and upstream watershed is shown in **Figure 3-2**. The main criteria for selecting the case study location were (1) tidal influence on the river, (2) the availability of the fifteen-

minute stage-discharge data and tidal data, and (3) availability of ADCIRC-simulated peak storm surge data for synthetic storms. These data were required to develop the representative predictive models that will be discussed in Section 3.4.2.

We are interested in estimating river discharge caused by compound effects of the surge, precipitation, tides, and river antecedent flow. Observed and synthetic data were used in this study to model these processes. Observed data sources include:

- Fifteen-minute river stage-discharge data related to the Delaware River in the study location were available for U.S. Geological Survey (USGS) gage 01463500 (https://waterdata.usgs.gov/nj/nwis/uv/?site_no=01463500&PARAMeter_cd=00065.00060).
- National Oceanic and Atmospheric Administration (NOAA) tide gage 8539993 (<https://tidesandcurrents.noaa.gov/stationhome.html?id=8539993>), which was selected as the closest tide gage to the study location.

The locations of both gages are shown in **Figure 3-2**. Synthetic data containing ADCIRC-estimated surge values as a function of hurricane parameters for a series of over 1,000 synthetic hurricane tracks were collected from the United States Army Corps of Engineers (USACE) Coastal Hazard System (CHS) (<https://chs.erdc.dren.mil/>). The USACE CHS is a national source of data and information related to coastal hazards, including numerical and probabilistic modeling results from regional studies. In this study, ADCIRC model results are collected for the *target study location* (i.e., the location that is the primary focus of this case study) at save point 5373, which is shown in **Figure 3-2**, along with additional geographic information that will be referenced throughout this paper.

The locations of the NOAA tide gage, USGS gage, and target study location (save point 5373) do not coincide, and some assumptions are made. The location of the USGS gage is located 1.5 km upstream of the target study location (save point 5373). While the target study location is affected by tides and surge, there are rock riffles (annotated in Figure 3-2) that prevent the tides and surge from propagating upwards from the study location to the USGS gage, unless the tidal/surge elevation is sufficiently high to overcome the rock riffles. The data available in this USGS gage is used to develop stage-discharge data and estimate river antecedent flow. It is assumed that the river characteristics that contribute to the development of stage-discharge curve and river antecedent flow data do not change noticeably and are similar in 1.5 kilometers distance between the USGS gage and the target study location. The NOAA tide gage is located 2.5 kilometers downstream of the target study location. Further discussions regarding the site selection can be found in Mohammadi et al. (2021).

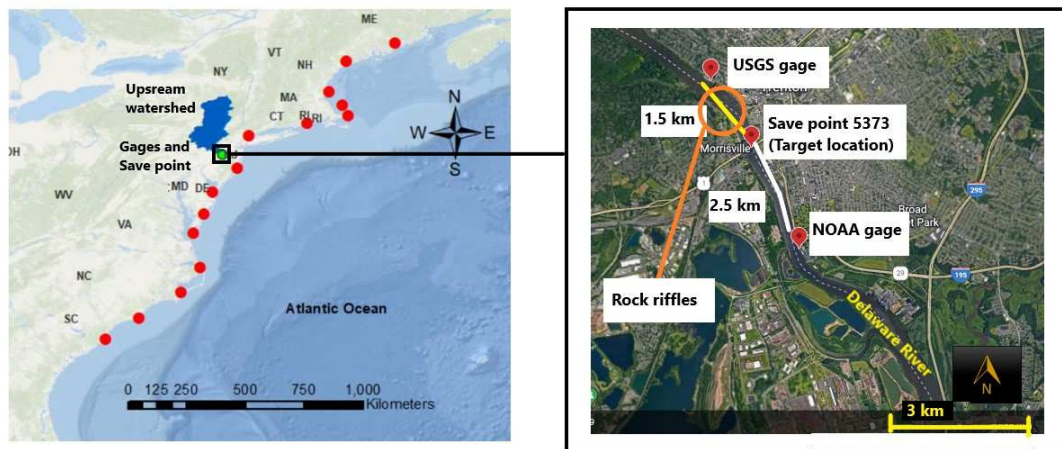


Figure 3-2. Left: The case study location with simulated landfall locations (red dots) and upstream watershed (blue dots); Right: The location of the USGS gage, NOAA tide gage, save point 5373, and the location of the rock riffles upstream of the save point 5373.

3.4 *Model Assumptions: Distributions and Predictive Models*

The subsections that follow describe the assumptions used to generate the marginal and conditional distributions required by the BN and perform the calculations needed to define the joint distributions and generate the hazard curve in accordance with Equation (3-3). As noted previously, these placeholder models are selected/developed to demonstrate the proposed framework and can be replaced with more sophisticated or application-specific models.

3.4.1 Storm Parameter Distributions

The development of probability distributions related to storm parameters typically requires the statistical assessment of historical storm data. This study uses the distributions developed by USACE as part of the North Atlantic Coast Comprehensive Study (NACCS) (Nadal-Caraballo et al. 2015). **Table 3-1** shows the NACCS-developed distributions that are leveraged in this study. Distributions and corresponding parameters in **Table 3-1** are for NACCS' region 2, where the area under study in the current analysis is located. In this study, 15 discrete points along the coast were considered as landfall locations (see **Figure 3-2**) and they were assumed to be equally likely (discrete uniform distribution).

3.4.2 Predictive Models Developed for Estimating Conditional Distributions

This study has developed five predictive models to generate conditional distributions for variables $\hat{\eta}$, \widehat{V}_w , \widehat{P}_{BA} , $\widehat{Q}_{\{\eta,R,T\}}$, and \widehat{Q}_P as a function of their parent nodes. The

following predictive models are shown in **Figure 3-1** (grey boxes) and will be discussed as the subsections that follow:

- **Surge model:** Surrogate model to predict surge height as a function of Δp , V_f , R_{max} , θ , and X_0 .
- **Wind model:** Statistical model to predict maximum wind velocity as a function of Δp .
- **Precipitation model:** Statistical and empirical model to predict hurricane-induced precipitation as a function of V_w , V_f , θ , and X_0 .
- **Precipitation-induced discharge model:** Statistical model to predict precipitation-induced discharge as a function of P_{BA} .
- **Surge-, tide-, river antecedent flow-induced discharge model (combined discharge model):** Statistical model to predict surge-induced river discharge as a function of η , T , and Q_R .

It is emphasized that these models are developed primarily to illustrate the proposed BN framework and can be replaced with more sophisticated models in future applications. Nonetheless, the models have been assessed for “reasonableness, as described in the following sections.

Table 3-1. Distributions and corresponding parameters for hurricane parameters (based on Nadal-Caraballo et al. (2015))

No.	Hurricane Parameter	Distribution	Functional form	Distribution Parameters
1	Δp	Doubly truncated Weibull distribution (DTWD)	$P[\Delta p > x]$ $= \frac{\exp\left[-\left(\frac{x}{U}\right)^k\right] - \exp\left[-\left(\frac{\Delta p_2}{U}\right)^k\right]}{\exp\left[-\left(\frac{\Delta p_1}{U}\right)^k\right] - \exp\left[-\left(\frac{\Delta p_2}{U}\right)^k\right]}$ $10 \leq x \leq 93$	$\Delta p_1 = 10 \text{ hpa}$ $\Delta p_2 = 93 \text{ hpa}$ $U = 35.77$ $k = 1.41$
2	R_{max}	Lognormal distribution	$f(x) = \frac{1}{x \zeta \sqrt{2\pi}} \exp\left[-\frac{1}{2} \left(\frac{\ln(x) - \lambda}{\zeta}\right)^2\right]$ $x > 0$	$\lambda = 4.215,$ $\zeta = 0.45$
3	V_f	Normal distribution	$f(x) = \frac{1}{\sigma \sqrt{2\pi}} \exp\left[-\frac{1}{2} \left(\frac{x - \mu}{\sigma}\right)^2\right]$ $x > 0$	$\mu = 44.05,$ $\sigma = 16.06$
4	θ	Normal distribution	$f(x) = \frac{1}{\sigma \sqrt{2\pi}} \exp\left[-\frac{1}{2} \left(\frac{x - \mu}{\sigma}\right)^2\right]$	$\mu = 16.48,$ $\sigma = 36.17$
5	x_0	Uniform distribution	n/a	n/a

3.4.2.1 Surge Model

Surge height is estimated as a function of predicted surge ($\hat{\eta}$) and the prediction error term (ε_η):

$$\eta = \hat{\eta} + \varepsilon_\eta \quad (3-4)$$

The function mentioned above is used to generate the conditional distribution $p(\eta|\hat{\eta}, \varepsilon_\eta)$ shown in Equation (3-3) and estimate the CPT related to the node η in **Figure 3-1**.

To generate the conditional distribution $p(\hat{\eta}|R_{max}, \theta, x_0, V_f, \Delta p)$ in Equation (3-3) and estimate the CPT associated with the node $\hat{\eta}$ in **Figure 3-1**, a simple surrogate model was developed. In this study, a simple, site-specific surrogate model was trained to

predict surge height ($\hat{\eta}$, MSL) as a deterministic function of representative synthetic hurricane track parameters and is represented as:

$$\hat{\eta} = g(\Delta p, V_f, \theta, R_{max}, x_0) \quad (3-5)$$

In this Equation, the quantities Δp , V_f , θ , R_{max} , and x_0 are defined in Section 3.2.2 ADCIRC modeling simulation results for peak surge for the target study location (save point 5373) were downloaded from the USACE CHS website (<https://chs.erdc.dren.mil/>). These simulation results provide peak surge height for over 1000 synthetic storm tracks and corresponding storm parameters. These simulations are available for several conditions. In this study, we used the base conditions with no consideration of tides or sea-level rise. The data was used to train and develop a location-specific Gaussian process regression model (e.g., as proposed in Al Kajbaf and Bensi 2020; Bass and Bedient 2018; Jia et al. 2016; Jia and Taflanidis 2013) for prediction of surge as a function of storm parameters.

While sophisticated modeling can be done for large regions using, for example, principal component analysis (Jia et al. 2016; Jia and Taflanidis 2013; Taflanidis et al. 2014), a target location-specific model was developed in this study. A holdout validation (random repeated subsampling) was performed using 50 holdout sets to assess the Gaussian process regression model's out-of-sample prediction abilities to estimate peak storm surge. Each holdout set consisted of a 70/30 split of randomly selected training and testing (holdout) data. 70% of the data was designated data used to fit the model in each holdout fold. The remaining 30% of the data was withheld for testing the fitted model against the data that was unseen. The (Pearson) correlation

coefficients for the out-of-sample data across all fifty holdout sets varied from approximately 0.96 to 0.99. The root mean square error (RMSE) varied between 0.14 m and 0.22 m across the fifty folds with a mean RMSE of 0.16 m. The mean RMSE was used in characterizing the distribution of the model error term used in the analysis. The overall bias (mean error) ranged between -0.02 and 0.02 m. However, an increased error was noted for high surge values (i.e., a tendency to underestimate surge height using the surrogate model for large surge values). After assessing model performance using the holdout validation approach, a surrogate model was trained using the complete data set. This surrogate model was then used to predict surge height and generate the CPT for node $\hat{\eta}$ in **Figure 3-1**.

The marginal distribution $p(\varepsilon_{\eta})$ in Equation (3-3) is generated by assuming ε_{η} as the sum of the surrogate model error ($\varepsilon_{\eta,S}$) and the error associated with the ADCIRC simulations ($\varepsilon_{\eta,A}$); i.e.:

$$\varepsilon_{\eta} = \varepsilon_{\eta,S} + \varepsilon_{\eta,A} \quad (3-6)$$

In which: $\varepsilon_{\eta,S}$ is normally distributed with a mean of zero and a standard deviation equal to the mean RMSE of the testing set for fifty holdout folds. $\varepsilon_{\eta,A}$ is assumed normally distributed with parameters as defined in the NACCS study (Nadal-Caraballo et al. 2015) ; i.e, mean of zero and standard deviation equal to 0.48 m.

3.4.2.2 Wind Velocity Model

The wind model was developed to define the conditional distribution $p(\widehat{V}_w | \Delta p)$ in Equation (3-3) and equivalently, the CPT assigned to the node V_w as a function of Δp

in **Figure 3-1**. Wind velocity (V_w) is defined as a function of a statistical model prediction (\widehat{V}_w) and a prediction error term (ε_{V_f}):

$$V_w = \widehat{V}_w + \varepsilon_{V_w} \quad (3-7)$$

The conditional distribution for \widehat{V}_w is generated using a statistical equation that relates V_w and Δp . In this case study, the statistical equation introduced in the NACCS report to predict V_w (km/hr) as a function of Δp (hPa) is used (Nadal-Caraballo et al. 2015):

$$\widehat{V}_w = 42.4807 - 0.0084\Delta p^2 + 2.9752\Delta p \quad (3-8)$$

The marginal distribution $p(\varepsilon_{V_w})$ in Equation (3-3) and equivalently, the marginal probability table for the node ε_{V_w} in **Figure 3-1**) is generated under the assumption that ε_{V_w} is normally distributed with a mean value equal to zero and standard deviation equal to 18.66 km/hr, consistent with the error for the wind velocity prediction equation (Equation (3-8)) documented in the NACCS study (Nadal-Caraballo et al. 2015).

3.4.2.3 Precipitation Model

Basin-wide average precipitation (P_{BA}) is defined as a function of a statistical model prediction (\widehat{P}_{BA}) and a prediction error term ($\varepsilon_{P_{BA}}$):

$$P_{BA} = \widehat{P}_{BA} + \varepsilon_{P_{BA}} \quad (3-9)$$

This function is used to generate the conditional probability distribution $p(P_{BA}|\widehat{P}_{BA}, \varepsilon_{P_{BA}})$ in Equation (3-3) and equivalently, to generate the CPT assigned to the node P_{BA} in **Figure 3-1**). A precipitation model is used to estimate precipitation in the upstream area shown as \widehat{P}_{BA} in **Figure 3-1**. This precipitation is a function of storm

parameters, including V_w , θ , x_0 , and V_f . This model, which generates the conditional distribution $p(\hat{P}_{BA}|V_w, \theta, x_0, V_f)$ (or equivalently, the CPT for the node \hat{P}_{BA} in **Figure 3-1**), is a statistical model that relates a regional rain field and hurricane parameters and is a multi-part model.

The precipitation model used herein is based on the Tropical Rainfall Rate (TRR) model suggested in the study by Tuleya et al. (2007). In the TRR model, the rainfall rate at a point location is a function of the storm's maximum wind speed and the distance from the storm center. The RMSE of the TRR model fitted to the Tropical Rainfall Measuring Mission rain rate is estimated by Tuleya et al. (2007) as 7.11 mm/day.

In the TRR model, the amount of precipitation at a point is a function of the distance between the point of interest and the storm center. Considering the extent of the upstream area and the storm movement, this distance changes with the time after landfall and the location of the point relative to the storm center. Therefore, the upstream area is divided into 1862 grid points on a $4km \times 4km$ resolution to cover these spatiotemporal factors affecting precipitation depth.

For each combination of storm parameters (as required to assess the hazard in accordance with Equation (3-3)), we determined the location of the storm center at each hour after landfall using θ , x_0 , and V_f . To incorporate the decay of wind velocity into the TRR model, a wind decay model suggested by Kaplan and DeMaria (1995; 2001) is used (Kaplan and DeMaria 1995; Kaplan and Demaria 2001).

The hourly precipitation is estimated for each grid point after determining the location of the storm center at each hour, estimating the distance between the storm center and

each grid point, and incorporating the wind decay. However, the TRR model mentioned above computes rainfall rate at a daily scale, whereas we have estimated hourly rainfall by dividing daily rainfall by 24.

A synthetic storm track (in red) and related rain field for the upstream watershed (colored surface) are shown in **Figure 3-3** to illustrate the implementation of the precipitation model used in this study. As shown in this figure, the rain field is estimated at discrete time steps (five of which are shown in the figure). **Figure 3-3** also shows the total daily upstream rainfall (map shown in the lower right of the figure). Daily total rainfall is estimated as the sum of the hourly rainfalls for each grid in the watershed. Next, total (average) daily upstream rainfall for the entire watershed is estimated as the average of the daily rainfalls taken over all grid points. The error term ($\epsilon_{P_{BA}}$) related to the precipitation model used (see Equation (3-9)) is assumed to be normally distributed with mean zero and standard deviation equal to the RMSE of the TRR model. Consideration of a more sophisticated approach to defining this error, accounting for error in precipitation and wind decay models, is identified as a potential area for future research.

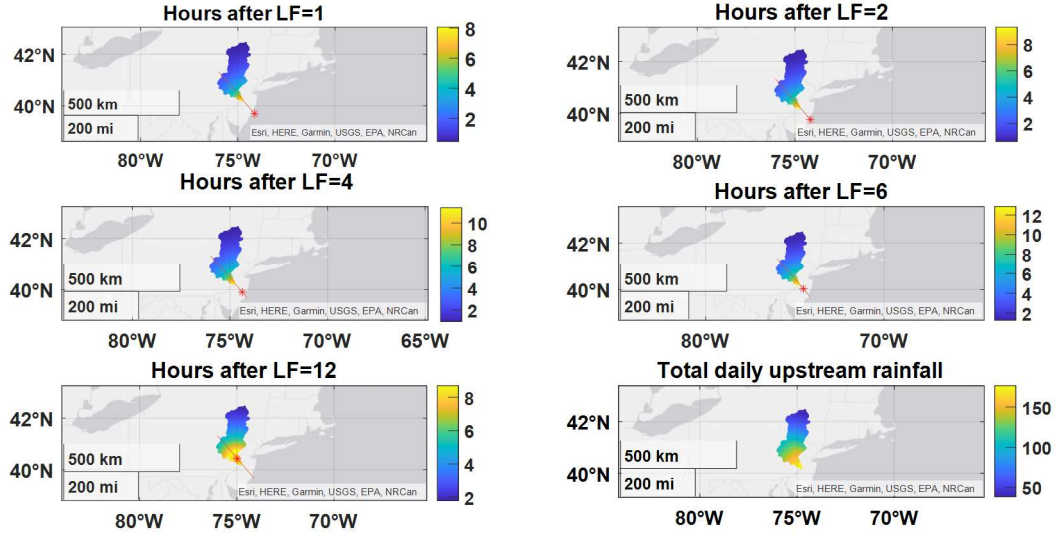


Figure 3-3. Hurricane-induced precipitation in the upstream area (mm/hr) for an example storm track at discrete time steps (represented as hours after storm landfall, LF) and total daily upstream rainfall (mm/day) (lower right map); the red star represents storm center at specific points after landfall; the color bar represents rainfall (mm/hr for hourly precipitation and mm/day for daily precipitation).

3.4.2.4 Precipitation-Induced Discharge Model

A precipitation-induced discharge model was developed to predict changes in river discharge caused by hurricane-induced precipitation. It is presented as:

$$Q_P = \hat{Q}_P + \varepsilon_{Q_P} \quad (3-10)$$

Where: \hat{Q}_P is the predicted change in river discharge (units of cms) caused by precipitation and ε_{Q_P} is a prediction error term. This function is used to generate the distribution $p(Q_P | \hat{Q}_P, \varepsilon_{Q_P})$ in Equation (3-3) (or equivalently, the CPT assigned to the node Q_P in **Figure 3-1**).

\hat{Q}_P is predicted as a function of the upstream basin-wide average precipitation (P_{BA}):

$$\hat{Q}_P = g(P_{BA}) \quad (3-11)$$

In this study, the predictive model represented in Equation (3-11) was developed by using observed daily basin average precipitation and simulated daily discharge by a

calibrated Variable Infiltration Capacity (VIC) model organized by (Naz et al. 2016; Oubeidillah et al. 2013) for the period of 1980 to 2015. **Figure 3-4** shows the time series of discharge (top left panel) and precipitation (bottom left panel) data for the noted period, as well as the filtered time series related to dates within hurricane season (orange). This hurricane-season filtered dataset is used to develop a regression model relating precipitation and discharge. **Figure 3-4** (Right) also shows the scatterplot of daily discharge and basin-wide average precipitation for all data and hurricane-season data.

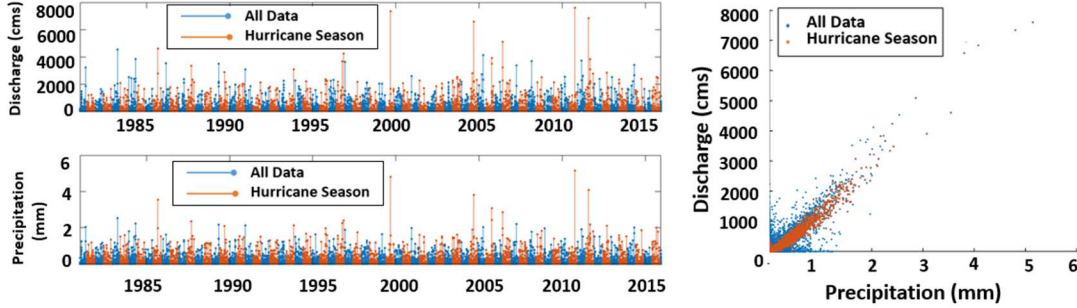


Figure 3-4. Left: Time series of precipitation-induced discharge (top) and basin-wide average daily precipitation (bottom); Right: Scatterplot of discharge and basin-wide average daily precipitation.

Based on the trend between discharge and precipitation in **Figure 3-4**, generalized linear models (GLM) and polynomial models were selected as candidate models for fitting the data. Among these models, the second-degree polynomial model showed the best overall performance and is presented as:

$$\hat{Q}_P = \alpha_1 + \alpha_2 P_{BA} + \alpha_3 P_{BA}^2 \quad (3-12)$$

Figure 3-5 shows the second-degree polynomial regression line. The R -squared and RMSE values related to the second-order model are 0.96 and 84.1 cms, respectively. To assess the RMSE (units of cms) and the correlation coefficient (R) between

predicted and observed discharge values, a holdout validation was performed using 50 holdout folds (random subsampling) considering a 70/30 split of randomly selected training and testing data. The correlation coefficients varied from approximately 0.97 to 0.98. The RMSE varied between approximately 65.1 cms and 87.8 cms across the fifty folds with a mean RMSE of 76.7 cms, which is used in characterizing the distribution of the model error term used in the analysis. The overall bias (mean error) is relatively small (ranging between approximately -4.6 and 5.6 cms).

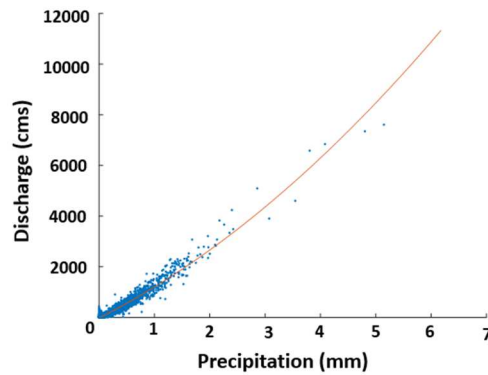


Figure 3-5. Scatterplot of discharge and basin-wide average daily precipitation (blue dots) superimposed with second-order polynomial regression line (red line).

3.4.2.5 Combined Discharge Model

The combined discharge model was developed to predict river discharge due to the simultaneous occurrence of storm surge, tides, and river antecedent flow. It takes the following form:

$$Q_{\{\eta,R,T\}} = \hat{Q}_{\{\eta,R,T\}} + \varepsilon_{Q_{\{\eta,R,T\}}} \quad (3-13)$$

where $\hat{Q}_{\{\eta,R,T\}}$ is the (equivalent) total discharge (units of cms) caused by surge, river antecedent flow, and tides. $\varepsilon_{Q_{\{\eta,R,T\}}}$ is a prediction error term. To estimate $\hat{Q}_{\{\eta,R,T\}}$, river antecedent flow was first converted to an equivalent depth, then it was superimposed

with the tide and surge water levels to estimate the total water level (h). In the next step, this total water level was converted back to river discharge to estimate the equivalent discharge caused by the surge, tide, and river antecedent flow. Thus, the predictive model takes the form:

$$\hat{Q}_{\{\eta,R,T\}} = g(\eta, T, Q_R) \quad (3-14)$$

Where: $g(\eta, T, Q_R)$ is a function that maps surge, river baseflow-equivalent depth, and tidal elevations, respectively, to an equivalent discharge. A stage-discharge relationship developed for a gage near the case study location was used to map the water level and the equivalent discharge value. In the area under study, the error caused by non-linear interaction between tides and storm surge is judged to be negligible (Nadal-Caraballo et al. 2015). Therefore, the simple superposition of tides and surges is judged to generate reasonable results. Equation (3-14) facilitates the specification of $p(\hat{Q}_{\{\eta,R,T\}}|\eta, Q_R, T)$ in Equation (3-3) and, equivalently, the definition of the CPT for node $\hat{Q}_{\{\eta,R,T\}}$ in **Figure 3-1**. Equation (3-13) is used to generate the conditional distribution of $p(Q_{\{\eta,R,T\}}|\hat{Q}_{\{\eta,R,T\}}, \varepsilon_{Q_{\{\eta,R,T\}}})$ in Equation (3-3) and equivalently, the definition of the CPT for node $Q_{\{\eta,R,T\}}$ in **Figure 3-1**. In this study, the interaction between river flow and storm surge is not addressed to reduce computational effort. However, this interaction can be captured using hydraulic models in future applications of the proposed framework.

Fifteen-minute stage-discharge data related to USGS gage 01463500 located on the Delaware River at Trenton was used for developing the stage-discharge relationship. The location of this gage is shown in **Figure 3-2**. These fifteen-minute stage-discharge

data were available for 14 years from 2007 to 2020. **Figure 3-6** shows the scatter plot relating stage and discharge (left) and the time series of stage and discharge (right).

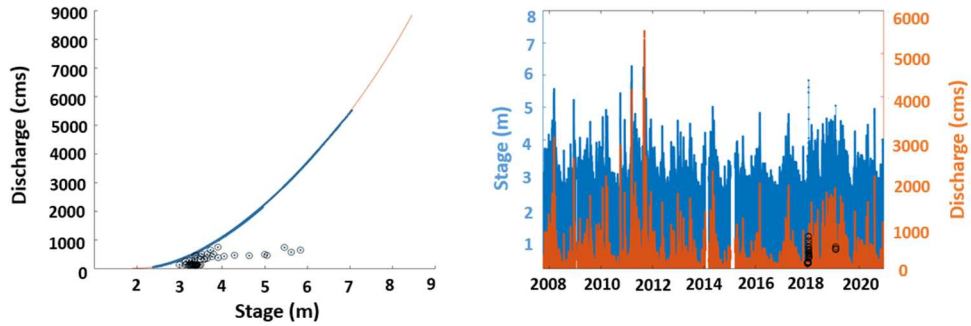


Figure 3-6. Left: Scatterplot of stage and discharge (blue dots) with poor fitted data highlighted in black circles and fitted third-order polynomial model (red line) ;Right: time series of stage (blue) and discharge (orange) with poor fitted data highlighted using black circles.

Based on the relationship shown between the quantities in **Figure 3-6** (left), a polynomial model was considered an appropriate candidate model. The third-order polynomial was selected as the predictive model with the highest accuracy and is shown in **Figure 3-6** (left). This model is represented as:

$$\hat{Q}_{\{\eta,R,T\}} = \alpha_1 + \alpha_2 h + \alpha_3 h^2 + \alpha_4 h^3 \quad (3-15)$$

Where: h is the sum of the river antecedent flow-equivalent depth, tides, and surge.

Figure 3-6 (left) shows that there are several points for which the model does not perform well (these represent 0.012% of the total data set). These points are highlighted with black circles. The poor-fit points are found to be related to two distinct segments of the overall time series in **Figure 3-6** (right), which are associated with moderate events and judged to not affect the overall appropriateness of the model.

To assess model performance, a holdout validation was performed using 50 holdout folds considering a 70/30 split of randomly selected training and testing data. The

correlation coefficients varied from approximately 0.998 to 0.999. The RMSE varied between approximately 10.25 cms and 17.3 cms across the fifty folds with a mean RMSE of 12.68 cms, which is used in characterizing the distribution of the model error term used in the analysis. The overall bias (mean error) is relatively small (ranging between approximately -0.09 and 0.08 cms).

To develop the marginal distribution for river antecedent flow, $f(Q_R)$ in Equation (3-3) and generate the probability table assigned to the node Q_R in **Figure 3-1**), a statistical analysis was performed using discharge data available for the USGS gage 01463500 located near the case study region (see **Figure 3-2**). We first extracted and removed the portion of the time series related to the hurricane season (i.e., portions of the time series that corresponded to dates when hurricanes were known to be in the area were removed). This is to ensure the antecedent flow was not capturing the effects of hurricane-induced precipitation, which are already included in the proposed model. Finally, to approximate a random sample of discharge data, a random set of 5% of the overall time series was selected, and a series of candidate distributions were fit to the data set. The estimated Akaike information criterion (AIC) and Bayesian information criterion (BIC) values for the candidate distributions were used to select the best fit distribution. Ultimately, the lognormal distribution was selected to model the marginal river antecedent flow distribution.

Tidal effects were incorporated into the analysis (shown as T in **Figure 3-1**) using predicted tidal elevations from NOAA gage 8539993. Positive and negative tidal elevations were separated and empirical CDFs related to high (positive) and low (negative) tides were generated. There is assumed to be a 0.5 probability of peak

surge occurring at high tide and a 0.5 probability of peak surge occurring at low tide. That is:

$$P(T = t_i) = P(T = t_i|low)P(low) + P(T = t_i|high)P(high) \quad (3-16)$$

Figure 3-7 shows the empirical CDF and probability mass function (PMF) for high and low tides.

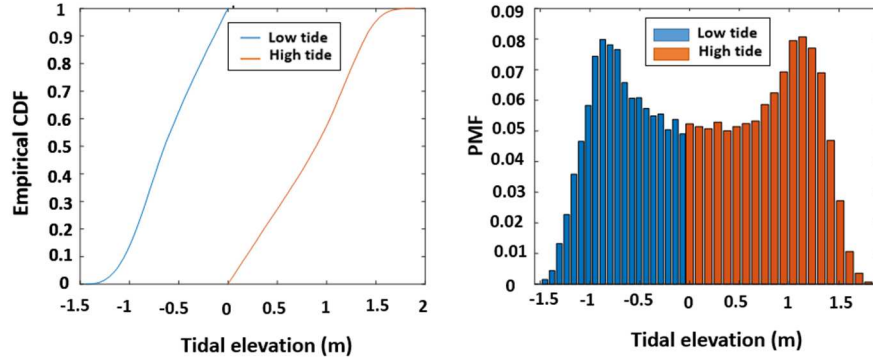


Figure 3-7. Empirical CDF (left) and PMF related to high and low tides.

3.4.2.6 Calculation of Total Discharge

In this study, total equivalent discharge caused by tides, river antecedent flow, storm surge, and storm-induced precipitation is modeled as the simple superposition of the precipitation-induced discharge and surge-, tide-, river antecedent flow-equivalent discharge and is represented as:

$$Q_{total} = Q_{\{\eta,R,T\}} + Q_P \quad (3-17)$$

The conditional distribution $p(Q_{total}|Q_{\{\eta,R,T\}}, Q_P)$ (and equivalently, conditional probabilities for the node Q_{total} shown in the BN in **Figure 3-1**) was generated using the simple superposition mentioned in Equation (3-17). The conditional distribution $p(Q_{total}|Q_{\{\eta,R,T\}}, Q_P)$ facilitates calculation of $p(Q_{total} > q|Q_{\{\eta,R,T\}}, Q_P)$.

3.4.2.7 Discretization of Distributions

Implementation of the joint probability method, in general, requires the discretization of all modeled random variables in Equation (3-3). Discretization is likewise required to support calculations performed using the BN. Discrete landfall locations and the edges of discretized bins related to constitute random variables are shown in **Table 3-2**. Monte Carlo simulation was used to generate the CPTs in the BN to reduce discretization error. To generate the CPT for a child node as a function of the parent nodes, a Monte Carlo simulation was performed for each combination of the discrete states of its parent nodes. **Figure 3-8** shows an example of performing a Monte Carlo simulation. As shown in this figure, a combination of the bins colored in grey represents one combination of the states of the parent nodes related to node η (excluding landfall location). To generate N_{sim} simulated values related to parent nodes randomly, N_{sim} values are drawn from within the four gray bins, resulting in N_{sim} combinations of the hurricane parameters. In the next step, surge height is computed for each of these N_{sim} combinations of hurricane parameters using the surrogate model. Then N_{sim} surge values are binned into the state intervals related to node η , and the discrete conditional probability table assigned to node η was computed for the combination of parent nodes. The conditional probability table of node η is a component for estimating the probability distribution of the final random variable which is total river discharge. The process described above is implemented for all combinations of parent nodes and all nodes in the BN. For the case shown in **Figure 3-8**, the functional form of the distribution of the parent nodes is analytically defined. For other nodes, where an

analytical expression is not readily defined, simulations are drawn from a uniform distribution defined on the bin.

Table 3-2. Discretized values for the parameters required in the Bayesian formulation.

No	variable	Discretized values
1	X_0 (lat, lon)	(33.16417, -79.2011), (33.94843, -77.9277), (34.93409, -76.2995), (35.8801, -75.5935), (37.19846, -75.8545), (37.92462, -75.4296), (38.78565, -75.0918), (39.68712, -74.1428), (40.92737, -73.7382), (41.39125, -71.4794), (41.67301, -69.9293), (42.08063, -70.1512), (42.60478, -70.6388), (43.75627, -69.982), (44.47684, -68.1531)
2	Δp (hpa)	10, 23.83, 37.66, 51.50, 65.33, 79.16, 93
3	V_w (km/h)	0, 38, 76, 114, 152, 190, 228, 266, 304, 342, 380
4	R_{max} (km)	0, 50, 87.50, 125, 162.50, 200, inf
5	V_f (km. h ⁻¹)	0, 20, 35, 50, 65, 80, inf
6	θ (degree)	-60, -40, -20, 0, 20, 40
7	Q_R (cms)	20 values interpolated between 0 and 2831 and interval of 141 cms
8	T (m)	-1.45, -1.38, -1.30, -1.23, -1.16, -1.08, -1.01, -0.94, -0.87, -0.79, -0.72, -0.65, -0.57, -0.50, -0.43, -0.36, -0.28, -0.21, -0.14, -0.07, 0, 0.09, 0.18, 0.28, 0.37, 0.47, 0.56, 0.66, 0.75, 0.85, 0.94, 1.03, 1.13, 1.22, 1.32, 1.41, 1.51, 1.60, 1.70, 1.79, 1.89
9	η (m)	40 values interpolated between 0 and 6.5 and interval of 0.16 m
10	P_{BA} (mm. day ⁻¹)	15 values interpolated between 0 and 76 mm and interval of 5.08 mm.day ⁻¹
11	$Q_{\{\eta,R,T\}}$ (cms)	80 values interpolated between 0 and 26901 cms and interval of 336 cms
12	Q_P (cms)	80 values interpolated between 0 and 7362 and interval of 92 cms
13	Q_{total} (cms)	300 values interpolated between 0 and 34702 and interval of 115.6 cms

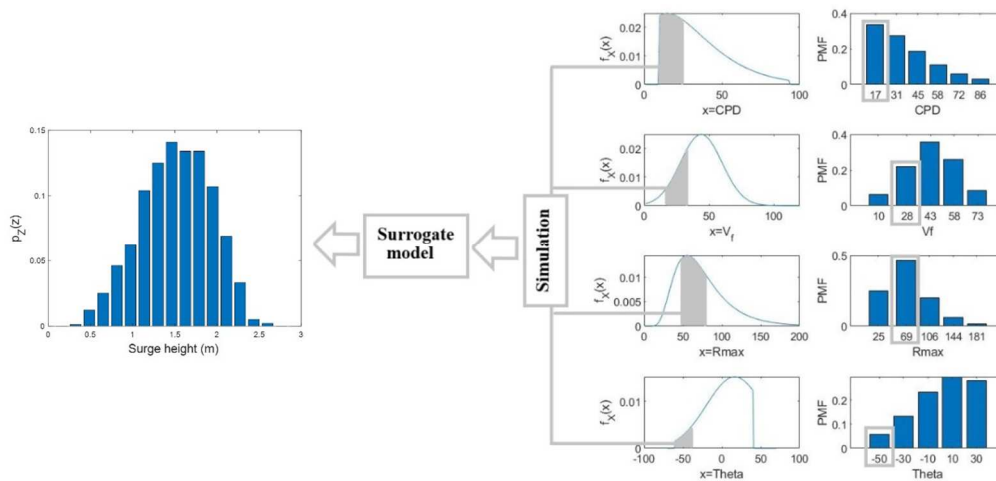


Figure 3-8. Illustration of Monte Carlo simulation approach for generating CPTs.

3.5 Generation of the Hazard Curve

Finally, the integral shown in Equation (3-3) is solved in discrete form for a range of values related to Q_{total} . The final (representative) hazard curve showing the annual exceedance rate for each value of the Q_{total} is shown in **Figure 3-9**. In this figure, the annual occurrence rate of 0.18 storms per year applied for hurricanes occurring in the study area to generate the hazard curve is taken from the NACCS analysis (Nadal-Caraballo et al, 2015)). This storm rate (storm/year) leverages the results of the statistical analysis performed by USACE for the NACCS (Nadal-Caraballo et al. 2015). Nadal-Caraballo et al (2015) obtained the published rate of 0.18 storms/year is obtained by scaling an omnidirectional rate (storms/year/km) using an optimal kernel size (radius) of 200 km. In the present study, the size of the study area includes over 1500 km of coastline over which 15 candidate landfall values are distributed. The distance between landfall values varies but is approximately in the range 150-200 km, and each landfall location is assumed to be equally likely. Thus, while track spacing was not

explicitly considered in the hazard calculations, the rate of storms affecting the region and attributed to each landfall location is judged to be generally reasonable for the purposes of the study.

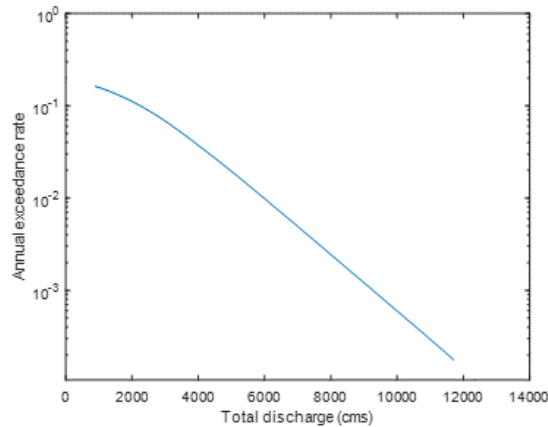


Figure 3-9. Illustrative/representative hazard curve showing annual exceedance frequency for river discharge caused by hurricane occurrence, developed considering simplified/illustrative modeling assumptions.

3.6 Assessment of the Model Performance

This section includes a performance assessment of all models used in the study. To assess the model's performance in this section, the capability of the BN for information updating is leveraged. Information updating is applied by entering the evidence to the nodes in the BN (i.e., the states of certain nodes are set as known). In the next step, posterior distribution related to the target response variable (i.e., total river discharge) are estimated and used for model performance assessment.

The evidence was introduced to the BN by specifying storm parameters, river antecedent flow, and tides associated with historical events that affected the area. The posterior distribution of the total discharge was then compared with peak river discharge observed at USGS gage 01463500 during the hurricane event. As mentioned

in Section 3.3, the location of the USGS gage is 1.5 km upstream of the study location at save point 5373. There are rock riffles between the study location and the USGS gage that can limit (but not prevent in case of high tides and surges) the movement of water upstream to the USGS gage. Furthermore, it is assumed that modeled peak total river discharge occurs at the time of peak surge, which will lead to a conservative estimation of the discharge. For these reasons, the posterior distribution for discharge is expected to be biased consistently higher than the discharge observed at the USGS river gage.

In this study, a limited number of historical storms were available to assess the model performance. This limited availability was specially related to R_{max} data. **Figure 3-10** shows observed storm tracks of three storms affecting the case study region. These figures also include the synthetic storm track modeled in this study (i.e., the storm track as represented by the most closely aligned set of storm parameters).

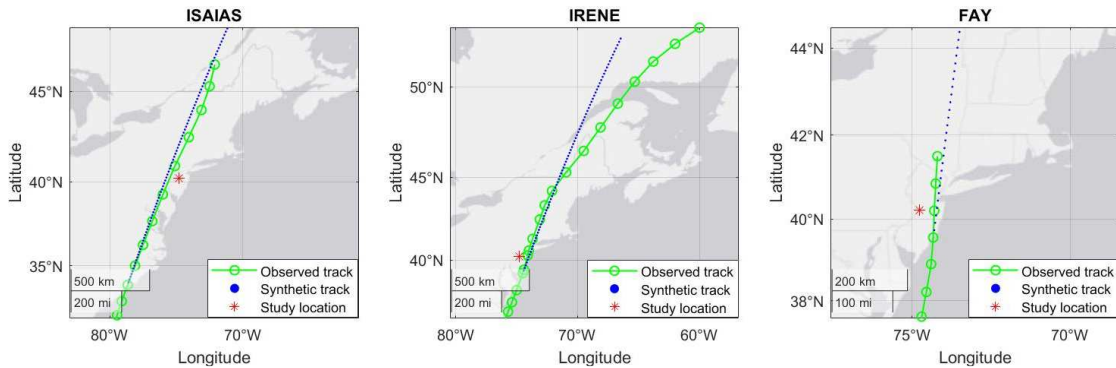


Figure 3-10. Synthetic and observed storm track related to historical storms.

Table 3-3 shows key variables for the three storms affecting the area: representative storm parameters, observed peak river discharge (column labeled “USGS Q”), the tide at the time of the observed peak water level at the USGS gage 01463500 (column labeled “Tide at peak water level (WL)”)), and river antecedent flow (column labeled

“QR”). The representative storm parameters are the values related to storm parameters specified in the NOAA IBTrACS database (<https://www.ncdc.noaa.gov/ibtracs/>) taken at the point right before landfall (is the last observation available before the storm makes landfall). The location of these representative points is shown in **Figure 3-11**. These representative values of the parameters were entered as evidence for corresponding nodes in BN related to storm parameters. River antecedent flow and peak river discharge were extracted using fifteen-minute discharge data at the USGS river gage 01463500. Tidal elevations were extracted at the time of the peak discharge (or peak WL) from NOAA tide predictions at NOAA station 8539993.

Table 3-3. Storm parameters and surge and discharge values related to USGS gage and modeling results.

Name of the storm	Time	LAT	LON	ΔP (hPa)	V_w (km/h)	θ (degree)	V_f (km/h)	R_{max} (km)	Tide at peak WL (m)	Q_R (cms)	USGS Q (cms)	Modal bin ¹ of PMF for discharge
ISAIAS	8/4/2020 0:00	33.7244	-78.5834	25.25	138	19	37	37	1.38	113	2146	3354-3470
FAY	7/10/2020 18:00	39.5473	-74.3161	15.25	92	7	25	166	-0.56	127	538	1272-1388
IRENE	8/28/2011 9:00	39.1783	-74.49	55.25	111	20	42	185	1.6	424	4134	6709-6824

¹ Bin associated with the highest probability mass

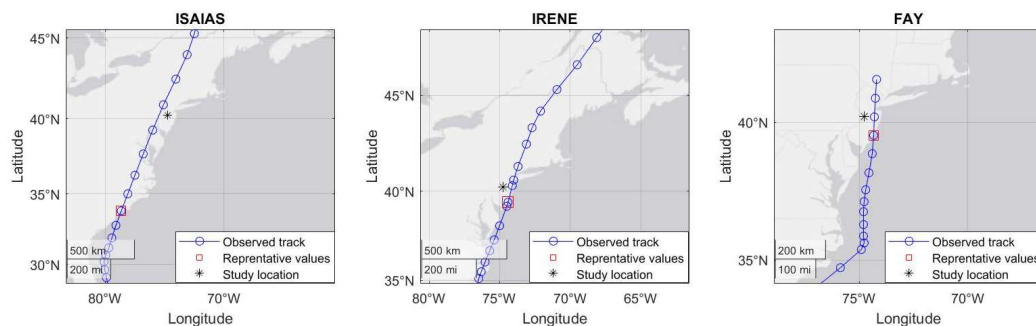


Figure 3-11. Location of the representative point for extracting information at landfall location for historical storms.

After setting the known evidence for the nodes in the BN, posterior distributions of the total discharge are computed. **Figure 3-12** shows the modeled posterior distribution of the total discharge (PMF of total discharge). The modal bin of the posterior distribution, which is the bin with the highest probability in the PMF is also represented in **Table 3-3** and column labeled modal bin. As shown in this table, the limits of the modal bins are consistently showing higher values than USGS observed discharge values. As noted earlier, this result is expected due to the model simplifications used in the overall assessment. One reason for this could be the presence of rock riffles that limit the propagation of surges and tides to the USGS gage. Furthermore, the conservative assumption related to the simultaneous occurrence of the peak surge and peak total river discharge could also contribute to higher modeling values for the limits of modal bins.

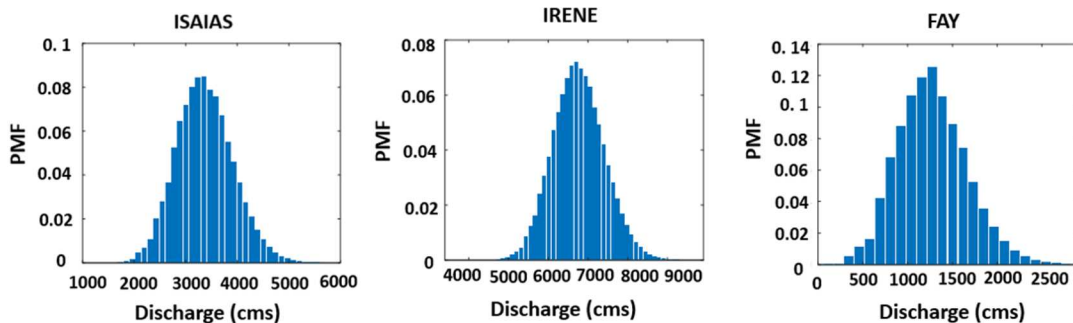


Figure 3-12. Posterior distribution of the modeled discharge values for historical storms.

As shown in **Table 3-3** and **Figure 3-12**, the modeling results generally seem reasonable, considering the high level of uncertainty involved in the analysis, the limited fidelity of the predictive models used in this study, and the assumption of temporal concurrence of peak surge and discharge. For example, an important source of uncertainty in this study is related to the limited number of the landfall locations

modeled (however, the number is consistent with other similar probabilistic studies). An approximation in landfall location can affect the simulated peak surge height and, subsequently, river discharge since the topographic/bathymetric and hydrodynamic conditions will differ at each point along the coast. Furthermore, landfall locations have a notable impact on storm track paths and the spatial distribution of the precipitation in the upstream area. Storms can make landfall at each point along the coast; however, it is computationally expensive to model a high number of landfall locations.

The change in storm characteristics after landfall also contributes to the aggregation of uncertainty in the model. Many factors that affect storm path inland after landfall are not considered while modeling synthetic storm track paths. Storm paths for synthetic tracks are generated as an ideal straight line using the landfall location and heading direction. However, in reality, storms follow a path on the land that is not straight. A different storm path can affect the decay of storm intensity and the amount of precipitation experienced at each point.

To estimate rainfall in this study, storm location and wind decay were estimated at hourly resolution. Then precipitation was estimated based on the distance between points of interest and storm center and the maximum wind speed. The rainfall rate was estimated using the TRR model, which estimates rainfall rate at daily resolution. To convert daily rainfalls estimated using the TRR model to hourly rainfall, the assumption of the uniform distribution of the rainfall was made, and a factor of twenty-four was used. Finally, there was no well-developed statistical or analytical model for capturing the storm's forward velocity decay on the land after landfall. In this study, to estimate the location of the storm center at each hour, a constant forward velocity was

considered. This approximations can affect the amount of precipitation in the upstream area estimated as a function of storm location and wind speed.

3.7 Conclusion

This study demonstrated a Bayesian-motivated approach for the probabilistic assessment of MMFs in a coastal area. The Bayesian-motivated approach has the advantage of incorporating the knowledge of the physical processes (consistent with the limitations of the existing state of knowledge) into the probabilistic assessment of flood hazards. These physical relationships between quantities are represented via a series of deterministic equations to generate conditional probability distributions. The Bayesian-motivated approach builds up the joint distributions using these conditional distributions, and then marginal distributions are derived by integrating over these conditional distributions. In cases where available data are limited, the capability of the Bayesian-motivated approach to integrate knowledge of the physical processes is considered a significant advantage. However, the application of the Bayesian-motivated approach is challenging in different ways. For example, Bayesian-motivated approaches require statistical analysis of the input data (e.g., storm parameters, river discharge data), which is affected by the quantity of data available for a region.

Furthermore, to compute conditional distributions, a high computational effort is necessary for predicting the child nodes as a function of the parent nodes. In this case study, five efficient predictive models plus two simple superposition models were used. While constructing these representative predictive models was not a trivial task, the use of high fidelity and sophisticated models to increase the accuracy of the results will

noticeably increase the computational effort. Several simplifying assumptions were made in this study to reduce the computational effort. One of these assumptions was the simplified treatment of the interaction between storm surge and river flow (precipitation-induced and antecedent) using superposition. Complex interactions can be better captured using more sophisticated hydraulic models in future applications of the proposed framework.

Finally, solving the integral in Equation (3-3) in discrete form requires the discretization of the continuous variables, introducing a discretization error. To minimize this error, Monte Carlo simulations were used in this study. There are areas where research is necessary to increase the accuracy of this model. For example, incorporating the non-linearity between tide, storm surge, and precipitation-induced water levels into the analysis could increase the performance of the model. In addition, more sophisticated models for modeling storm path and forward velocity after landfall can contribute to a more realistic assessment of compound flood hazard in this study.

While a series of placeholder models were developed for the purposes of demonstrating the proposed framework, the framework can be directly adapted to include outputs from more sophisticated models in generating the CPTs between variables. Thus, this study developed and demonstrated a flexible framework to assess compound flood hazards using a Bayesian motivated approach.

Chapter 4: Further applications of the developed Bayesian framework

4.1 Introduction

Bayesian Networks (BNs) are directed acyclic graphs that represent the relationships among the involved random variables. BNs consist of nodes (circles) representing random variables and directed links (arrows) representing the probabilistic dependence (typically reflecting causal relationships among random variables). A family terminology is conventionally used to describe BNs. For example, Figure 4-1 represents a BN with nodes X_1 , X_2 and Y , and links from X_1 to Y , and X_2 to Y . X_1 and X_2 are referred to as the *parents* of node Y and conversely Y is referred to as the *child* of X_1 and X_2 . X_1 and X_2 are called root nodes because they have no parents, and a marginal probability distribution is assigned to each of these nodes. Y is assigned conditional probability distributions that changes based on the states of its parents X_1 and X_2 .

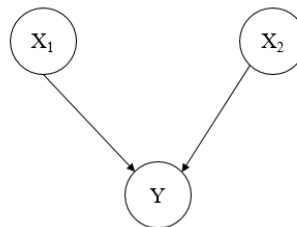


Figure 4-1. A simple BN with two parent nodes and a child node

This chapter illustrates how the capability of the BN for information updating can be leveraged for different applications. By specifying the state of one or multiple nodes

(typically referred to as entering evidence), the distributions of other nodes can be updated through a process known as *inference*. The values that are selected as evidence can be observed values or assumed values that reflect states for which we want to understand the impacts of new information. Figure 4-2 shows the BN developed in this study, which will be used to illustrate the notion of information updating. The BN in Figure 4-2 is the same as the BN presented earlier in Figure 3-1; it is repeated here for convenience.

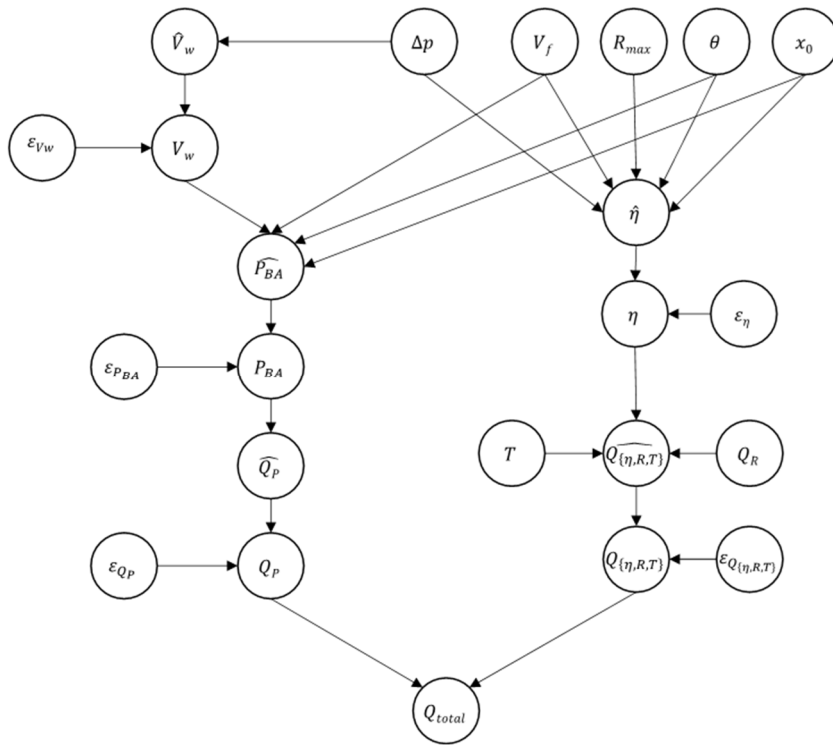


Figure 4-2. Developed BN for information updating

4.2 Information Updating in BNs

Equation 4-1) shows conceptually how inference is conducted in a BN to update the beliefs (probabilities) about variables based on entered evidence. This equation is based on Bayes' theorem. However, in practice, more efficient algorithms such as clustering,

polytree, and stochastic sampling are used to conduct Bayesian inference for information updating (“GeNIe Modeler – BayesFusion” 2022). In this equation, $P(A|B)$ is the posterior probability distribution of event A , and it represents a belief about the probability of event A after observing an occurrence of the event B . $P(B|A)$ is the probability of event B conditioned on the occurrence of event A . $P(A)$, which is also known as the prior probability of the event A , is the marginal probability of the event A . $P(A)$ represents the belief about the probability of the event A prior to any information about event B . $P(B)$, is known as a “normalization constant” and can be estimated using the Theorem of Total Probability (Kjærulff and Madsen 2013).

$$P(A|B) = \frac{P(B|A).P(A)}{P(B)} \quad 4-1)$$

Information updating can be conducted in different directions, including forward, backward, or in both directions, referred to as forward inference, backward inference, and mixed inference, respectively. These three types of inferences are described in the following subsections.

4.2.1 Forward Inference

Forward inference, also called predictive inference, is a process in which information propagates in the direction of the causal relationships between variables. In this process, the observed values related to the parent node are set as evidence, and then the probability distribution of the child node is updated. This type of inference is called forward inference since the information in the BN flows in the same direction as the causal relationships (Bensi and Groth 2020; Ding 2010). For example, in Figure 4-1,

propagation from X_1 to Y (i.e. fixing the state of X_1 and then observing the effect on Y) and from X_2 to Y are forward inferences. This capability of BN was used in chapter 3 for assessing the model performance by setting observed values related to the input parameters (root nodes) as evidence for those nodes and then updating the beliefs (probabilities) of other nodes, including total river discharge. After conducting the information updating, the posterior distribution of the node related to the target variable, total hurricane-affected river flow, was estimated and compared with the observed value of this variable. Figure 4-3 shows the prior and posterior distribution of total river flow using forward inference for three historical events considered in Chapter 3 and listed in Table 4-1. In this figure, the prior distribution represents the marginal distribution of total river flow as obtained when integrating over all nodes. The posterior distribution was estimated by setting evidence for certain states of nodes related to model input parameters and then reintegrating over all nodes given those observed states. The Bayesian model input parameters included the storm's central pressure deficit (Δp), forward velocity (V_f), radius to the maximum wind (R_{max}), heading direction (θ), landfall location (x_0), river antecedent flow (Q_R), and tidal elevation (T). Observed values related to these parameters, which were set as evidence in BN, are listed in columns 3 to 10 in Table 4-1. As shown in Figure 4-3, the updated distribution is narrower than the prior distribution because of uncertainty reduction by setting evidence related to model input parameters. As presented in Figure 4-3, the updated total river discharge value related to the bin with the highest probability of occurrence for each storm is shifted to the values that are closer to the observed values.

For storm Isaias and storm Irene, the distribution shifts to the right, and for storm Fay a shift to the left is observed.

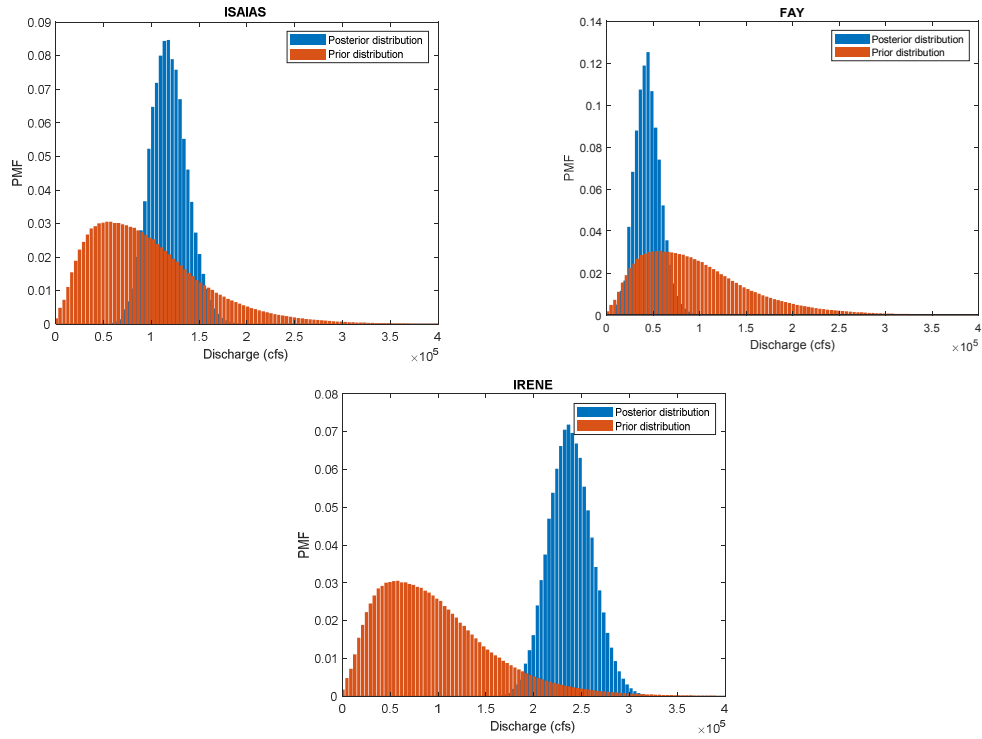


Figure 4-3. Updated distributions of effect (target) node using forward inference.

Table 4-1. Parameters and corresponding storm surges and discharges related to historical storms.

1	2	3	4	5	6	7	8	9	10	11	12
Storm	Date	LAT	LON	ΔP (hPa)	θ (degree)	V_f (km/h)	R_{max} (km)	Tide (ft)	Q_{River} (cfs)	Observed Q (cfs)	Surge (ft)
ISAIAS	8/4/2020	33.7244	-78.5834	25.25	19	37	37	4.56	4000	75800	6.5
FAY	7/10/2020	39.5473	-74.3161	15.25	7	25	166	-1.86	4500	19000	2.5
IRENE	8/28/2011	39.1783	-74.49	55.25	20	42	185	5.25	15000	146000	8.2

4.2.2 Backward Inference

Backward inference, also called a diagnostic inference, is the process by which the information in the BN flows in the opposite direction of the causal relationships. For example, in Figure 4-1, propagation from Y to X_1 and from Y to X_2 are examples of backward inferences. To illustrate the concept of backward inference in this study,

observed data related to total river discharge was used (column 11 of Table 4-1). These observations are related to three historical storms that affected the area. To update the beliefs related to nodes representing the model input parameters (ΔP , V_f , R_{max} , θ , x_0 , Q_R , and T), the observation of total river discharge for each hurricane was set as evidence, then probability distributions related to input parameters were updated. Figure 4-4 shows updated distributions of nodes representing model input parameters. In this figure, the values on the horizontal axis for each distribution correspond to the middle value of each bin. The first row of Figure 4-4 shows the prior and posterior distribution of ΔP . As shown in this figure, the updated distribution for storm Isaias shows a higher probability of occurrence for the bin with lower and upper limits of 10 and 28 hPa. This range for the maximum probable values is consistent with the observed value of ΔP for this storm, which is 25 hPa. However, in case of storm Fay, a higher probability of occurrence for the bin with lower and upper limits of 10 and 23 hPa is observed. This range is consistent with the observed value for this storm (i.e., 15 hPa). Furthermore, in Figure 4-4, an increase in the probability of occurrence for the bin with limits of 37 to 65 hPa related to the storm Irene is observed, which is also consistent with the observed value of ΔP for this storm (i.e., 55 hPa).

The second row of Figure 4-4 shows the prior and posterior distribution of V_f . As shown in this figure, the changes in the updated probability of the storm Isaias is not noticeable. However, an increase in the probability of occurrence for the bin with limits of 20 to 35 km/h is observed for storm Fay. This increase in the probability of occurrence for this bin is consistent with the observed value of V_f for this storm at

landfall, which was 25 km/h. In the case of storm Irene, an increase in the probability of occurrence for V_f is noticed for the bin with limits of 35 and 50 km/h. The observed value of V_f for this storm is 42 km/h and is in the bin with the highest probability mass related to V_f .

The trends in updated probabilities of R_{max} and θ , which are shown in rows 3 and 4 of Figure 4-4, are not as noticeable as in the cases of ΔP and V_f . Fifth row of the Figure 4-4 shows the updated probability of landfall location. To analyze these updated probabilities, the locations of simulated and observed landfall for three historical storms are shown in Figure 4-5. As shown in Figure 4-5, the observed landfall location for storm Isaias is close to simulated landfall location 2 (southern part of the coastline in Figure 4-5), and the observed landfall locations for storms Fay and Irene are close to landfall location 8 (northern part of the coastline in Figure 4-5). However, the updated probabilities for landfall location are not consistent with the observed location of these storms. The sixth row of Figure 4-4 presents the updated distributions for antecedent river flow. As shown in this figure, the changes in probability for storm Isaias is not noticeable. However, a higher probability of occurrence for the bin with limits of 1000 to 5000 cfs is observed for storm Fay which is consistent with the observed river flow value of this storm (i.e., 4500 cfs). The third figure in this row, which is related to storm Irene, shows an increase in the probability of occurrence for the bin limits of 10,000 and 25,000, consistent with the observed value of river flow for this storm (15000 cfs).

Finally, the last row in Figure 4-4 represents the updated distributions for tidal elevations. As shown in this figure, the updated probability of tidal elevations for storm Isaias is not consistent with the value of the observed high tide for this storm (i.e., 4.56 ft). However, an increased probability of occurrence is noticed for the bins with lower and upper limits of -3 and -2 ft for storm Fay, consistent with the observed tidal elevation of -1.86 ft for this storm. Similarly, an increase in the probability of high tide for the storm Irene is observed for the bins with limits of 4 and 5.5 ft which is also consistent with the observed value of 5.25 ft tide for this storm.

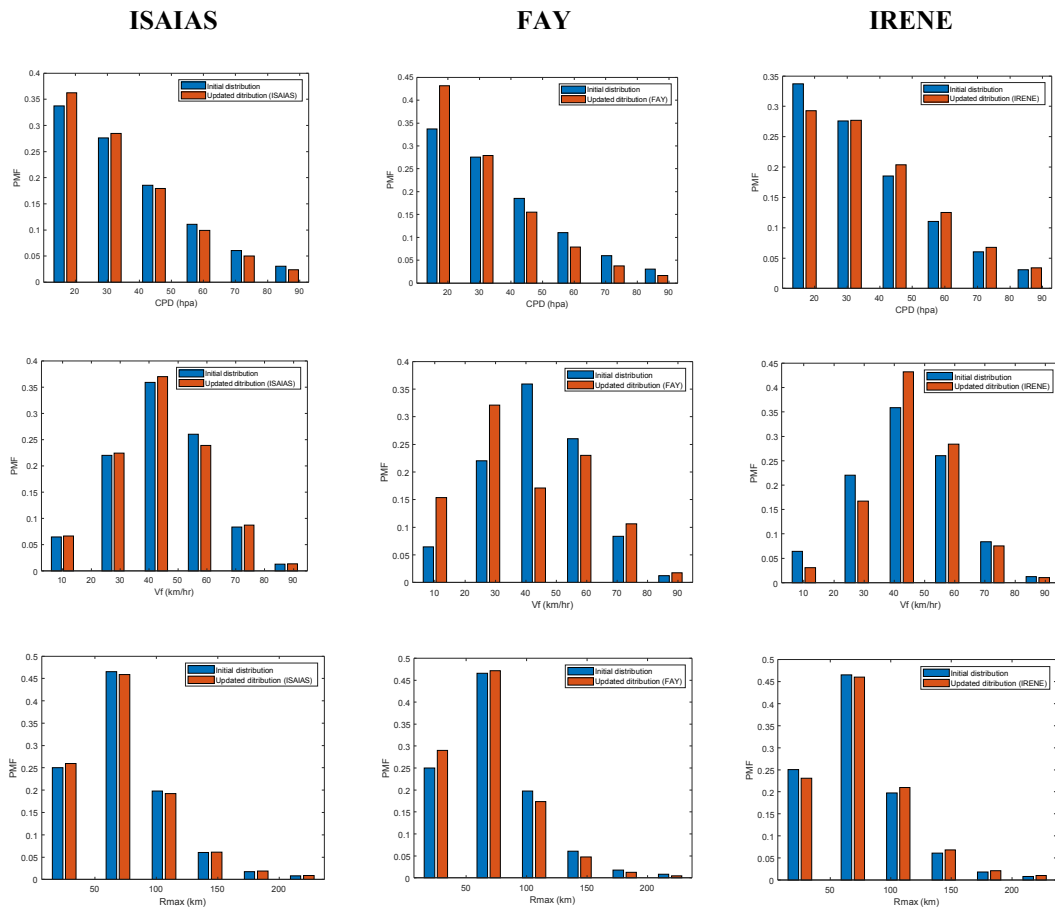


Figure 4-4. Updated distributions of nodes representing model input parameters using observations related to the total river discharge node.

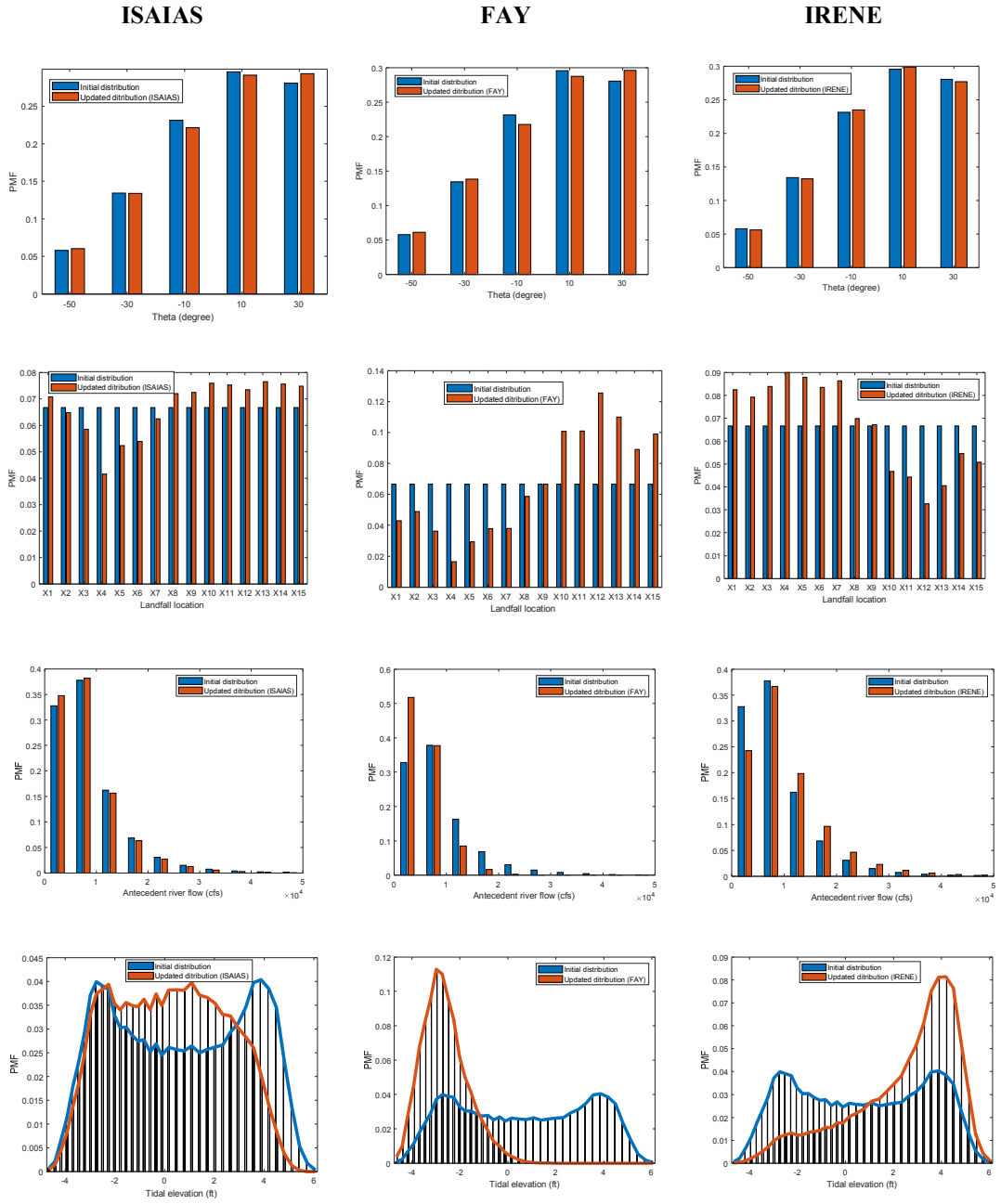


Figure 4-4. Continued

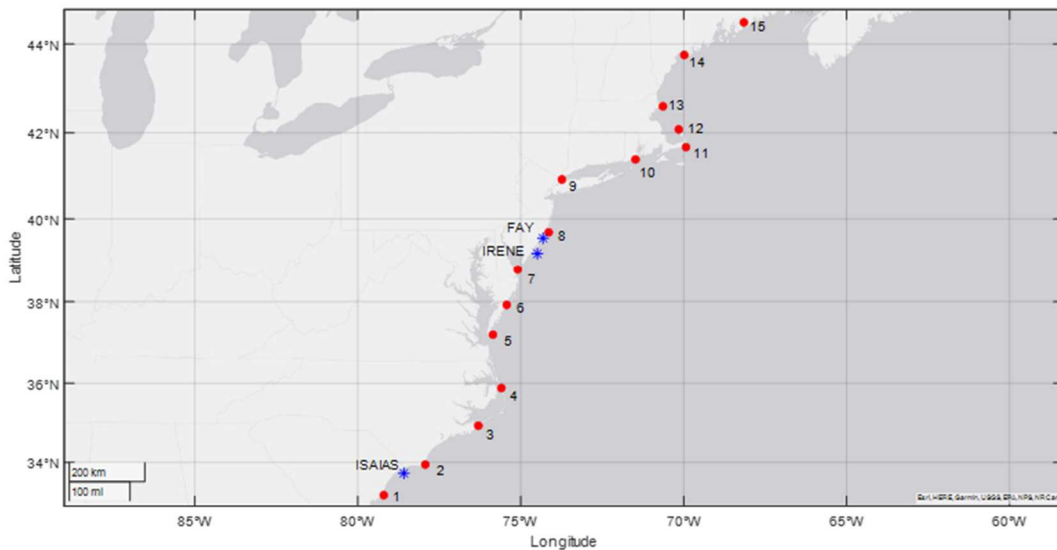


Figure 4-5. Landfall locations of three historical storms (blue stars) along with fifteen simulated landfall locations in this study (red circles)

4.2.3 Mixed Inference

In addition to forward and backward inference in the BN, information updating can flow in a combination of directions while setting evidence related to the nodes that have both the role of a parent and a child. If observed information related to these nodes is set as evidence, propagation occurs in both directions. For parent nodes of these nodes, it is called backward inference, and for child nodes of these nodes, it is called forward inference. An example of this type of inference can be conducted in the BN shown in Figure 4-2 by setting observed storm surge values for each storm listed in column 12 of Table 4-1. After setting observed storm surge values as evidence in the BN, mixed propagation will update the probability distribution of nodes that act as parent or child nodes for this node. These nodes include storm parameters (parent nodes of storm surge node) and total river discharge (child node of storm surge node). Similar to the forward

and backward inference cases explained here, the observed storm surge values related to three historical storms listed in Table 4-1 are used for information updating using mixed inference. Figure 4-6 shows updated probabilities of storm parameters and total river flow nodes in the BN shown in Figure 4-2, using observed values related to the storm surge node (η). As shown in the first row of the Figure 4-2 updated probabilities of ΔP related to storm Fay and Isaias did not show a noticeable change, however, an increase in the probability of occurrence for the bin with lower and upper limits of 37 to 65 hPa was noticed for storm Irene. This updated probability was consistent with observed value of 55 hPa for this storm. The second row of Figure represents the updated probability of V_f . As shown in this figure, an increase in the probability of V_f for the bin limits of 35 to 65 km/h is observed for storm Isaias. This updated probability of V_f is consistent with the observed value of 37 km/h for this storm. A similar trend is observed for storm Irene and the probability of V_f in similar bin limits has increased and is consistent with the observed value of the 42 km/h for this storm. Updated probability for storm Fay did not show any noticeable changes. The third and the fourth row of Figure 4-6 show updated probabilities of R_{max} and θ for which a meaningful trend is not observed.

As shown in the fifth row of Figure 4-6, landfall locations for storms Isaias and Fay are shifted to the southern and the northern part of the coast, which are consistent with observed values of the landfall for these storms located in the southern and northern part of the coast. However, a shift of probability of storm Irene to the south part of the coast is not consistent with the observed value of landfall location for this storm. The last row of Figure 4-6 shows updated probabilities of total river discharge. As shown

in this figure, a higher probability of 100,000 cfs for storm Isaias and 150,000 cfs for storm Irene is observed. These updated probabilities are consistent with observed values of 75,000 and 146,000 cfs for these storms, respectively. The updated probability of the storm Fay was not noticeable and did not provide any insights to discuss.

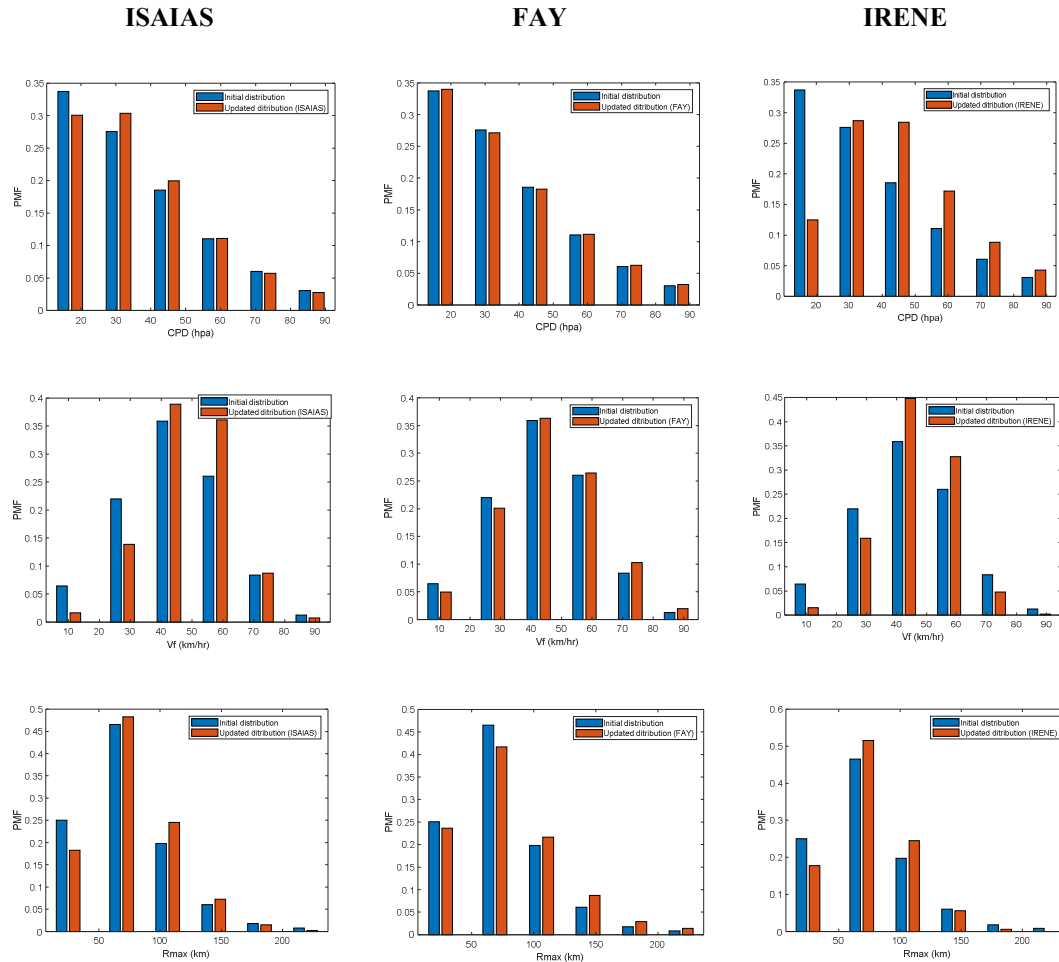


Figure 4-6. Updated distributions of nodes using observed values of storm surge related to historical storms.

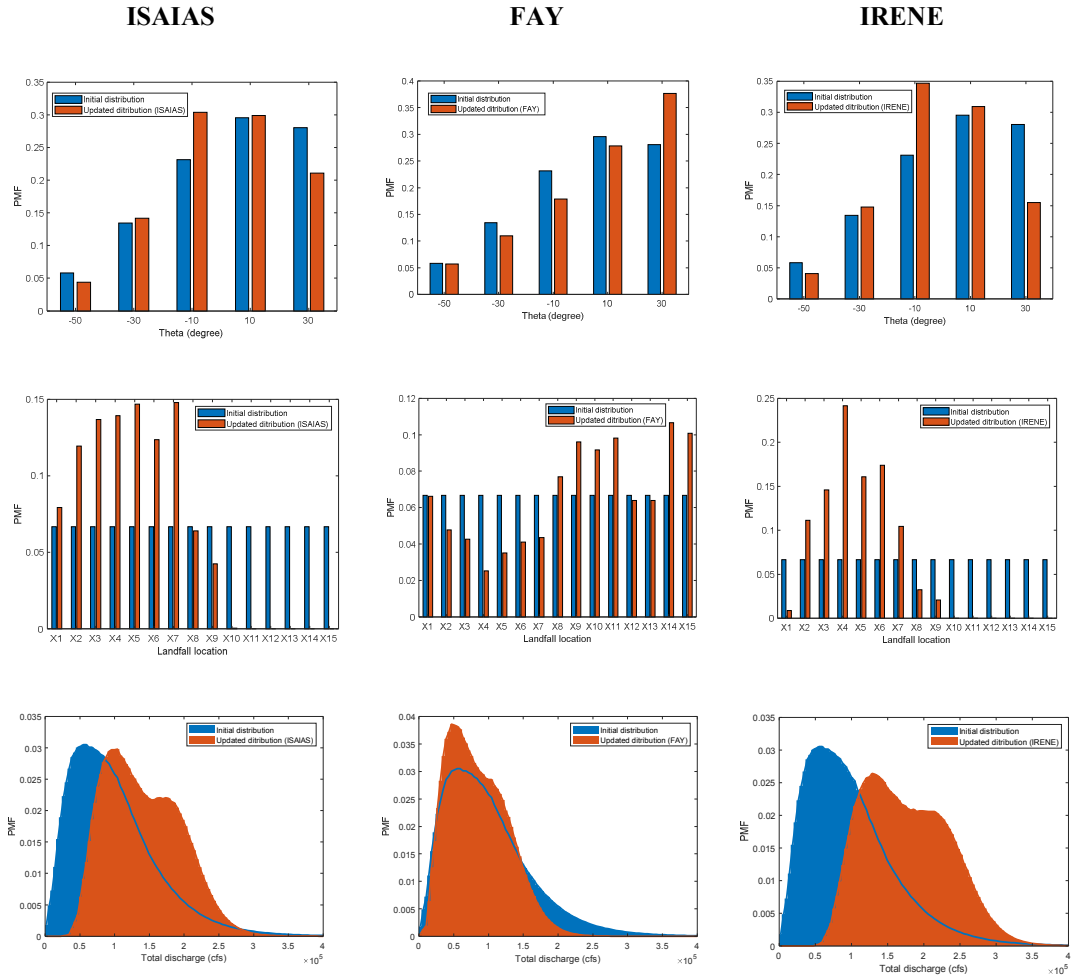


Figure 4-6. Continued.

4.3 *Conclusion*

Information updating is a powerful capability of BNs that can be used to update beliefs about different nodes in a BN. Information updating can be conducted by setting the state of one or several nodes as evidence and then propagating new information in the BN. These updated beliefs of nodes can help decision-makers to know about the updated probability of variables of interest (nodes in BN) based on the observed evidence or assumed evidence of other nodes (e.g., an assumed high discharge value). Observed values may be entered as part of post-event forensic studies. However, the

values set as evidence are not necessarily observed values. Instead, this evidence could be assumed values used in sensitivity studies by decision-makers to support scenario planning. For example, suppose an engineered system has been protected by a barrier that has been designed for a specified stillwater elevation. However, there may be interest in the potential for overtopping of the barrier by wind-generated waves. In this case, the BN can be used to understand the posterior distribution of variables affecting wind-generated waves (e.g., wind speed, heading direction, and landfall location) given an assumed water level against the barrier. This assumed value related to water level can be set as evidence in the BN, and then the beliefs about other variables in the BN (including storm characteristics) can be updated. This information updating will inform decision-makers about the probability distribution of storm characteristics that can lead to this high water level. For example, they will know about the probability distribution of the wind speed, precipitation depth, heading direction, and landfall location of the storm and can be prepared more efficiently for this storm to avoid its negative impacts. In addition, information updating can work in the opposite direction using forward inference. In this type of inference, the evidence related to nodes representing the input parameters of the model can be set to update the belief about the node representing the target variable in the BN (total hurricane-affected river discharge). For example, suppose a storm is forecasted or being considered in the analysis, and the parameters of the storm are predicted or specified. In that case, these parameters can be set as evidence to the model, and the information in the BN can be updated to regenerate the probability distribution of the total river discharge or storm surge caused by this storm. Knowing this updated information will help decision-makers to be informed about the

probable hazard that will affect the infrastructure or engineering system and take more effective protective measures.

Chapter 5: Conclusion, a Summary of the Contributions and Next Steps

5.1 Conclusion

Multi mechanism floods (MMFs) can lead to more severe and differing consequences on societies and built environments than single mechanism floods. To achieve a realistic assessment of flood hazards, consideration of multiple flood mechanisms is necessary. This study focused on the probabilistic assessment of MMFs. Specifically, this study sought to achieve the following goals:

- (1) Develop a lexicon and a framework to support the systematic review of the current literature and practices related to the assessment of MMF hazards and define the related gaps and challenges
- (2) Develop a Bayesian model for the probabilistic assessment of MMF hazards in a coastal area, including a series of representative models
- (3) Evaluate the performance (reasonableness) of the developed Bayesian model using historical data
- (4) Leverage and demonstrate the capability of the developed Bayesian Network (BN) to update the probability distributions of involved variables using observed data.

The primary conclusions of this study are:

- A high portion of the current literature addressing MMFs is focused on coastal hazards, specifically combinations of flood mechanisms involving storm surge

with precipitation and/or river flow. A small portion of these coastal-focused studies focused on the joint probability analysis (JPA) of waves and water levels. Inland MMFs received less attention than coastal floods; a high portion of the related studies focused on assessing flood hazards caused by the compounding effect of multiple river flows at riverine confluences. A noticeable gap was recognized in addressing rain on snow and dam failure caused by excessive precipitation-induced river flow combined with precipitation and river flow.

- In terms of modeling objectives, existing studies related to MMF hazard assessment generally fell into one of three categories. The first group includes studies that conducted a full probabilistic assessment of MMFs and generated a hazard curve (or surface) for the target severity metric(s) that accounts for multiple mechanisms. The second group of studies focused on modeling deterministic combinations of flood mechanisms, typically using computationally expensive numerical models. These studies mainly focused on accurately modeling the physical interactions between multiple flood mechanisms and assessed compound flood hazards using deterministic scenarios. Finally, the third group of the studies are building block studies that provide information and tools to support the probabilistic assessment of MMFs. This category includes studies focused on developing physical models to predict hurricane-induced precipitation or understand the physical interactions among multiple flood mechanisms.

- A key step in the extremal analysis of compound floods is the preparation of paired data related to the simultaneous occurrence of multiple flood mechanisms. The conventional method of annual maximum series of both random variables is considered conservative and raises a key challenge since it is unlikely for the annual maxima values of two variables to occur at the same time. To address this challenge, second group of studies considered the maximum value of one variable and the simultaneous value of the second variable at the time of maximum value for the first variable. The third group of the studies considered the maximum value of the first variable and the maximum value of the second variable within a fixed time interval, typically one day after the occurrence of the maximum value related to the first variable. In general, there is no unified method for extremal analysis of MMFs and preparation of paired data which is a critical step in the analysis.
- Overall the current literature has made progress related to PFHA of MMFs. However, the substantial remaining challenge is capturing the dependence structure between involved variables. This dependence has a nonstationary nature and varies by time and location. The lack of a comprehensive framework to analyze this dependence structure considering this nonstationary and spatiotemporal nature is recognized.
- This study has developed a framework for probabilistic assessment of MMFs in coastal areas using a Bayesian approach. Involved flood mechanisms in this analysis include hurricane-induced surge and precipitation, tides, and antecedent river flow. The developed framework can be applied for other

combinations of flood mechanisms and non-coastal floods. Five predictive models were developed as placeholder models in the developed framework and can be replaced with more sophisticated models based on the desired accuracy level in different projects. While models were used as placeholders in the BN, the overall model was assessed using historical data to determine if model results were reasonable.

- A robust characteristic of the developed BN in this study is the capability for information updating using observed data or assumptions to support sensitivity studies or to support scenario planning. This capability of the developed framework is used to update the probability distribution of different nodes using observed values related to three historical storms that affected the study area.

5.2 *Summary of contributions*

This dissertation has made several contributions:

- This study introduced a framework that provides a conceptual structure and a lexicon to describe and analyze different elements in probabilistic assessments of MMFs. Using this framework, the study focused on summarizing the current literature and practices regarding the approaches used for PFHA of MMFs and the scope of the studies. Then, this study critically reviewed existing studies to define the gaps and shortcomings of the current state of the art in assessing compound flood hazards.

- This dissertation developed a framework for probabilistic assessment of compound coastal floods using a Bayesian approach. This framework is novel in terms of application to the probabilistic evaluation of MMFs. The current framework is implemented using computationally efficient surrogate and statistical models. The developed framework is flexible, and the predictive models developed for the estimation of conditional probabilities can be replaced with more robust and accurate models, as appropriate.
- The developed framework has the advantage of incorporating the knowledge of the physical process into the analysis. This is valuable in cases where the data related to representative variables of flood mechanisms are limited.
- The developed framework relaxes the limitations of current statistically-based methods for probabilistic assessment of compound floods, including the choice of an appropriate functional form for the copula and the assumption of the similarity between marginal and joint distributions.
- The developed framework can be used to update information for each variable using observed information related to the other variables. This can be conducted by setting the observed values of the nodes as evidence and then updating the probabilities of other nodes using this new information. Information updating can be conducted using assumed values instead of observed values to support scenario planning.
- The framework developed in this study is not site-specific and can be applied to different case study locations. Furthermore, the input parameters to this model are storm parameters, river flow, and tidal elevation, which are readily

available. Therefore, after building a probabilistic model using the framework developed in this study, the Bayesian model can be run for different scenarios with short computation time. After introducing the input parameters to the model and running the probabilistic model, a probability distribution will be generated for the target variable (i.e., total river discharge).

5.3 *Future research*

Several aspects of this study can be expanded in future works to achieve a more realistic assessment of flood hazards. The following is a list of recommended directions for future research:

1. The developed framework starts with introducing storm parameters, tidal elevations, and concurrent river flow to the BN. When storms are observed and are predicted to make landfall, National Hurricane Center (NHC) releases predictions related to storm parameters that can be used as input to the developed model in this study. However, there is a level of uncertainty related to these predictions. To make the probabilistic assessment in this study more robust, one step could be incorporating the uncertainty in predicted hurricane parameters into the developed framework.
2. This study has considered the annual occurrence rate for hurricanes affecting the area. This hurricane annual occurrence rate was used for generation of hazard curve and was multiplied by the probability of exceedance of total river discharge to estimate annual exceedance rate. However, due to climate change,

there is a nonstationary trend in hurricane occurrence rate. Therefore, a dynamic framework that accounts for the climate change effect on the frequency of hurricane events can provide a more robust assessment of flood hazards. Consequently, an additional step to this study will be incorporating the effect of climate change on the annual occurrence rate of hurricanes.

3. This study considered four flood mechanisms in the analysis (storm surge, tides, river flow, and precipitation) that can contribute to river discharge. However, other flood severity parameters could also be incorporated into the analysis, such as water elevation and wave runup. Furthermore, even though this developed framework is for the coastal case study, similar Bayesian frameworks may be adapted for inland case studies and urban flooding.
4. This study aimed to develop a framework for the probabilistic assessment of MMFs. This framework was based on a Bayesian approach. These conditional distributions required by the model are estimated using five efficient predictive models. Even though these models were tested for accuracy and reasonableness, the focus of this study was on framework development instead of the high accuracy of the predictive models. Therefore, this study was conducted using simplified assumptions and predictive models that were computationally justifiable. One of these assumptions was simplifying the interaction between storm surge, river flow, and precipitation-induced discharge and simply adding them up. However, the application of complex hydraulic and hydrodynamic models as predictive models can increase the accuracy of the results and capture the complex interaction between multiple flood mechanisms.

5. In this study, the GeNie modeler was used to model different BN nodes and their relationships. In this model, corresponding values related to each node were defined as discrete values, which introduces a discretization error. Some solutions for decreasing this error could be the increasing number of discretized bins and using Monte Carlo simulation to generate a large sample inside each bin. However, these strategies increase computational effort noticeably. Therefore, an important area for further research could be defining a structured method for the discretization of random variables which is efficient and accurate. A sensitivity analysis is suggested to achieve this optimal discretization method.

Acknowledgement and Disclaimer

This work was supported by the U.S. Nuclear Regulatory Commission (NRC) Office of Nuclear Regulatory Research through Oak Ridge National Laboratory as part of the NRC Probabilistic Flood Hazard Assessment Research Program. Any opinions, findings, and conclusions expressed in this dissertation are those of the authors and do not necessarily reflect the views of the funding agency or any other organization.

Appendices

Appendix 1: Summary of Reviewed Research Studies

This appendix presents summaries of existing research studies, broken down by flooding type. Table 1 summarizes studies that addresses coastal flooding mechanisms. Tables 2 and 3 summarize studies that address coastal mechanisms along with fluvial and pluvial flooding mechanisms, respectively. Table 4 summarizes studies that address fluvial flooding mechanisms.

Notes regarding the tables:

- The entry “—” under the column “Flood-forcing mechanism” is used to indicate that information was not explicitly stated in the subject paper or that the information is otherwise not available or applicable for the study. In some cases, the flood-forcing phenomena listed in this table is based on the judgment of this report’s authors regarding the flood-forcing of relevance to the process under consideration in a particular study.
- Different terminology is used across the literature to describe flood-forcing phenomena, mechanisms, and severity (including multiple terms used to describe similar metrics). In the tables, terms used to describe flood-forcing phenomena, mechanisms, and severity metrics are taken from the source papers. To link to the MMF Framework and terminology, the flood mechanism as described in that terminology is shown in the column “MMF Term Flood Mechanism.”
- The column labeled “Joint Probability Approach” identifies which of the joint probability approaches introduced in Section 2.3 are applicable to the study being summarized. When the study does not utilize one of the approaches noted in Section

2.3, the statistical method is identified as “n/a” (not applicable) and a note is included regarding the alternate focus of the paper. Studies not directly related to statistical methods are included in this table because they are judged to provide information/insights, building blocks, or formulations that may be relevant to addressing Compound floods.

Table 2: Summary of research studies for coastal flood type

Reference	Flood-forcing Phenomena	Flood Mechanism	Flood Severity Metric	MMF Term Flood Mechanism	Joint Probability Approach	Data Sources	Case Study / Focus Area	Models and Software
(De Michele et al. 2007)	Sea storm	Surge, waves	Sea Storm Magnitude (function of significant wave height and storm duration)	Storm Surge, Waves	Copula-based approach	Wave buoy data	Sardinia, Italy	—
(Hawkes et al. 2002b)	Meteorological conditions (wind), astronomic forces	Sea water level (storm surge, waves, tides)	Water level, wave height, wave period, overtopping rate	Storm surge, waves, tides	Fitting of Parametric Joint Distributions [also used stochastic simulation; Monte Carlo]	Observed data, hindcasting, synthetic data	Locations around England and Wales	—
(Kowalik and Proshutinsky 2010)	Earthquake in water bodies, astronomic forces	Tsunami, tide	Sea level	Tsunami, tide	n/a [Process-based, Numerical model addressing interactions of tide and tsunami]	Empirical/simulated data	Cook Inlet in Alaska	—
(Masina et al. 2015)	Meteorological conditions (strong onshore winds and low atmospheric pressure systems.), astronomical forces	Sea level and waves	Peak Water level, Significant Wave Height	Storm surge, waves, tides	Copula-based approach	Observed data from meteorological-marine database operated by the Hydro-Meteorological and Climate Service of ARPA	Ravenna coast in Italy	—
(Orton et al. 2016)	Tropical cyclones and extratropical cyclones	Storm tide	Water level	Storm surge, wave, tide	Statistical analysis using the results of the physical models and extreme value analysis	Extratropical storm set and tide gauge data, historical tropical cyclone data	New York Harbor	The Stevens ECOM (sECOM) three-dimensional hydrodynamic model

Table 1: Continued

Reference	Flood-forcing Phenomena	Flood Mechanism	Flood Severity Metric	MMF Term Flood Mechanism	Joint Probability Approach	Data Sources	Case Study / Focus Area	Models and Software
(Tebaldi et al. 2012)	Storms, SLR forcing, astronomic forces	Storm, tide, sea level rise	Water level	Storm surge, waves, tide, sea level rise	n/a [EVA considering impacts of SLR on water levels]	Hourly and monthly tide records	Coasts of the contiguous U.S.	—
(Toro et al. 2008)	Hurricane	Storm surge	Water level	Storm surge	[compares JPM and JPM-OS methods]	Historical/synthetic storm data	Mississippi coast	—
(Vitousek et al. 2017)	Coastal storms/ meteorological conditions, astronomical forces, SLR forcing	Wave (runup = setup + swash), storm surge, tide, sea level rise	Total water level	Rainfall-runoff processes– river flow, storm surge, wave, tides, sea level rise	n/a [EVA considering impacts of SLR on water levels]	Reanalysis data and model results	Global-scale	—
(Wadey et al. 2015)	Winter sea storm, astronomical forces	Storm surge, waves and tides	Sea level and significant wave height	Storm surge, waves, tides	Parametric joint distribution [Bivariate normal distribution]	Tide gauge records and wave buoy data	United Kingdom coastal regions (Sefton in northwest coast; and Suffolk in east coast)	—
(Zhang et al. 2011)	Earthquake in water bodies, astronomical forces	Tsunami, tide	Wave runup, inundation extent	Tsunami, tide	n/a [Process-based, numerical model addressing interactions of tides and tsunamis]	Observed tide and wave data	Prince William Sound Earthquake in the Gulf of Alaska	SELFEE

Table 3: Summary of research studies for coastal and fluvial flood type

Reference	Flood-forcing Phenomena	Flood Mechanism	Flood Severity Metric	MMF Term Flood Mechanism	Joint Probability Approach	Data Sources	Case Study / Focus Area	Models and Software
(Bass and Bedient 2018)	Tropical cyclones	Sea level (surge, tide), precipitation-induced runoff	Peak inundation levels	Rainfall-runoff processes– river flow, storm surge, wind	Bayesian-motivated approach [Surrogate modeling focus]	Gridded hourly observed rainfall, observed river streamflow and stage (for validation); HURDAT tropical cyclone parameters; synthetic storms and flood peaks	Southeast Houston, Texas	HEC-HMS, ADCIRC and SWAN, HEC-RAS
(Bevacqua et al. 2017)	Low-pressure system, winds	Sea level (surge, tide), precipitation-induced runoff	Flood level	Rainfall-runoff processes– river, storm surge	Copula-based approach (pair-copula construction)	Daily winter season water level; reanalysis dataset	Ravenna (Italy)	—
(Bunya et al. 2010)	Hurricane, astronomical forcing	River flow, tide, wind, wave, and storm surge	Water level	Rainfall-runoff processes– river, storm surge, wave, tide	n/a [Process-based, Numerical method; (coupled model for simulation of river flow, tide, wind waves and storm surge)]	Anemometers, airborne and land-based Doppler radar, airborne stepped-frequency microwave radiometer, buoys, ships, aircraft, coastal stations, satellite measurements, and observed water marks	Southern Mississippi and Louisiana	Wave Model (WAM) offshore and Steady- State Irregular Wave (STWAVE), Advanced Circulation (ADCIRC) model

Table 2: Continued

Reference	Flood-forcing Phenomena	Flood Mechanism	Flood Severity Metric	MMF Term Flood Mechanism	Joint Probability Approach	Data Sources	Case Study / Focus Area	Models and Software
(Chen and Liu 2014)	Typhoons, monsoon (or other rain inducing storms)	River flow (runoff-induced flooding), tides and storm surge	Flood depth, inundation area	Rainfall-runoff processes– river, storm surge, tides	n/a [Process-based methods, Numerical model; considered scenarios involving a historical typhoon and concurrent river floods with specified return periods]	Observed data related to Typhoon Krosa (2007), Typhoon Kalmagei (2008), and Typhoon Morakot (2009)	Tsengwen River basin and neighboring coastal area in southern Taiwan	SELFE
(Kew et al. 2013)	Meteorological conditions	Surge and precipitation-induced runoff	Winds and n-day precipitation (proxies for storm surge and river discharge)	Rainfall-runoff processes– river flow, storm surge, tides	n/a [Statistical analysis addressing conditional probability of winds and surge given occurrence of extreme precipitation]	ESSENCE synthetic data set	Rhine delta in the Netherlands	ECHAM5/MPI-OM coupled global climate model
(Lian et al. 2012)	Typhoon and astronomical forcing	Typhoon-induced precipitation and tide level (storm tide)	ratio of the flooded length of the rivers to the total length of the rivers	Rainfall-runoff processes– river flow, storm surge, tide	Copula-based approach (optimal copula)	Precipitation and tidal level records	Fuzhou city on southeast coast of China	HEC-RAS

Table 2: Continued

Reference	Flood-forcing Phenomena	Flood Mechanism	Flood Severity Metric	MMF Term Flood Mechanism	Joint Probability Approach	Data Sources	Case Study / Focus Area	Models and Software
(Moftakhari et al. 2017)	Storms, astronomical forces, SLR forcing	Fluvial flow, surge, tide, and sea level rise	Water level	Rainfall-runoff processes– river flow, storm surge, tides, sea level rise	Copula-based approach	Hourly (coastal) water levels, daily river flow, and future local sea level rise (SLR) projections	Multiple coastal estuaries, USA	—
(Orton et al. 2018)	Tropical, wet extratropical and extratropical cyclones, SLR forcing	Storm tide, river flow, sea level rise	Water level	Rainfall-runoff processes– river flow, storm surge, tide, sea level rise	Statistical analysis involving combination of numerical modeling, Bayesian-motivated approaches, and extreme value analysis	HURDAT2 TC data, USGS river gauge flow data, meteorological reanalysis data	Hudson River, USA	The Stevens ECOM (sECOM) three-dimensional hydrodynamic model
(Petroliaqkis 2018)	Weather event	Storm surge and wave	—	Rainfall-runoff processes– river, storm surge, wave	n/a [Analysis of statistical dependence between quantities]	Hindcast wind and pressure field data	32 rivers along European coasts	Delf3D-Flow
(Serafin et al. 2019)	Oceanographic and riverine processes	Fluvial (river) flow and coastal water level	Water levels	Rainfall-runoff processes– river flow, storm surge, wave	n/a [Process model involving numerical model, machine learning, probabilistic simulation model]	Hourly discharge and stage observations; hourly still water level	Washington state coast	HEC-RAS

Table 2: Continued

Reference	Flood-forcing Phenomena	Flood Mechanism	Flood Severity Metric	MMF Term Flood Mechanism	Joint Probability Approach	Data Sources	Case Study / Focus Area	Models and Software
(Svensson and Jones 2002)	Mid-latitude cyclones	Sea surge, precipitation-induced runoff, tide	Flow and surge residuals	Rainfall-runoff processes—river flow, storm surge, wave, tide	n/a [Analysis of statistical dependence between (extremal) quantities]	Daily mean river flows; daily precipitation observations; hourly sea surge and total sea levels	Eastern Britain	—
(Svensson and Jones 2004)	Mid-latitude cyclones	Sea surge, precipitation-induced runoff, tide	Flow and Surge Residuals	Rainfall-runoff processes—river flow, storm surge, wave, tide	n/a [Analysis of statistical dependence between (extremal) quantities]	Hourly sea surge and total sea level; daily river flow data; daily precipitation data	Coastal areas located in south and west Britain	—
(van den Hurk et al. 2015)	Meteorological condition, astronomical forcing	Storm surge and precipitation-induced runoff, tides	Water level	Rainfall-runoff processes—river flow, storm surge, wave, tides	Empirical joint distributions [Statistical and process-based method using regional climate model]	Observations from in situ stations and rainfall radar data, local surge data	Netherlands	—
(Ward et al. 2018)	Coastal and inland storms	Surge, river flow	Water level, (skew surge), peak discharge	Rainfall-runoff processes—river flow, storm surge, waves	Copula-based method	Observations of high sea levels and high river discharge	Global	—

Table 2: Continued

Reference	Flood-forcing Phenomena	Flood Mechanism	Flood Severity Metric	MMF Term Flood Mechanism	Joint Probability Approach	Data Sources	Case Study / Focus Area	Models and Software
(Zheng et al. 2014)	Hurricane, meteorological conditions	Runoff-induced flooding and surge	Flood level	Rainfall-runoff processes– river flow, storm surge	n/a [Extremal dependence study using multiple statistical assessments]	Synthetic data sets; daily rainfall gauges and the storm tide gauge (case study)	Hawkesbury-Nepean catchment, north of Sydney, Australia	—
(Zhong et al. 2013)	Astronomical forces, meteorological conditions, SLR forcing, operations	Astronomical tide, wind-induced storm surge, fluvial (river) flow	Water levels	Rainfall-runoff processes– river flow, storm surge, wave, tides, snowmelt, river structure operations, sea level rise	Copula-based approach [also used Monte Carlo simulation]	Observed sea level; predicted astronomic tidal level; observed discharges	Lower Rhine Delta (Europe)	—

Table 4: Summary of research studies for coastal and pluvial flood type

Reference	Flood-forcing Phenomena	Flood Mechanism	Flood Severity Metric	MMF Term Flood Mechanism	Joint Probability Approach	Data Sources	Case Study / Focus Area	Models and Software
(Archetti et al. 2011)	Storms, astronomical forces	Sea level (storm surge, tide, waves), precipitation	Number of flooded nodes	Rainfall-runoff processes, storm surge, wave, tide	Copula-based approach	Regional tide gauge, observed data for rainfall and sea level	Drainage system along the Adriatic coast in Italy	—
(Langousis and Veneziano 2009)	Hurricane	Hurricane-induced precipitation	—	Rainfall-runoff processes	n/a [Combined process-based (physics-based) and statistical model of hurricane precipitation as a function of multiple hurricane parameters]	Precipitation radar data	New Orleans	—
(Lin et al. 2010)	Tropical cyclone	Rainfall, surge, and tides (storm tide)	—	Storm surge, tide, rainfall-runoff processes– river flow	n/a [Process-based, numerical model addressing hurricane rainfall, winds, and surge]	Surge gauge data, radar rainfall fields, time-series related to local wind from stations located at the coastal area	Hurricane Isabel (2003) and the urbanized coastal area located in the Chesapeake Bay watershed	2-dimensional Advanced Circulation Model (ADCIRC)
(Lonfat et al. 2007)	Hurricane	Precipitation-induced runoff	—	Rainfall-runoff processes– river flow	n/a [Parametric hurricane rainfall model (PHRAM)]	Gridded rainfall data (rain gauges), radar data	All storms that made landfall along U.S. coasts in 2004	—
(Lu et al. 2012)	Tropical cyclone	Runoff-induced flooding	Discharge	Rainfall-runoff processes– river flow	n/a [Process- and physics-based model of hurricane-induced rainfall]	Outputs from WRF model	Hurricanes Isabel (2003) and Irene (2011), Delaware River Basin	CUENCAS
(Wahl et al. 2015b)	Hurricane	Storm surge and precipitation	—	Storm surge, rainfall-runoff processes– river	Copula-based approach	Storm surge; mean daily precipitation data	Contiguous U.S.	—
(Zheng et al. 2013)	Cyclonic systems	Storm surge and precipitation	—	Storm surge, Rainfall-runoff processes– river flow	n/a [Dependence study involving bivariate logistic threshold-excess model]	Processed tide level data daily precipitation data	Australian coast	—

Table 5: Summary of research studies for fluvial flood type

Reference	Flood-forcing Phenomena	Flood Mechanism	Flood Severity Metric	MMF Term Flood Mechanism	Joint Probability Approach	Data Sources	Case Study / Focus Area	Models and Software
(Bender et al. 2016)	Winter storm and snowmelt	Runoff-induced flooding	Flood level, discharge	Rainfall-runoff processes– river flow	Copula-based approach	Daily mean discharge time-series	Rhine and Sieg rivers (Germany)	Hydro_AS-2D
(Gilja et al. 2018)	Hydrologic Event (rain and snowmelt)	Runoff-induced flooding	Flood discharge	Rainfall-runoff processes– river flow	Copula-based approach	Measured river discharge data	Sava River (a tributary of Danube River)	—
(Kao and Chang 2012)	—	Runoff-induced flooding	Peak streamflow discharge,	Rainfall-runoff processes– river flow	Copula-based approach (Gaussian copulas)	Peak annual and daily discharge data	Nashville, Tennessee	—
(Sui and Koehler 2001)	Precipitation-producing events	Precipitation on snow and snow melt	Runoff depth, peak discharge	Rainfall-runoff processes– river, rain-on-snow, snowmelt	n/a [Statistical analysis (EVA) of rain-on-snow events]	Average monthly and annual precipitation data, snow depth and snow water equivalent data; discharge	A forest region located in Southern Germany	—
(Wang et al. 2009)	—	Runoff-induced flooding	Discharge	Rainfall-runoff processes– river	Copula-based approach (Archimedean copulas)	Daily/hourly observed data for flow rate	Des Moines River in Iowa	—

Bibliography

- Al Kajbaf, A., and M. Bensi. 2020. "Application of surrogate models in estimation of storm surge: A comparative assessment." *Applied Soft Computing*, 91: 106184. <https://doi.org/10.1016/j.asoc.2020.106184>.
- Angelikopoulos, P., C. Papadimitriou, and P. Koumoutsakos. 2012. "Bayesian uncertainty quantification and propagation in molecular dynamics simulations: A high performance computing framework." *J. Chem. Phys.*, 137 (14): 144103. American Institute of Physics. <https://doi.org/10.1063/1.4757266>.
- Annaka, T., K. Satake, T. Sakakiyama, K. Yanagisawa, and N. Shuto. 2007. "Logic-tree Approach for Probabilistic Tsunami Hazard Analysis and its Applications to the Japanese Coasts." *Tsunami and Its Hazards in the Indian and Pacific Oceans*, Pageoph Topical Volumes, K. Satake, E. A. Okal, and J. C. Borrero, eds., 577–592. Basel: Birkhäuser.
- Archetti, R., A. Bolognesi, A. Casadio, and M. Maglionico. 2011. "Development of flood probability charts for urban drainage network in coastal areas through a simplified joint assessment approach." *Hydrology and Earth System Sciences*, 15 (10): 3115–3122. <https://doi.org/10.5194/hess-15-3115-2011>.
- Baker, J. 2008. "An Introduction to Probabilistic Seismic Hazard Analysis (PSHA), Ver. 1.3."
- Balakrishnan, N., and C. D. Lai. 2009. *Continuous bivariate distributions*. Dordrecht ; New York: Springer.
- Bass, B., and P. Bedient. 2018. "Surrogate modeling of joint flood risk across coastal watersheds." *Journal of Hydrology*, 558: 159–173. <https://doi.org/10.1016/j.jhydrol.2018.01.014>.
- Bender, J., T. Wahl, A. Müller, and J. Jensen. 2016. "A multivariate design framework for river confluences." *Hydrological Sciences Journal*, 61 (3): 471–482. <https://doi.org/10.1080/02626667.2015.1052816>.
- Bensi, M., A. D. Kiureghian, and D. Straub. 2013. "Efficient Bayesian network modeling of systems." *Reliability Engineering & System Safety*, 112: 200–213. <https://doi.org/10.1016/j.ress.2012.11.017>.
- Bensi, M., S. Mohammadi, S.-C. Kao, and S. T. DeNeale. 2020. "Multi-Mechanism Flood Hazard Assessment: Critical Review of Current Practice and Approaches." Oak Ridge National Lab. (ORNL), Oak Ridge, TN (United States), ORNL/TM-2020/1447, doi: 10.2172/1637939.
- Bensi, M. T., and K. M. Groth. 2020. "On the value of data fusion and model integration for generating real-time risk insights for nuclear power reactors." *Progress in Nuclear Energy*, 129: 103497. <https://doi.org/10.1016/j.pnucene.2020.103497>.
- Berghuijs, W. R., S. Harrigan, P. Molnar, L. J. Slater, and J. W. Kirchner. 2019. "The Relative Importance of Different Flood-Generating Mechanisms Across

- Europe.” *Water Resources Research*, 55 (6): 4582–4593.
<https://doi.org/10.1029/2019WR024841>.
- Bermúdez, M., J. F. Farfán, P. Willems, and L. Cea. 2021. “Assessing the Effects of Climate Change on Compound Flooding in Coastal River Areas.” *Water Resources Research*, 57 (10): e2020WR029321.
<https://doi.org/10.1029/2020WR029321>.
- Bevacqua, E., D. Maraun, I. Hobæk Haff, M. Widmann, and M. Vrac. 2017. “Multivariate statistical modelling of compound events via pair-copula constructions: analysis of floods in Ravenna (Italy).” *Hydrology and Earth System Sciences*, 21 (6): 2701–2723. <https://doi.org/10.5194/hess-21-2701-2017>.
- Bevacqua, E., M. I. Vousdoukas, T. G. Shepherd, and M. Vrac. 2020. “Brief communication: The role of using precipitation or river discharge data when assessing global coastal compound flooding.” *Natural Hazards and Earth System Sciences*, 20 (6): 1765–1782. Copernicus GmbH.
<https://doi.org/10.5194/nhess-20-1765-2020>.
- Bevacqua, E., M. I. Vousdoukas, G. Zappa, K. Hodges, T. G. Shepherd, D. Maraun, L. Mentaschi, and L. Feyen. 2020. “More meteorological events that drive compound coastal flooding are projected under climate change.” *Commun Earth Environ*, 1 (1): 1–11. Nature Publishing Group.
<https://doi.org/10.1038/s43247-020-00044-z>.
- Brody, S. D., S. Zahran, W. E. Highfield, H. Grover, and A. Vedlitz. 2008. “Identifying the impact of the built environment on flood damage in Texas.” *Disasters*, 32 (1): 1–18. <https://doi.org/10.1111/j.1467-7717.2007.01024.x>.
- Brussee, A. R., J. D. Bricker, K. M. De Bruijn, G. F. Verhoeven, H. C. Winsemius, and S. N. Jonkman. 2021. “Impact of hydraulic model resolution and loss of life model modification on flood fatality risk estimation: Case study of the Bommelerwaard, The Netherlands.” *Journal of Flood Risk Management*, 14 (3): e12713. <https://doi.org/10.1111/jfr3.12713>.
- Bunya, S., J. C. Dietrich, J. J. Westerink, B. A. Ebersole, J. M. Smith, J. H. Atkinson, R. Jensen, D. T. Resio, R. A. Luettich, C. Dawson, V. J. Cardone, A. T. Cox, M. D. Powell, H. J. Westerink, and H. J. Roberts. 2010. “A High-Resolution Coupled Riverine Flow, Tide, Wind, Wind Wave, and Storm Surge Model for Southern Louisiana and Mississippi. Part I: Model Development and Validation.” *Monthly Weather Review*, 138 (2): 345–377.
<https://doi.org/10.1175/2009MWR2906.1>.
- Chen, W.-B., and W.-C. Liu. 2014. “Modeling Flood Inundation Induced by River Flow and Storm Surges over a River Basin.” *Water*, 6 (10): 3182–3199.
<https://doi.org/10.3390/w6103182>.
- Cheung, S. H., T. A. Oliver, E. E. Prudencio, S. Prudhomme, and R. D. Moser. 2011. “Bayesian uncertainty analysis with applications to turbulence modeling.” *Reliability Engineering & System Safety*, Quantification of Margins and Uncertainties, 96 (9): 1137–1149. <https://doi.org/10.1016/j.ress.2010.09.013>.
- Cialone, M., C. Massey, M. Anderson, A. Grzegorzewski, R. Jensen, A. Cialone, D. Mark, D. Pevey, B. GUNKEL, T. Mcalpin, N. C. Nadal-Caraballo, J. Melby,

- and J. Ratcliff. 2015. *North Atlantic Coast Comprehensive Study (NACCS) – Coastal Storm Model Simulations: Waves and Water Levels*.
- Cigler, B. A. 2017. “U.S. Floods: The Necessity of Mitigation.” *State and Local Government Review*, 49 (2): 127–139. SAGE Publications Inc. <https://doi.org/10.1177/0160323X17731890>.
- Couason, A., A. Sebastian, and O. Morales-Nápoles. 2018. “A Copula-Based Bayesian Network for Modeling Compound Flood Hazard from Riverine and Coastal Interactions at the Catchment Scale: An Application to the Houston Ship Channel, Texas.” *Water*, 10 (9): 1190. Multidisciplinary Digital Publishing Institute. <https://doi.org/10.3390/w10091190>.
- Crawford, S. E., M. Brinkmann, J. D. Ouellet, F. Lehmkuhl, K. Reicherter, J. Schwarzbauer, P. Bellanova, P. Letmathe, L. M. Blank, R. Weber, W. Brack, J. T. van Dongen, L. Menzel, M. Hecker, H. Schüttrumpf, and H. Hollert. 2022. “Remobilization of pollutants during extreme flood events poses severe risks to human and environmental health.” *Journal of Hazardous Materials*, 421: 126691. <https://doi.org/10.1016/j.jhazmat.2021.126691>.
- De Michele, C., G. Salvadori, G. Passoni, and R. Vezzoli. 2007. “A multivariate model of sea storms using copulas.” *Coastal Engineering*, 54 (10): 734–751. <https://doi.org/10.1016/j.coastaleng.2007.05.007>.
- Ding, J. 2010. “Probabilistic Inferences in Bayesian Networks.” <https://doi.org/10.5772/46968>.
- Eilander, D., A. Couason, H. Ikeuchi, S. Muis, D. Yamazaki, H. C. Winsemius, and P. J. Ward. 2020. “The effect of surge on riverine flood hazard and impact in deltas globally.” *Environ. Res. Lett.*, 15 (10): 104007. <https://doi.org/10.1088/1748-9326/ab8ca6>.
- England Jr., J. F., T. A. Cohn, B. A. Faber, J. R. Stedinger, W. O. Thomas Jr., A. G. Veilleux, J. E. Kiang, and R. R. Mason, Jr. 2019. *Guidelines for determining flood flow frequency—Bulletin 17C. Guidelines for determining flood flow frequency—Bulletin 17C*, Techniques and Methods, 168. USGS Numbered Series. Reston, VA: U.S. Geological Survey.
- Fan, Y. R., L. Yu, X. Shi, and Q. Y. Duan. 2021a. “Tracing Uncertainty Contributors in the Multi-Hazard Risk Analysis for Compound Extremes.” *Earth’s Future*, 9 (12): e2021EF002280. <https://doi.org/10.1029/2021EF002280>. <https://doi.org/10.1016/j.jhydrol.2021.126406>.
- Flath, H. P., L. C. Wilcox, V. Akçelik, J. Hill, B. van Bloemen Waanders, and O. Ghattas. 2011. “Fast Algorithms for Bayesian Uncertainty Quantification in Large-Scale Linear Inverse Problems Based on Low-Rank Partial Hessian Approximations.” *SIAM J. Sci. Comput.*, 33 (1): 407–432. Society for Industrial and Applied Mathematics. <https://doi.org/10.1137/090780717>.
- Gall, M., T. L. Sheldon, and L. Collins. n.d. “The economic impact of school closures during the 2015 flood in Richland County, South Carolina.” *Risk, Hazards & Crisis in Public Policy*, n/a (n/a). <https://doi.org/10.1002/rhc3.12242>.
- Genest, C., and A.-C. Favre. 2007. “Everything You Always Wanted to Know about Copula Modeling but Were Afraid to Ask.” *Journal of Hydrologic Engineering*, 12 (4).

- “GeNIe Modeler – BayesFusion.” 2022. Accessed June 16, 2022.
<https://www.bayesfusion.com/genie/>.
- Ghanbari, M., M. Arabi, S.-C. Kao, J. Obeysekera, and W. Sweet. 2021. “Climate Change and Changes in Compound Coastal-Riverine Flooding Hazard Along the U.S. Coasts.” *Earth’s Future*, 9 (5): e2021EF002055.
<https://doi.org/10.1029/2021EF002055>.
- Gilja, G., E. Ocvirk, and N. Kuspilić. 2018. “Joint probability analysis of flood hazard at river confluences using bivariate copulas.” *Građevinar*, 70 (04): 267–275. <https://doi.org/10.14256/JCE.2173.2017>.
<https://doi.org/10.14256/jce.2173.2017>.
- Gori, A., N. Lin, and D. Xi. 2020. “Tropical Cyclone Compound Flood Hazard Assessment: From Investigating Drivers to Quantifying Extreme Water Levels.” *Earth’s Future*, 8 (12): e2020EF001660.
<https://doi.org/10.1029/2020EF001660>.
- Hallegatte, S., C. Green, R. J. Nicholls, and J. Corfee-Morlot. 2013. “Future flood losses in major coastal cities.” *Nature Climate Change*, 3 (9): 802–806. Nature Publishing Group. <https://doi.org/10.1038/nclimate1979>.
- Harris, R., E. Furlan, H. Vuong Pham, S. Torresan, J. Mysiak, and A. Critto. 2021. “A Bayesian network approach for multi-sectoral flood damage assessment and multi-scenario analysis.” EGU21-14996.
- Haugh, M. 2016. “An Introduction to Copulas.”
- Hawkes, P. J. 2008. “Joint probability analysis for estimation of extremes.” *Journal of Hydraulic Research*, 46 (sup2): 246–256.
<https://doi.org/10.1080/00221686.2008.9521958>.
- Hawkes, P. J., B. P. Gouldby, J. A. Tawn, and M. W. Owen. 2002. “The joint probability of waves and water levels in coastal engineering design.” *Journal of Hydraulic Research*, 40 (3): 241–251.
<https://doi.org/10.1080/00221680209499940>.
- “HEC-HMS.” Accessed February 23, 2022.
<https://www.hec.usace.army.mil/software/hec-hms/>.
- Helderop, E., and T. H. Grubestic. 2019. “Hurricane storm surge in Volusia County, Florida: evidence of a tipping point for infrastructure damage.” *Disasters*, 43 (1): 157–180. <https://doi.org/10.1111/disa.12296>.
- Hill, T. U. of N. C. at C. n.d. “- ADCIRC.” Accessed February 23, 2022.
<https://adcirc.org/>.
- Hsiao, S.-C., W.-S. Chiang, J.-H. Jang, H.-L. Wu, W.-S. Lu, W.-B. Chen, and Y.-T. Wu. 2021. “Flood risk influenced by the compound effect of storm surge and rainfall under climate change for low-lying coastal areas.” *Science of The Total Environment*, 764: 144439.
<https://doi.org/10.1016/j.scitotenv.2020.144439>.
- Hsieh, B., and J. Ratcliff. 2013. “Coastal Hurricane Inundation Prediction for Emergency Response Using Artificial Neural Networks.” *Engineering Applications of Neural Networks, Communications in Computer and Information Science*, L. Iliadis, H. Papadopoulos, and C. Jayne, eds., 102–111. Berlin, Heidelberg: Springer.

- Hsu, C.-H., F. Olivera, and J. L. Irish. 2018. "A hurricane surge risk assessment framework using the joint probability method and surge response functions." *Nat Hazards*, 91 (1): 7–28. <https://doi.org/10.1007/s11069-017-3108-8>.
- Hu, X., M. Wang, K. Liu, D. Gong, and H. Kantz. 2021. "Using Climate Factors to Estimate Flood Economic Loss Risk." *Int J Disaster Risk Sci*, 12 (5): 731–744. <https://doi.org/10.1007/s13753-021-00371-5>.
- Huang, W., F. Ye, Y. J. Zhang, K. Park, J. Du, S. Moghimi, E. Myers, S. Pe'eri, J. R. Calzada, H. C. Yu, K. Nunez, and Z. Liu. 2021. "Compounding factors for extreme flooding around Galveston Bay during Hurricane Harvey." *Ocean Modelling*, 158: 101735. <https://doi.org/10.1016/j.ocemod.2020.101735>.
- Huard, D., and A. Mailhot. 2008. "Calibration of hydrological model GR2M using Bayesian uncertainty analysis." *Water Resources Research*, 44 (2). <https://doi.org/10.1029/2007WR005949>.
- van den Hurk, B., E. van Meijgaard, P. de Valk, K.-J. van Heeringen, and J. Gooijer. 2015. "Analysis of a compounding surge and precipitation event in the Netherlands." *Environmental Research Letters*, 10 (3): 035001. <https://doi.org/10.1088/1748-9326/10/3/035001>.
- Jalili Pirani, F., and M. R. Najafi. 2020. "Recent Trends in Individual and Multivariate Compound Flood Drivers in Canada's Coasts." *Water Resources Research*, 56 (8): e2020WR027785. <https://doi.org/10.1029/2020WR027785>.
- Jane, R., L. Cadavid, J. Obeysekera, and T. Wahl. 2020. "Multivariate statistical modelling of the drivers of compound flood events in south Florida." *Natural Hazards and Earth System Sciences*, 20 (10): 2681–2699. Copernicus GmbH. <https://doi.org/10.5194/nhess-20-2681-2020>.
- Jang, J.-H., and T.-H. Chang. 2022. "Flood risk estimation under the compound influence of rainfall and tide." *Journal of Hydrology*, 606: 127446. <https://doi.org/10.1016/j.jhydrol.2022.127446>.
- Jelesnianski, C. P. 1992. *SLOSH: Sea, Lake, and Overland Surges from Hurricanes*. U.S. Department of Commerce, National Oceanic and Atmospheric Administration, National Weather Service.
- Jensen, F. 1996. *An Introduction To Bayesian Networks*. Taylor & Francis.
- Jia, G., and A. A. Taflanidis. 2013. "Kriging metamodeling for approximation of high-dimensional wave and surge responses in real-time storm/hurricane risk assessment." *Computer Methods in Applied Mechanics and Engineering*, 261–262: 24–38. <https://doi.org/10.1016/j.cma.2013.03.012>.
- Jia, G., A. A. Taflanidis, N. C. Nadal-Caraballo, J. A. Melby, A. B. Kennedy, and J. M. Smith. 2016. "Surrogate modeling for peak or time-dependent storm surge prediction over an extended coastal region using an existing database of synthetic storms." *Nat Hazards*, 81 (2): 909–938. <https://doi.org/10.1007/s11069-015-2111-1>.
- Kao, S.-C., and N.-B. Chang. 2012. "Copula-Based Flood Frequency Analysis at Ungauged Basin Confluences: Nashville, Tennessee." *Journal of Hydrologic Engineering*, 17 (7): 790–799. American Society of Civil Engineers. [https://doi.org/10.1061/\(ASCE\)HE.1943-5584.0000477](https://doi.org/10.1061/(ASCE)HE.1943-5584.0000477).

- Kaplan, J., and M. DeMaria. 1995. "A Simple Empirical Model for Predicting the Decay of Tropical Cyclone Winds after Landfall." *Journal of Applied Meteorology (1988-2005)*, 34 (11): 2499–2512. American Meteorological Society.
- Kaplan, J., and M. Demaria. 2001. "On the Decay of Tropical Cyclone Winds after Landfall in the New England Area." *Journal of Applied Meteorology (1988-2005)*, 40 (2): 280–286. American Meteorological Society.
- Kew, S. F., F. M. Selten, G. Lenderink, and W. Hazeleger. 2013. "The simultaneous occurrence of surge and discharge extremes for the Rhine delta." *Natural Hazards and Earth System Sciences*, 13 (8): 2017–2029. <https://doi.org/10.5194/nhess-13-2017-2013>.
- Kick, E. L., J. C. Fraser, G. M. Fulkerson, L. A. McKinney, and D. H. De Vries. 2011. "Repetitive flood victims and acceptance of FEMA mitigation offers: an analysis with community-system policy implications." *Disasters*, 35 (3): 510–539. <https://doi.org/10.1111/j.1467-7717.2011.01226.x>.
- Kim, S.-W., J. A. Melby, N. C. Nadal-Caraballo, and J. Ratcliff. 2015. "A time-dependent surrogate model for storm surge prediction based on an artificial neural network using high-fidelity synthetic hurricane modeling." *Nat Hazards*, 76 (1): 565–585. <https://doi.org/10.1007/s11069-014-1508-6>.
- Kjærulff, U., and A. Madsen. 2013. *Bayesian networks and influence diagrams. A guide to construction and analysis. 2nd ed.*
- Kjeldsen, T., C. Svensson, and D. Jones. 2010. "A joint probability approach to flood frequency estimation using Monte Carlo simulation." *Proceedings of the BHS Third International Symposium: Role of Hydrology in Managing Consequences of a Changing Global Environment*, C. Kirby, ed., 278–282. Newcastle: British Hydrological Society.
- Koç, G., S. Natho, and A. H. Thielen. 2021. "Estimating direct economic impacts of severe flood events in Turkey (2015–2020)." *International Journal of Disaster Risk Reduction*, 58: 102222. <https://doi.org/10.1016/j.ijdrr.2021.102222>.
- de Kok, T. 2021. "Temporal Assessment of Hybrid Flood Defenses: A Dynamic Bayesian Network."
- Kowalik, Z., and A. Proshutinsky. 2010. "Tsunami–tide interactions: A Cook Inlet case study." *Continental Shelf Research, Tides in Marginal Seas - A special issue in memory of Prof Alexei Nekrasov*, 30 (6): 633–642. <https://doi.org/10.1016/j.csr.2009.10.004>.
- Kumbier, K., R. C. Carvalho, A. T. Vafeidis, and C. D. Woodroffe. 2018. "Investigating compound flooding in an estuary using hydrodynamic modelling: a case study from the Shoalhaven River, Australia." *Natural Hazards and Earth System Sciences*, 18 (2): 463–477. Copernicus GmbH. <https://doi.org/10.5194/nhess-18-463-2018>.
- Kyprioti, A. P., A. A. Taflanidis, M. Plumlee, T. G. Asher, E. Spiller, R. A. Luettich, B. Blanton, T. L. Kijewski-Correa, A. Kennedy, and L. Schmied. 2021. "Improvements in storm surge surrogate modeling for synthetic storm parameterization, node condition classification and implementation to small

- size databases.” *Nat Hazards*, 109 (2): 1349–1386.
<https://doi.org/10.1007/s11069-021-04881-9>.
- Langousis, A., and D. Veneziano. 2009. “Long-term rainfall risk from tropical cyclones in coastal areas.” *Water Resources Research*, 45 (11).
<https://doi.org/10.1029/2008WR007624>.
- Lazin, R., X. Shen, and E. Anagnostou. 2021. “Estimation of flood-damaged cropland area using a convolutional neural network.” *Environ. Res. Lett.*, 16 (5): 054011. IOP Publishing. <https://doi.org/10.1088/1748-9326/abeba0>.
- Lian, J. J., K. Xu, and C. Ma. 2012. “Joint impact of rainfall and tidal level on flood risk in a coastal city with a complex river network: a case study for Fuzhou city, China.” *Hydrology and Earth System Sciences Discussions*, 9 (6): 7475–7505. <https://doi.org/10.5194/hessd-9-7475-2012>.
- Lin, N., J. A. Smith, G. Villarini, T. P. Marchok, and M. L. Baeck. 2010. “Modeling Extreme Rainfall, Winds, and Surge from Hurricane Isabel (2003).” *Weather and Forecasting*, 25 (5): 1342–1361.
<https://doi.org/10.1175/2010WAF2222349.1>.
- Liu, Z., L. Cheng, K. Lin, and H. Cai. 2021. “A hybrid bayesian vine model for water level prediction.” *Environmental Modelling & Software*, 142: 105075.
<https://doi.org/10.1016/j.envsoft.2021.105075>.
- Lonfat, M., R. Rogers, T. Marchok, and F. D. Marks. 2007. “A Parametric Model for Predicting Hurricane Rainfall.” *Monthly Weather Review*, 135 (9): 3086–3097. <https://doi.org/10.1175/MWR3433.1>.
- Lu, C., S. V. P. S. Guo, H. Zenchao, and L. Tianyuan. 2012. “Flood Coincidence Risk Analysis Using Multivariate Copula Functions.” *Journal of Hydrologic Engineering*, 17 (6): 742–755. [https://doi.org/10.1061/\(ASCE\)HE.1943-5584.0000504](https://doi.org/10.1061/(ASCE)HE.1943-5584.0000504).
- Lu, P., N. Lin, K. Emanuel, D. Chavas, and J. Smith. 2018. “Assessing Hurricane Rainfall Mechanisms Using a Physics-Based Model: Hurricanes Isabel (2003) and Irene (2011).” *Journal of the Atmospheric Sciences*, 75 (7): 2337–2358. American Meteorological Society. <https://doi.org/10.1175/JAS-D-17-0264.1>.
- Lu, W., L. Tang, D. Yang, H. Wu, and Z. Liu. 2022. “Compounding Effects of Fluvial Flooding and Storm Tides on Coastal Flooding Risk in the Coastal-Estuarine Region of Southeastern China.” *Atmosphere*, 13 (2): 238. Multidisciplinary Digital Publishing Institute.
<https://doi.org/10.3390/atmos13020238>.
- Lucey, J. T. D., and T. W. Gallien. 2021. “Compound coastal flood risk in a semi-arid urbanized region: The implications of copula choice, sampling, and infrastructure.” *Natural Hazards and Earth System Sciences Discussions*, 1–33. Copernicus GmbH. <https://doi.org/10.5194/nhess-2021-241>.
- Lüdtke, S., K. Schröter, M. Steinhausen, L. Weise, R. Figueiredo, and H. Kreibich. 2019. “A Consistent Approach for Probabilistic Residential Flood Loss Modeling in Europe.” *Water Resources Research*, 55 (12): 10616–10635.
<https://doi.org/10.1029/2019WR026213>.
- Luetlich, R. A. (Richard A., J. J. Westerink, and N. W. Scheffner. 1992. “ADCIRC : an advanced three-dimensional circulation model for shelves, coasts, and

- estuaries. Report 1, Theory and methodology of ADCIRC-2DD1 and ADCIRC-3DL.” *This Digital Resource was created from scans of the Print Resource*. Coastal Engineering Research Center (U.S.).
- Luo, Y., Z. Dong, X. Guan, and Y. Liu. 2019. “Flood Risk Analysis of Different Climatic Phenomena during Flood Season Based on Copula-Based Bayesian Network Method: A Case Study of Taihu Basin, China.” *Water*, 11 (8): 1534. Multidisciplinary Digital Publishing Institute. <https://doi.org/10.3390/w11081534>.
- Lv, H., Y. Meng, Z. Wu, X. Guan, and Y. Liu. 2021. “Construction of flood loss function for cities lacking disaster data based on three-dimensional (object-function-array) data processing.” *Science of The Total Environment*, 773: 145649. <https://doi.org/10.1016/j.scitotenv.2021.145649>.
- Marzocchi, W., M. Taroni, and J. Selva. 2015. “Accounting for Epistemic Uncertainty in PSHA: Logic Tree and Ensemble Modeling.” *Bulletin of the Seismological Society of America*, 105 (4): 2151–2159. GeoScienceWorld. <https://doi.org/10.1785/0120140131>.
- Masina, M., A. Lamberti, and R. Archetti. 2015. “Coastal flooding: A copula based approach for estimating the joint probability of water levels and waves.” *Coastal Engineering*, 97: 37–52. <https://doi.org/10.1016/j.coastaleng.2014.12.010>.
- Mayo, T., and N. Lin. 2019. “The Effect of the Surface Wind Field Representation in the Operational Storm Surge Model of the National Hurricane Center.” *Atmosphere*, 10 (4): 193. Multidisciplinary Digital Publishing Institute. <https://doi.org/10.3390/atmos10040193>.
- Mazzoleni, M., J. Mård, M. Rusca, V. Odongo, S. Lindersson, and G. Di Baldassarre. 2021. “Floodplains in the Anthropocene: A Global Analysis of the Interplay Between Human Population, Built Environment, and Flood Severity.” *Water Resources Research*, 57 (2): e2020WR027744. <https://doi.org/10.1029/2020WR027744>.
- Mileti, D. 1999. *Disasters by Design: A Reassessment of Natural Hazards in the United States*.
- Moftakhari, H. R., G. Salvadori, A. AghaKouchak, B. F. Sanders, and R. A. Matthew. 2017. “Compounding effects of sea level rise and fluvial flooding.” *Proceedings of the National Academy of Sciences*, 114 (37): 9785–9790. <https://doi.org/10.1073/pnas.1620325114>.
- Mohammadi, S., M. Bensi, S.-C. Kao, and S. Deneale. 2021. *Multi-Mechanism Flood Hazard Assessment: Example Use Case Studies*. Oak Ridge National Lab. (ORNL), Oak Ridge, TN (United States).
- Nadal-Caraballo, N. C., J. A. Melby, V. M. Gonzalez, and A. T. Cox. 2015. “Coastal Storm Hazards from Virginia to Maine.” 221.
- Naseri, K., and M. Hummel. 2022. “A Bayesian Copula-Based Nonstationary Framework for Compound Flood Risk Assessment along US Coastlines.” *Journal of Hydrology*, 128005. <https://doi.org/10.1016/j.jhydrol.2022.128005>.

- Nasr, A. A., T. Wahl, M. M. Rashid, P. Camus, and I. D. Haigh. 2021. "Assessing the dependence structure between oceanographic, fluvial, and pluvial flooding drivers along the United States coastline." *Hydrology and Earth System Sciences*, 25 (12): 6203–6222. Copernicus GmbH. <https://doi.org/10.5194/hess-25-6203-2021>.
- Naz, B. S., S.-C. Kao, M. Ashfaq, D. Rastogi, R. Mei, and L. C. Bowling. 2016. "Regional hydrologic response to climate change in the conterminous United States using high-resolution hydroclimate simulations." *Global and Planetary Change*, 143 (C). <https://doi.org/10.1016/j.gloplacha.2016.06.003>.
- Nelsen, R. B. 2002. *Properties and Applications of Copulas: A Brief Survey*.
- Oliver, T. A., and R. D. Moser. 2011. "Bayesian uncertainty quantification applied to RANS turbulence models." *J. Phys.: Conf. Ser.*, 318 (4): 042032. IOP Publishing. <https://doi.org/10.1088/1742-6596/318/4/042032>.
- Orton, P. M., F. R. Conticello, F. Cioffi, T. M. Hall, N. Georgas, U. Lall, A. F. Blumberg, and K. MacManus. 2018. "Flood hazard assessment from storm tides, rain and sea level rise for a tidal river estuary." *Nat Hazards*. <https://doi.org/10.1007/s11069-018-3251-x>.
- Orton, P. M., T. M. Hall, S. A. Talke, A. F. Blumberg, N. Georgas, and S. Vinogradov. 2016. "A validated tropical-extratropical flood hazard assessment for New York Harbor." *Journal of Geophysical Research: Oceans*, 121 (12): 8904–8929. <https://doi.org/10.1002/2016JC011679>.
- Oubeidillah, A. A., S.-C. Kao, M. Ashfaq, B. Naz, and G. Tootle. 2013. "A large-scale, high-resolution hydrological model parameter dataset for climate change impact assessment for the conterminous United States." *Hydrology and Earth System Sciences Discussions*, 10: 9575–9613. <https://doi.org/10.5194/hessd-10-9575-2013>.
- Pappadà, R., F. Durante, G. Salvadori, and C. De Michele. 2018. "Clustering of concurrent flood risks via Hazard Scenarios." *Spatial Statistics*, 23: 124–142. <https://doi.org/10.1016/j.spasta.2017.12.002>.
- Park, Y. H., and D. Youn. 2021. "Characteristics of Storm Surge Based on the Forward Speed of the Storm." *Journal of Coastal Research*, 114 (SI): 71–75. <https://doi.org/10.2112/JCR-SI114-015.1>.
- Rajasekaran, S., S. Gayathri, and T.-L. Lee. 2008. "Support vector regression methodology for storm surge predictions." *Ocean Engineering*, 35 (16): 1578–1587. <https://doi.org/10.1016/j.oceaneng.2008.08.004>.
- Razmkhah, H., A. Fararouie, and A. R. Ravari. 2022. "Multivariate Flood Frequency Analysis Using Bivariate Copula Functions." *Water Resour Manage*, 36 (2): 729–743. <https://doi.org/10.1007/s11269-021-03055-3>.
- Sahana, M., S. Rehman, H. Sajjad, and H. Hong. 2020. "Exploring effectiveness of frequency ratio and support vector machine models in storm surge flood susceptibility assessment: A study of Sundarban Biosphere Reserve, India." *CATENA*, 189: 104450. <https://doi.org/10.1016/j.catena.2019.104450>.
- Saharia, A. M., Z. Zhu, and J. F. Atkinson. 2021. "Compound flooding from lake seiche and river flow in a freshwater coastal river." *Journal of Hydrology*, 603: 126969. <https://doi.org/10.1016/j.jhydrol.2021.126969>.

- Santos, V. M., M. Casas-Prat, B. Poschlod, E. Ragno, B. van den Hurk, Z. Hao, T. Kalmár, L. Zhu, and H. Najafi. 2020. “Multivariate statistical modelling of extreme coastal water levels and the effect of climate variability: a case study in the Netherlands.” *Hydrology and Earth System Sciences Discussions*, 1–25. Copernicus GmbH. <https://doi.org/10.5194/hess-2020-536>.
- Santos, V. M., T. Wahl, R. Jane, S. K. Misra, and K. D. White. 2021. “Assessing compound flooding potential with multivariate statistical models in a complex estuarine system under data constraints.” *Journal of Flood Risk Management*, 14 (4): e12749. <https://doi.org/10.1111/jfr3.12749>.
- Sarhadi, A., D. H. Burn, M. Concepción Ausín, and M. P. Wiper. 2016. “Time-varying nonstationary multivariate risk analysis using a dynamic Bayesian copula.” *Water Resources Research*, 52 (3): 2327–2349. <https://doi.org/10.1002/2015WR018525>.
- Schoppa, L., M. Barendrecht, T. Sieg, N. Sairam, and H. Kreibich. 2021. “Augmenting a Sociohydrological Flood Risk Model for Companies with Process-oriented Loss Estimation.” EGU21-10064. <https://doi.org/10.5194/egusphere-egu21-10064>.
- Schröter, K., S. Lüdtke, R. Redweik, J. Meier, M. Bochow, L. Ross, C. Nagel, and H. Kreibich. 2018. “Flood loss estimation using 3D city models and remote sensing data.” *Environmental Modelling & Software*, 105: 118–131. <https://doi.org/10.1016/j.envsoft.2018.03.032>.
- Sebastian, A., E. J. C. Dupuits, and O. Morales-Nápoles. 2017. “Applying a Bayesian network based on Gaussian copulas to model the hydraulic boundary conditions for hurricane flood risk analysis in a coastal watershed.” *Coastal Engineering*, 125: 42–50. <https://doi.org/10.1016/j.coastaleng.2017.03.008>.
- Serafin, K. A., P. Ruggiero, K. Parker, and D. F. Hill. 2019. “What’s streamflow got to do with it? A probabilistic simulation of the competing oceanographic and fluvial processes driving extreme along-river water levels.” *Nat. Hazards Earth Syst. Sci.*, 19 (7): 1415–1431. <https://doi.org/10.5194/nhess-19-1415-2019>.
- Shashank, V. G., S. Mandal, and S. Sil. 2021. “Impact of varying landfall time and cyclone intensity on storm surges in the Bay of Bengal using ADCIRC model.” *J Earth Syst Sci*, 130 (4): 194. <https://doi.org/10.1007/s12040-021-01695-y>.
- Shrestha, B. B., A. Kawasaki, and W. W. Zin. 2021. “Development of flood damage assessment method for residential areas considering various house types for Bago Region of Myanmar.” *International Journal of Disaster Risk Reduction*, 66: 102602. <https://doi.org/10.1016/j.ijdrr.2021.102602>.
- Smith, A. B. 2020. “U.S. Billion-dollar Weather and Climate Disasters, 1980 - present (NCEI Accession 0209268).” NOAA National Centers for Environmental Information.
- Sui, J., and G. Koehler. 2001. “Rain-on-snow induced flood events in Southern Germany.” *Journal of Hydrology*, 252 (1): 205–220. [https://doi.org/10.1016/S0022-1694\(01\)00460-7](https://doi.org/10.1016/S0022-1694(01)00460-7).

- Svensson, C., and D. A. Jones. 2002. "Dependence between extreme sea surge, river flow and precipitation in eastern Britain." *International Journal of Climatology*, 22 (10): 1149–1168. <https://doi.org/10.1002/joc.794>.
- Svensson, C., and D. A. Jones. 2004. "Dependence between sea surge, river flow and precipitation in south and west Britain." *Hydrology and Earth System Sciences*, 8 (5): 973–992. <https://doi.org/10.5194/hess-8-973-2004>.
- Taflanidis, A. A., G. Jia, N. C. Nadal-Caraballo, A. B. Kennedy, J. A. Melby, and J. M. Smith. 2014. "Development of Real-Time Tools for Hurricane Risk Assessment." 1341–1350. American Society of Civil Engineers. <https://doi.org/10.1061/9780784413609.135>.
- Tebaldi, C., B. H. Strauss, and C. E. Zervas. 2012. "Modelling sea level rise impacts on storm surges along US coasts." *Environ. Res. Lett.*, 7 (1): 014032. <https://doi.org/10.1088/1748-9326/7/1/014032>.
- Toro, G. R. 2008. *Joint Probability Analysis of Hurricane Flood Hazards for Mississippi, Final report in support of the FEMA-HMTAP flood study of the State of Mississippi (Rev. 1)*.
- Toro, G. R., D. T. Resio, D. Divoky, A. Wm. Niedoroda, and C. Reed. 2010. "Efficient joint-probability methods for hurricane surge frequency analysis." *Ocean Engineering, A Forensic Analysis of Hurricane Katrina's Impact: Methods and Findings*, 37 (1): 125–134. <https://doi.org/10.1016/j.oceaneng.2009.09.004>.
- Tu, X., Y. Du, V. P. Singh, and X. Chen. 2018. "Joint distribution of design precipitation and tide and impact of sampling in a coastal area." *International Journal of Climatology*, 38 (S1): e290–e302. <https://doi.org/10.1002/joc.5368>.
- Tuleya, R. E., M. DeMaria, and R. J. Kuligowski. 2007. "Evaluation of GFDL and Simple Statistical Model Rainfall Forecasts for U.S. Landfalling Tropical Storms." *Wea. Forecasting*, 22 (1): 56–70. American Meteorological Society. <https://doi.org/10.1175/WAF972.1>.
- Turan, C. K., Y. P. Kinfu, M. A. Samad, A. Farhadzadeh, and K. Ng. 2018. "Comparison of ADCIRC and SLOSH Model Simulations for Hurricanes Andrew and Irma near Miami, Florida." 176–187. American Society of Civil Engineers. <https://doi.org/10.1061/9780784481424.019>.
- USNRC. 2012. *Guidance for Performing the Integrated Assessment for External Flooding*.
- Valle-Levinson, A., M. Olabarrieta, and L. Heilman. 2020. "Compound flooding in Houston-Galveston Bay during Hurricane Harvey." *Science of The Total Environment*, 747: 141272. <https://doi.org/10.1016/j.scitotenv.2020.141272>.
- Vitousek, S., P. L. Barnard, C. H. Fletcher, N. Frazer, L. Erikson, and C. D. Storlazzi. 2017. "Doubling of coastal flooding frequency within decades due to sea-level rise." *Scientific Reports*, 7 (1): 1399. <https://doi.org/10.1038/s41598-017-01362-7>.
- Wadey, M. P., J. M. Brown, I. D. Haigh, T. Dolphin, and P. Wisse. 2015. "Assessment and comparison of extreme sea levels and waves during the 2013/14 storm season in two UK coastal regions." *Natural Hazards and Earth*

- System Sciences*, 15 (10): 2209–2225. Copernicus GmbH.
<https://doi.org/10.5194/nhess-15-2209-2015>.
- Wahl, T., S. Jain, J. Bender, S. D. Meyers, and M. E. Luther. 2015. “Increasing risk of compound flooding from storm surge and rainfall for major US cities.” *Nature Climate Change*, 5 (12): 1093–1097.
<https://doi.org/10.1038/nclimate2736>.
- Wang, C. 2016. “A joint probability approach for coincidental flood frequency analysis at ungauged basin confluences.” *Natural Hazards*, 82 (3): 1727–1741. <https://doi.org/10.1007/s11069-016-2265-5>.
- Wang, C., N.-B. Chang, and G.-T. Yeh. 2009. “Copula-based flood frequency (COFF) analysis at the confluences of river systems.” *Hydrological Processes*, 23 (10): 1471–1486. <https://doi.org/10.1002/hyp.7273>.
- Wang, H., J. Zhou, Y. Tang, Z. Liu, A. Kang, and B. Chen. 2021a. “Flood economic assessment of structural measure based on integrated flood risk management: A case study in Beijing.” *Journal of Environmental Management*, 280: 111701. <https://doi.org/10.1016/j.jenvman.2020.111701>.
- Wang, Y., Z. Guo, S. Zheng, M. Zhang, X. Shu, J. Luo, L. Qiu, and T. Gao. 2021b. “Risk assessment for typhoon-induced storm surges in Wenchang, Hainan Island of China.” *Geomatics, Natural Hazards and Risk*, 12 (1): 880–899. Taylor & Francis. <https://doi.org/10.1080/19475705.2021.1899060>.
- Westerink, J. J., J. Luetlich, C. A. Blain, and N. W. Scheffner. 1994. *ADCIRC: An Advanced Three-Dimensional Circulation Model for Shelves, Coasts, and Estuaries. Report 2. User's Manual for ADCIRC-2DDI*. ARMY ENGINEER WATERWAYS EXPERIMENT STATION VICKSBURG MS.
- Xu, K., C. Ma, J. Lian, and L. Bin. 2014. “Joint Probability Analysis of Extreme Precipitation and Storm Tide in a Coastal City under Changing Environment.” *PLoS ONE*, (G. J.-P. Schumann, ed.), 9 (10): e109341.
<https://doi.org/10.1371/journal.pone.0109341>.
- Yang, J., P. Reichert, and K. C. Abbaspour. 2007. “Bayesian uncertainty analysis in distributed hydrologic modeling: A case study in the Thur River basin (Switzerland).” *Water Resources Research*, 43 (10).
<https://doi.org/10.1029/2006WR005497>.
- Yang, W., Q. Yang, M. Gong, X. Xu, and B. Yang. 2021. “Assessment on typhoon prevention capability of fishing port based on numerical model calculations.” *IOP Conf. Ser.: Earth Environ. Sci.*, 861 (7): 072007. IOP Publishing.
<https://doi.org/10.1088/1755-1315/861/7/072007>.
- Yildirim, E., and I. Demir. 2019. “An integrated web framework for HAZUS-MH flood loss estimation analysis.” *Nat Hazards*, 99 (1): 275–286.
<https://doi.org/10.1007/s11069-019-03738-6>.
- Yue, S. 2001. “A bivariate gamma distribution for use in multivariate flood frequency analysis.” *Hydrological Processes*, 15 (6): 1033–1045.
<https://doi.org/10.1002/hyp.259>.
- Yue, S., T. B. M. J. Ouarda, B. Bobée, P. Legendre, and P. Bruneau. 1999. “The Gumbel mixed model for flood frequency analysis.” *Journal of Hydrology*, 226 (1): 88–100. [https://doi.org/10.1016/S0022-1694\(99\)00168-7](https://doi.org/10.1016/S0022-1694(99)00168-7).

- Zhang, H., W. Fang, H. Zhang, and L. Yu. 2021. "Assessment of direct economic losses of flood disasters based on spatial valuation of land use and quantification of vulnerabilities: a case study on the 2014 flood in Lishui city of China." *Natural Hazards and Earth System Sciences*, 21 (10): 3161–3174. Copernicus GmbH. <https://doi.org/10.5194/nhess-21-3161-2021>.
- Zhang, L., and V. P. Singh. 2006. "Bivariate Flood Frequency Analysis Using the Copula Method." *Journal of Hydrologic Engineering*, 11 (2): 150–164. [https://doi.org/10.1061/\(ASCE\)1084-0699\(2006\)11:2\(150\)](https://doi.org/10.1061/(ASCE)1084-0699(2006)11:2(150)).
- Zhang, Y. J., R. C. Witter, and G. R. Priest. 2011. "Tsunami–tide interaction in 1964 Prince William Sound tsunami." *Ocean Modelling*, 40 (3): 246–259. <https://doi.org/10.1016/j.ocemod.2011.09.005>.
- Zheng, F., S. Westra, M. Leonard, and S. A. Sisson. 2014. "Modeling dependence between extreme rainfall and storm surge to estimate coastal flooding risk." *Water Resources Research*, 50 (3): 2050–2071. <https://doi.org/10.1002/2013WR014616>.
- Zheng, F., S. Westra, and S. A. Sisson. 2013. "Quantifying the dependence between extreme rainfall and storm surge in the coastal zone." *Journal of Hydrology*, 505: 172–187. <https://doi.org/10.1016/j.jhydrol.2013.09.054>.
- Zhong, H., van P.-J. Overloop, and van P. H. A. J. M. Gelder. 2013. "A joint probability approach using a 1-D hydrodynamic model for estimating high water level frequencies in the Lower Rhine Delta." *Natural Hazards and Earth System Sciences*, 13 (7): 1841–1852. <https://doi.org/10.5194/nhess-13-1841-2013>.
- Zhong, M., T. Zeng, T. Jiang, H. Wu, X. Chen, and Y. Hong. 2021. "A Copula-Based Multivariate Probability Analysis for Flash Flood Risk under the Compound Effect of Soil Moisture and Rainfall." *Water Resour Manage*, 35 (1): 83–98. <https://doi.org/10.1007/s11269-020-02709-y>.
- Zscheischler, J., O. Martius, S. Westra, E. Bevacqua, C. Raymond, R. M. Horton, B. van den Hurk, A. AghaKouchak, A. Jézéquel, M. D. Mahecha, D. Maraun, A. M. Ramos, N. N. Ridder, W. Thiery, and E. Vignotto. 2020. "A typology of compound weather and climate events." *Nature Reviews Earth & Environment*, 1 (7): 333–347. Nature Publishing Group. <https://doi.org/10.1038/s43017-020-0060-z>.